Ilmenite-Pyrophanite and Niobian Rutile in the South Mountain Batholith, Nova Scotia

Karla M. Pelrine

Submitted in Partial Fulfillment of the Requirements
for the Degree of Bachelor of Sciences, Honours
Department of Earth Sciences
Dalhousie University, Halifax, Nova Scotia
April 30, 2003

Dalhousie University

Department of Earth Sciences
Halifax, Nova Scotia
Canada B3H 3J5
(902) 494-2358
FAX (902) 494-6889

DATE April 30, 2003

AUTHOR Karla M. Pelrine

TITLE Ilmenite-Pyrophanite and Niobian Rutile in the South Mountain Batholith, Nova Scotia.

Degree BSc. Convocation May Year 2003

Permission is herewith granted to Dalhousie University to circulate and to have copied for non-commercial purposes, at its discretion, the above title upon the request of individuals or institutions.

Abstract

Ilmenite and rutile are ubiquitous, but modally scarce (<0.5%), minerals in granitoid rocks of the differentiated peraluminous South Mountain Batholith (SMB). Ilmenite occurs as blocky 0.05-0.90 mm grains in biotite, and as discrete larger anhedral grains along silicate grain boundaries. Ilmenite grains show compositional zoning toward the pyrophanite ($MnTiO_3$) end-member, ranging from 3-15 wt.% MnO in the cores to 5-23 wt.% MnO on the rims. Rim-core differences range from 2-12 wt.% MnO, generally with larger variations in the more fractionated rocks. With increasing fractionation in the batholith as a whole, the MnO contents of the ilmenites tend to decrease, albeit with considerable scatter. Several anhedral ilmenite grains appear to exhibit the same characteristics as those that occur in the neighbouring Meguma Supergroup. Texturally and chemically, ilmenite appears to be a primary magmatic mineral of the SMB throughout its crystallization history, although some grains may be xenocrystic. Rutile occurs as 0.03-0.70 mm, euhedral to anhedral grains, mainly as inclusions in biotite. Compositionally, most rutiles contain Nb_2O_5 (up to 4 wt. %) and Ta_2O_5 (up to 2 wt. %), both elements becoming more highly concentrated in rutiles from the more fractionated granitic rocks (from 0.5-1.5 wt. % Nb_2O_5+Ta_2O_5 in the early rocks to 0.1-3.5 wt. % Nb_2O_5+Ta_2O_5 in the most evolved rocks). Rutile occurs as three texturally and chemically distinct types. Type 1 rutile occurs as large discrete grains with the highest concentrations of Nb and Ta, and appears to be primary magmatic in origin. Type 2 rutile grains occur within chloritized biotite, are smaller than Type 1 rutiles, have moderate concentrations of Nb and Ta, and appear to be the product of the hydrothermal alteration of biotite. Type 3 rutile grains occur within grains of ilmenite, are the smallest of the three types, have the lowest concentrations of Nb and Ta, and appear to be the product of ilmenite breakdown during hydrothermal alteration. In the early history of the batholith, ilmenite sequesters most of the titanium available in the silicate melt, whereas in the later stages of evolution, rutile sequesters most of the titanium and acts as a host to niobium and tantalum. During evolution of the batholith, whole-rock Nb+Ta remains roughly constant at about 10-15 ppm, but the latest and most evolved rocks show a wide variation from 5-50 ppm Nb+Ta. With this differentiation, the whole-rock Nb/Ta ratio decreases from ~15 to 3, whereas the rutile Nb/Ta ratio increases from ~5 to ~20. Niobium-tantalum fractionation, as indicated by the variation in whole-rock and rutile Nb/Ta ratios, has implications for the formation of tantalum mineral deposits in the late stages of differentiation of the batholith.

TABLE OF CONTENTS

TABLE OF FIGURES

TABLE OF TABLES

Acknowledgements

This project would not have been possible without the generous help of several important people. First and foremost, my thanks go to my supervisor, Professor Barrie Clarke. The extensive time he spent helping me experience true research, as well as his patient guidance, were crucial to the completion of this thesis. My co-supervisor, Mike MacDonald from the Department of Natural Resources, provided his time and allowed us access to the rock storage facility in Stellarton N.S. Thanks to Bob MacKay, who is our microprobe expert, who patiently put up with me while I made my best attempt at operating that intimidating machine. I am also grateful to Gordon Brown whose expertise cutting thin sections is unmatched. I am very thankful to Marcos Zentilli, who was the first person to ever ask me what I dreamed about for the future. Thanks go to Lexie Arnott, Norma Keeping, Darlene van der Rijt, R. Jamieson and Sandy Grist, for help with many pieces of my thesis puzzle. Also I want to thank the rest of my peers writing theses this year for their mutual support. Finally, thanks to my family who put up with the deadlines, time restraints, and the general havoc I produced in our household over the past year.

CHAPTER 1: INTRODUCTION

1.1 Introduction

Oxide minerals are "those natural compounds in which oxygen is combined with one or more metals" (Klein and Hurlbut 1985). Oxide minerals are common accessory phases in igneous, metamorphic, and sedimentary rocks. The minerals of this group are relatively hard, dense, and refractory. Rutile, magnetite, ilmenite, and titanite are common oxides in granites. The occurrences and compositions of oxide minerals are sensitive to temperature, pressure, oxygen fugacity, bulk rock and fluid composition; therefore, they are able to record partial melt episodes, degrees of melt extraction, and periods of metasomatic enrichment (Haggerty 1976, 1991).

Two major chemical divisions describe oxide minerals:

i) Simple oxides are those with the configuration $X_a:O_b$. Simple oxides can have the chemical structures of X_2O, XO, XO_2 and X_2O_3. Examples of these simple oxides are cuprite Cu_2O, zincite $(Zn,Mn)O$, rutile TiO_2, and hematite Fe_2O_3.

ii) Multiple oxides have two non-equivalent metal atom sites and generally have chemical structures of XYO_3, XY_2O_6, and XY_2O_4. Ilmenite $FeTiO_3$, columbite-tantalite $(Fe, Mn)(Nb, Ta)_2O_6$, and spinel $MgAl_2O_4$ are examples of multiple oxides.

Oxide minerals contain high concentrations of transition metals, which, in some cases, can result in their strong absorption colors. Impurities, such as chromium, zirconium, niobium, and tantalum in dislocation gaps cause some oxide minerals to have semiconducting properties, with silicates that insulate charge and are generally poor conductors (Haggerty 1991).

Niobium, tantalum, and titanium are metals with many uses. Niobium can be used in heat-resistant steels, high refractive index glass for cameras and eye glasses, superconductive magnets, acoustic wave filters for televisions, and carbide cutting tools (Fig. 1.1). The primary uses of tantalum are in capacitors, superalloys in aircraft engines and spacecraft, x-ray film, prosthetic limbs, and carbide cutting tools (Fig. 1.2). Titanium is used in commercial and military aircraft, surgical equipment, paint pigment, and jewellery (Fig. 1.3).

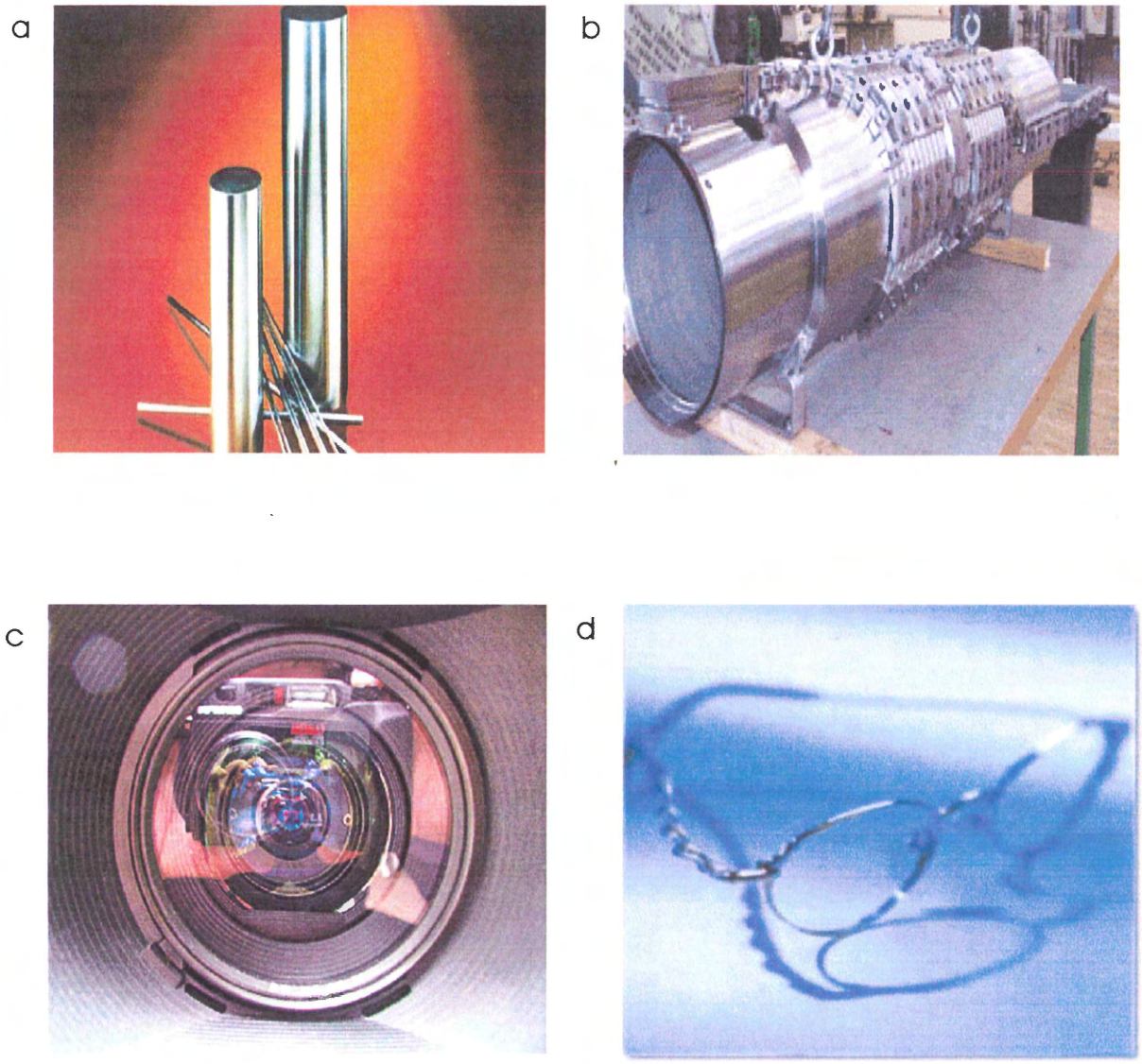

Figure 1.1: Uses of niobium: a) in heat-resistant steels, b) in superconductive magnets, c) in high refractive index glass in cameras, and d) in eye glasses.
(Sources: a) www.nonferrous-metal.com/ new-page/titanium07.htm;
b) www.jeo.com/nmr/mag_view/magnet_destruction.html;
c) www.sl66.com/sl66_lens_details/oberkochen.htm;
d) www.healthenterprises.com/contentmgr/ showdetails.php).

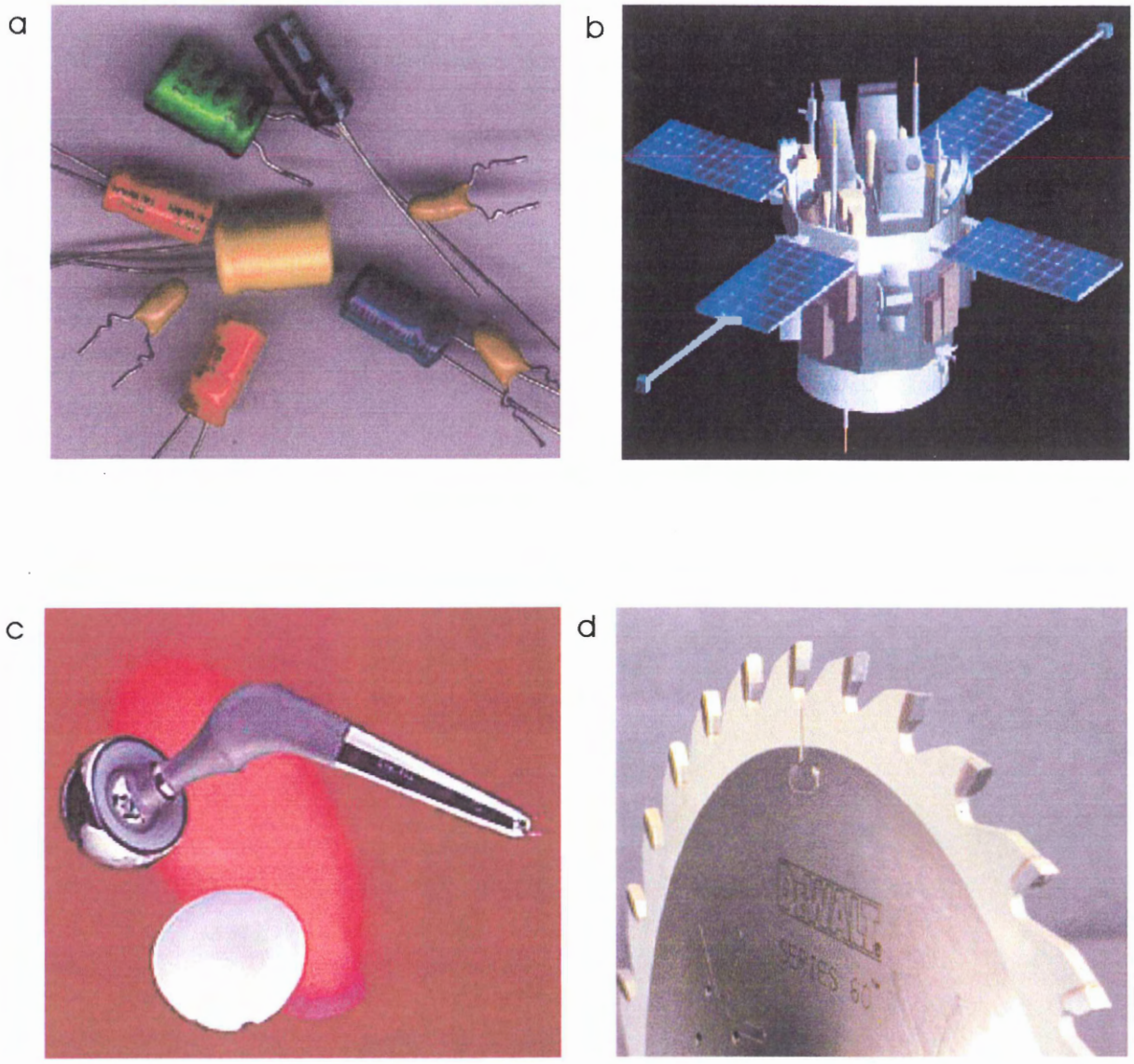

Figure 1.2: Uses of tantalum: a) in capacitors, b) in superalloys in aircraft engines and spacecraft, c) in prosthetic limbs, and d) as the carbide in cutting tools.
(Sources: a) www.hd.org/Damon/photos/electronics/;
b) helios.gsfc.nasa.gov/ ace_spacecraft.html;
c) www.twi.co.uk/j32k/getFile/ elec_medical.html;
d) www.dewalt.com/us/images/ articles/blades_02.jpg).

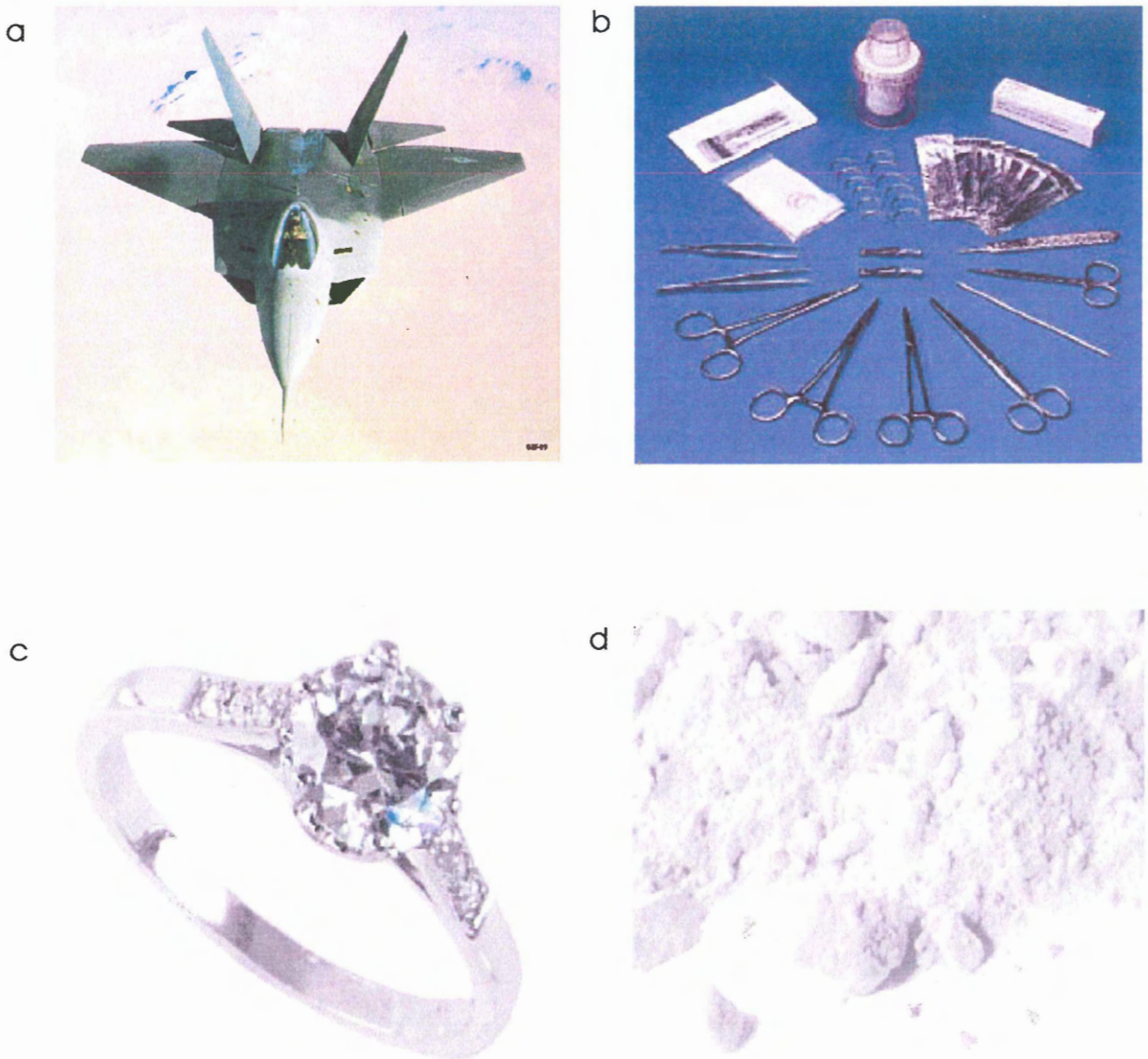

Figure 1.3: Uses of titanium: a) in commercial and military aircraft, b) in surgical equipment, c) in ring bands, and d) in white paint pigment.
(Sources: a) aae.www.ecn.purdue.edu/AAE/Career/Military.html;
b) www.bioanalytical.com/ products/md/sik.html;
c) www.luxury-line.com/diamonds/engagement/ashford-metals.htm;
d) www.mahavirminerals.com/ profile.html).

1.2 Occurrence of Oxide Minerals

Waychunas (1991) classified several main groups of oxide minerals based on their occurrences in nature. The first group contains those, such as ilmenite or rutile, that commonly occur in crystalline rocks. Mafic rocks tend to contain higher concentrations of these oxides than either intermediate or felsic rocks (Haggerty 1976). The second group of oxide minerals contains high concentrations of rare earth elements and generally occurs in pegmatites. Examples of these less common oxide minerals include columbite-tantalite and uraninite. The third group includes hydrous oxide minerals that are important in soil and surface environment chemistry and geochemistry, such as brucite or bauxite.

The essential minerals of granitic rocks are plagioclase, K-feldspar, and quartz. Biotite, muscovite, andalusite, chlorite, cordierite, garnet, tourmaline and ilmenite are minerals that occur in the South Mountain Batholith and are characteristic of peraluminous granites (MacDonald 2001). An absence of hornblende is also characteristic of these granites. The principal oxide minerals in granites are ilmenite, spinel, rutile, pseudobrookite-armalcolite, and perovskite. Oxide minerals in granites can vary extensively depending on the temperatures of crystallization of the granite. High temperature minerals are ilmenite, hematite, rutile, and pseudobrookite (Haggerty 1976). Low temperature replacement oxide minerals include maghemite, titanite, and hematite.

Most oxide minerals that occur in granites are minor phases or accessory minerals, and many variables can lead to different mineral assemblages. Globally magnetite-series granites contain several oxide phases including magnetite, hematite, and Cu, Pb, Zn ore deposits (Ishihara and Wang 1999). World wide the mineral components of ilmenite-series (peraluminous granites) include ilmenite, rutile, and W, Sn, REE, and Nb-Ta ore deposits (Ishihara and Wang 1999).

1.3 Statement of purpose

The objectives of this study are as follows:

i) to petrographically, and chemically, characterize the oxide minerals in the South Mountain Batholith;

ii) to examine Ti-oxides as possible mineralogical sinks for niobium and tantalum;

iii) to use the oxide minerals to infer the crystallization conditions, and sub-solidus cooling history of the South Mountain Batholith;

iv) to understand the chemical evolution of the South Mountain Batholith in terms of its oxide minerals;

v) to use the knowledge of partitioning of niobium and tantalum in oxide minerals of barren rocks to develop a method of locating niobium and tantalum mineral deposits; and

vi) to assess the input of the South Mountain Batholith oxides to the Ti-sands in the Shubenacadie River.

1.4 Scope of the investigation

The scope of this thesis exclusively includes the textures and compositions of the oxide minerals in the South Mountain Batholith. Other minerals such as silicates, phosphates, sulphides, and carbonates are beyond the scope of this investigation. The methods used include reflected light microscopy, and electron microprobe analysis. X-ray diffraction was not a method used in this thesis.

1.5 Organization of the thesis

Chapter 2 reviews the geological setting of the South Mountain Batholith, including previous work on the oxide minerals, with respect to mineral assemblages and chemical compositions. It also introduces an overview of several mineral deposits in the batholith. Chapter 3 presents the methods of sample preparation and separation, and reviews analytical methods, including petrographic analysis and electron microprobe analysis. Chapter 4 contains petrographic observations as well as mineral chemical data. Chapter 5 contains a discussion about oxide minerals in the South Mountain Batholith, along with a review of the differentiation and subsequent variations of mineral assemblages and chemical compositions. Chapter 6 presents conclusions and recommendations for future work.

CHAPTER 2: SOUTH MOUNTAIN BATHOLITH

2.1 Geological Setting

The bedrock of southern Nova Scotia consists of the meta-sedimentary rocks of the Meguma Supergroup, which is divided into the metawackes of the Goldenville Formation and the metapelites of the Halifax Formation (Schenk 1995). The Acadian Orogeny caused the metamorphism of the rocks of the Meguma Supergroup between 410 and 388 Ma (Hicks et al. 1999), where regional metamorphism in the area that reached the greenschist/ amphibolite facies. The Late Devonian – Early Carboniferous (~375 Ma) (Carruzzo 2003 in preparation) peraluminous South Mountain Batholith (Fig. 2.1) underlies one-third of southwestern Nova Scotia. The sediments overlying the South Mountain Batholith are those of the Horton Group (362-358 Ma) (Dunning et al. 2002).

2.2 Geology of the South Mountain Batholith

The South Mountain Batholith is approximately 180 km long and 50 km wide (McKenzie and Clarke 1975), covers an area of 7300 km^2, and is the largest granitoid intrusion in the Appalachians. The intrusion includes more than thirteen coalesced plutons (MacDonald et al 1992). The emplacement of the batholith has been estimated to be relatively rapid in geologic terms, possibly over a time span of approximately 5 Ma at a depth that correlates to a maximum pressure of 4 kbar (Clarke et al. 1993).

Xenoliths of Meguma country rock occur within the peraluminous granitic rocks of the batholith. These metamorphosed blocks enter the crystallizing magma by stoping (Fig. 2.2). The only physical evidence for this emplacement mechanism consists of these stoped blocks (Clarke et al. 1998).

MacDonald et al. (1992) classified the batholith into two separate stages of intrusions. Stage 1 is the early stage plutonic intrusions consisting mainly of granodiorite, and monzogranite. Stage 2 is later, and includes leucogranite, and leucomonzogranite.

Tate and Clarke (1997), and Clarke and Muecke (1985), suggested that the major processes controlling the petrological and chemical compositions of the SMB are fractional crystallization, hydrothermal / fluid phase alteration, and assimilation from

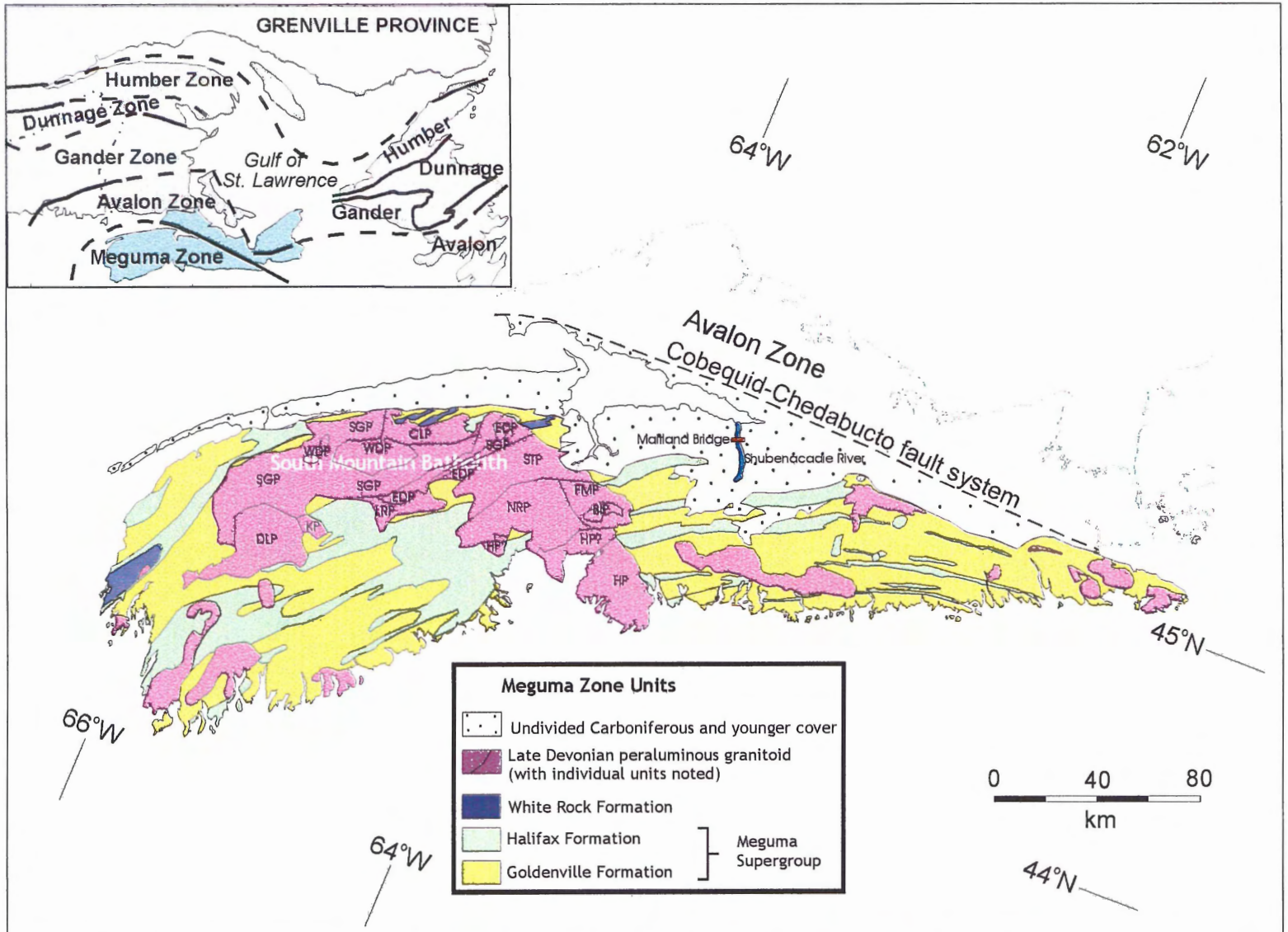

Figure 2.1: Geology of Nova Scotia. Unit names are abbreviated as follows: BIP - Big Indian Lake Pluton; CLP - Cloud Lake Pluton; DLP - Davis Lake Plutons; EDP - East Dalhousie Pluton; FMP - Five Mile Lake Pluton; HP - Halifax Pluton; KP - Kejimkujik Plutons; LRP - Little Round Lake Pluton; NRP - New Ross Pluton; SGP - Scrag Lake Pluton; STP - Salmontail Lake Pluton; and WDP - West Dalhousie Pluton (after Tate 1994 and MacDonald 2001).

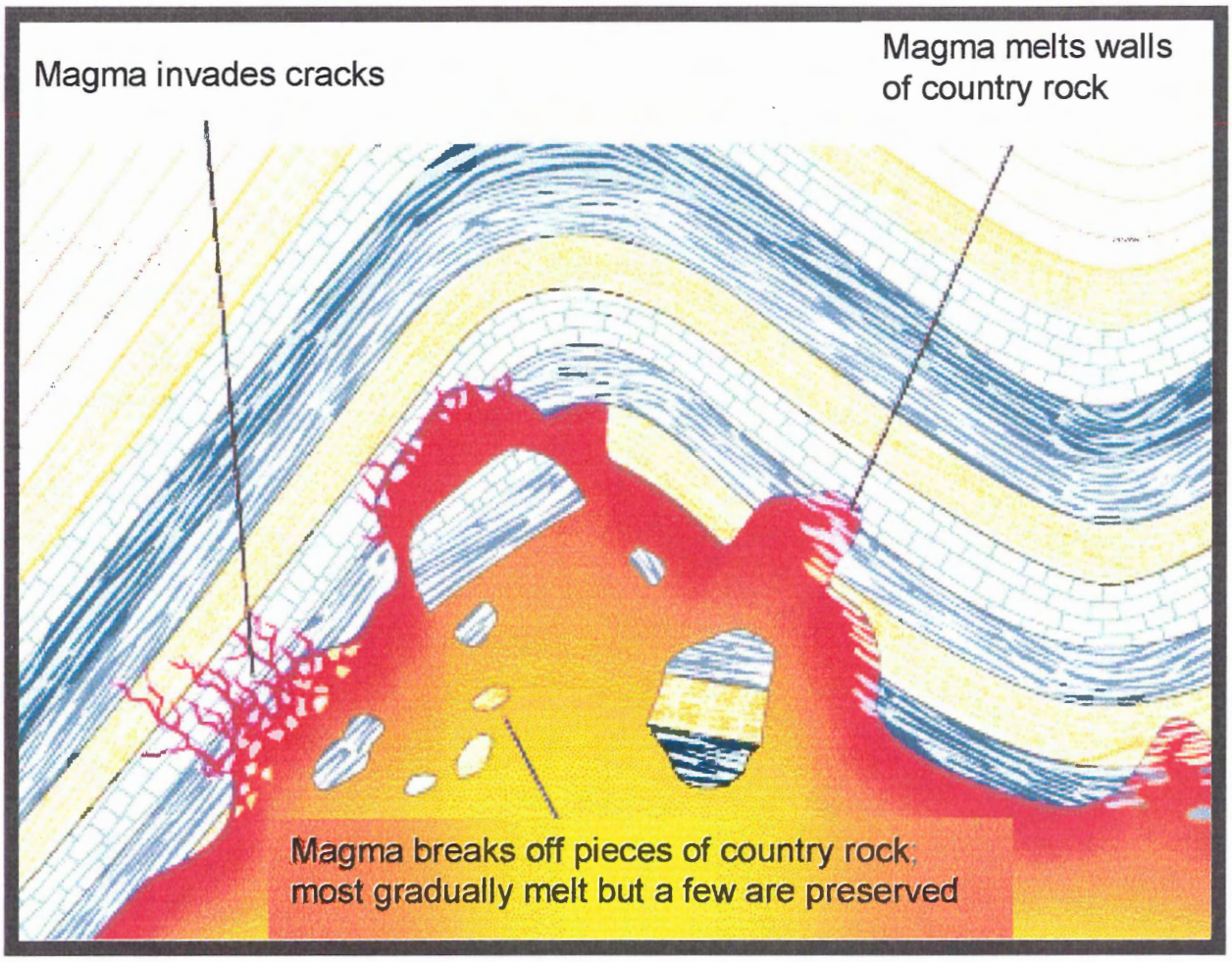

Figure 2.2: Diagram illustrating the process of stoping. The SMB is host to stoped blocks of the neighboring Meguma Supergroup. Evidence of these xenolithic blocks of the Meguma is scarce, because most of the blocks are assimilated into the granitic melt; however, there are several locations where xenoliths still occur (after Press and Siever 2001)

upper crustal contamination of the neighbouring Meguma Supergroup. Fractional crystallization produced magmatic trends in the SMB, and hydrothermal alteration and crustal contamination produced departures from these trends.

2.3 Review of petrology of the South Mountain Batholith

2.3.1 Main Rock types

Biotite granodiorite is the predominant rock type in the South Mountain Batholith. These granites are often hydrothermally altered, are gray and coarse grained and consist of K-feldspar phenocrysts, and a groundmass of quartz, plagioclase (An_{30}-An_{35}), and biotite. Accessory minerals include apatite, zircon, ilmenite, rutile, cordierite, andalusite, and garnet.

Monzogranite (further subdivided by MacDonald 2001) is another phase of granitic rock occurring in the South Mountain Batholith. The main mineralogy consists of quartz, K-feldspar, plagioclase (An_{30}-An_{32}), biotite, cordierite, and muscovite. K-feldspar is more abundant in these rocks than in the biotite granodiorite, and the proportions of biotite are lower. Greater amounts of muscovite, and andalusite, as well as hydrothermal alteration are present in this rock type. Accessory minerals include apatite, zircon, ilmenite, and rutile.

Leucomonzogranites (further subdivided by MacDonald 2001) consist of megacrysts of orthoclase and perthite with a groundmass of plagioclase (An_{20}-An_{10}), K-feldspar, quartz, biotite, cordierite, and muscovite. Included in these rocks are accessory minerals such as andalusite, garnet, apatite, zircon, ilmenite, and rutile.

Leucogranite in general contains quartz, plagioclase (An_0-An_{12}), K-feldspar, and topaz as well as small amounts of muscovite. Accessory minerals include biotite, apatite, zircon, uraninite, andalusite, Nb-Ta oxides, and economically interesting minerals such as cassiterite, sphalerite, chalcopyrite, pyrite, and pyrrhotite (MacDonald 2001). Fluorite concentrates mostly in fractures, and veins. These rocks are highly altered in some areas including massive greisen zones, as well as zones of sericitization (MacDonald 2001).

Aplites occur as dikes and irregular intrusions, and consist of quartz, plagioclase, K-feldspar, biotite, and muscovite. Accessory minerals in these rocks include apatite, zircon, andalusite, tourmaline, fluorite, garnet, and topaz (McKenzie and Clarke 1975).

Pegmatites also occur in dikes as well as in irregular pods. Quartz, plagioclase, K-feldspar, biotite, and muscovite comprise these relatively simple rocks. Pegmatites within the SMB are also known to concentrate minerals such as arsenopyrite, bornite, Nb-rutile, magnetite, hematite, bismuth metal, wittichenite, mawsonite, and tennantite (Farley 1979).

2.3.2 Specific Oxides

Oxide phases in the South Mountain Batholith are generally small (< 100 μm) and rare (< 0.5 %) and are not readily visible in hand specimen. Normally, reflected-light microscopy and an electron microprobe are needed to locate and identify these minerals. The following are those minerals most likely to occur in the batholith, based on previous work on peraluminous granites:

- ilmenite ($FeTiO_3$) - pyrophanite ($MnTiO_3$)
- niobian rutile (TiO_2)
- columbite ($(Fe,Mn)(Nb,Ta)_2O_6$) - tantalite ($(Fe,Mn)(Ta,Nb)_2O_6$) series

2.4 Differentiation of the South Mountain Batholith

MacKenzie and Clarke (1975) suggested that the lithologies within the SMB "constitute a single comagmatic series controlled by crystal-liquid fractionation processes". In the most elementary form, fractional crystallization can be represented by the transition from the least evolved biotite granodiorite occurring on the edges of the batholith, to the most evolved, and most fractionated leucogranite towards the center (MacDonald 2001; Dostal and Chatterjee 2000). If perfect equilibrium had been achieved during the entire cooling history of the batholith, the resulting rocks would have been homogenous throughout. Clarke and Chatterjee (1985) determined that the mechanisms of chemical differentiation that caused the SMB to have a heterogeneous composition include the following:

- Crystal-liquid fractionation in which practically all elements distribute themselves unevenly between any two phases, and incompatible elements become concentrated in the melt, whereas compatible elements remain principally in the solid residua.
- Assimilation of xenocrystic country rock involves melting and/or chemical exchange reactions that incorporate foreign material into the melt (Clarke 1992). Stoped blocks of the Meguma Supergroup are evidence of assimilation.
- Partitioning into a fluid phase in the final stages of crystallization involves further modification of highly fractionated rocks. Vapor phases allow for the mobilization of incompatible elements.

Mineral fractionation can account for some trends of major oxide, trace element, and REE evolution (Tate and Clarke 1997). For example, in the Davis Lake Pluton (Figure 2.1), Dostal and Chatterjee (1995) proposed that fluids released in the final stages of crystallization altered the highly fractionated rocks, and was probably the primary mechanism of fractionation during the later stages of evolution (Dostal and Chatterjee 2000). Logothetis (1985) and Chatterjee and Strong (1985) supported the idea of incompatible elements mobilizing via interaction between vapors and the melt in the SMB. Most incompatible elements tend to be immobile, but the vapor phase allows for movement between phases to veins, and greisens, possibly aiding in the creation of mineral deposits rich in rare-earth elements (Clarke and Chatterjee 1985).

2.5 Types of Mineral Deposits in the SMB

MacDonald et al. (2001) divided the 90 mineral deposits in the South Mountain Batholith into four main types based on mineralogy, alteration assemblages, and field relations:

- Pegmatite type - indicative of high temperatures, occurs in pods scattered throughout intrusion (Mo, Sn, W, Cu, Nb, and Ta);
- Greisen type - indicative of intermediate temperatures, usually occurs in the form of veins associated with faulting, and can be massive and highly altered (Sn, W, Mo, As, Cu, Pb, Zn, F, Au, and Ag);

- Vein type - indicative of low temperatures, occurs in zones that are highly fractured, and hemitization occurs readily in these areas (U, Cu, Mn, P, F, and Ag); and
- Breccia type - limited to very few plutons, as well as some meta-sedimentary rocks (Pb, Zn, Ba, Au, and Ag).

Individual plutons may have distinct types of mineral deposits, as many variables control the mineralogy of any granite. Prolonged fractionation causes the associated suite of elements to vary greatly from one area to the next. Other factors contributing to variations in bulk compositions include the amount of crustal contamination in the area, and the physical and chemical conditions during the emplacement and crystallization of the granite (MacDonald 2001).

2.6 Summary

The South Mountain Batholith is comprised of many rock types, including biotite granodiorite, monzogranite, leucomonzogranite, and leucogranite. Because the SMB is peraluminous, the oxide minerals likely to occur in the SMB are ilmenite, rutile, and columbite-tantalite. The primary mechanism controlling the bulk composition of the SMB is crystal-liquid fractionation, whereby incompatible elements become concentrated in the late stages of evolution. The concentration of incompatible elements has the potential to form mineral deposits. The four major types of mineral deposits that occur in the SMB are greisen, vein, breccia, and pegmatite types, each of which has characteristic mineralogy, alteration assemblages, and field relations.

CHAPTER 3: METHODOLOGY

3.1 Introduction

This thesis deals with the occurrence and chemical composition of opaque oxide minerals, particularly Ti-Fe-Mn-Nb-Ta bearing phases, as a function of magmatic evolution in the South Mountain Batholith. As such, the principal laboratory investigative tools are reflected-light microscopy and the electron microprobe.

3.2 Sample selection

Plots of 582 chemical analyses of whole-rock samples (NSDNR) from the South Mountain Batholith show a fractionation trend (Fig. 3.1). Strontium and zirconium decrease during fractional crystallization of the batholith. Strontium is depleted by early stage crystallization of Ca-rich plagioclase, and zirconium is depleted by zircon. As a measure of fractionation, I use the sum (Sr+Zr) as the value for the x-axis to reduce the amount of scatter in the fractionation trend that would occur if only one of the two elements were plotted alone.

As a method of organization, as well as a way to ensure representation of all the data, I arbitrarily divided the sample selection plots into five equal bins. Bin 1 is shown in blue and represents the early stages of evolution of the batholith (high Sr+Zr), and Bin 5, shown in red represents the most differentiated rocks (low Sr+Zr). These colors, as well as a yellow arrow representing fractionation, are used on each of the plots created from the data collected for this study.

Figure 3.2 shows that the sum (Nb+Ta) generally increases in highly fractionated rocks. Figure 3.3 shows that ratio of Nb/Ta changes during the fractionation of these otherwise very similar elements (similar atomic radii, and valence charges of +5) (Goldschmidt 1937) (Fig. 3.4). If niobium and tantalum did not fractionate, Nb/Ta would be constant. These diagrams were used to identify 104 samples evenly distributed over the Sr+Zr range for possible study. Sample selection is, therefore, based on chemical, not spatial relationships.

The Nova Scotia Department of Natural Resources granted access to the rock storage facility in Stellarton, Nova Scotia. I was able to locate 38 of the 104 samples as hand specimens and also nine as crushed samples. After careful re-examination, I

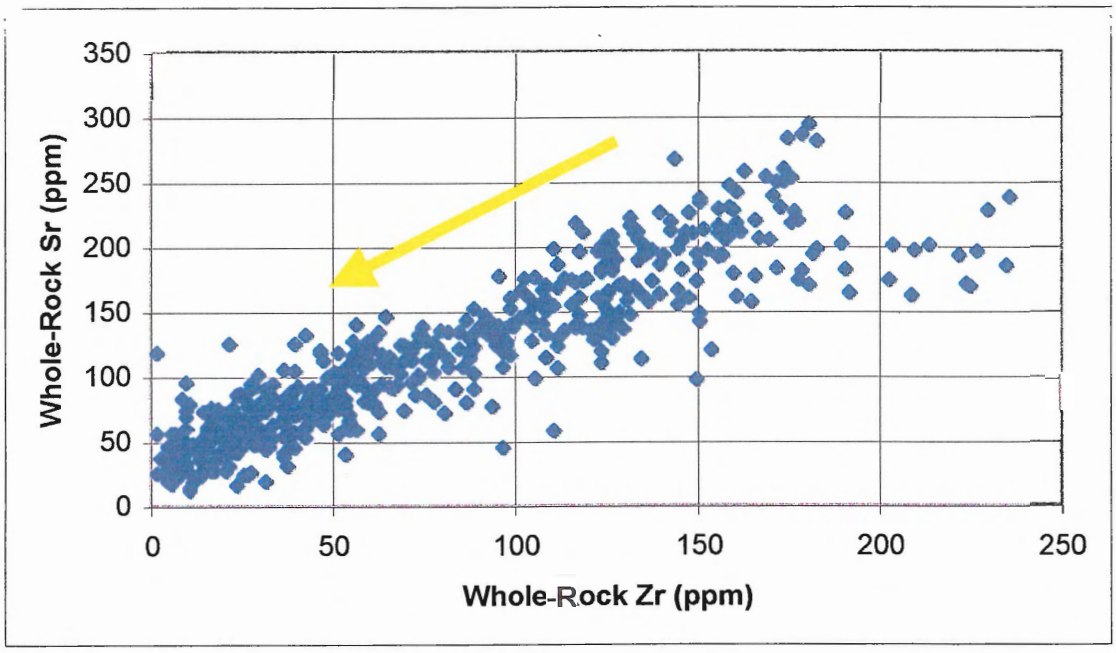

Figure 3.1: Concentrations of Zr and Sr from 582 rocks of the SMB. These two trace elements show a strong positive correlation. Early Stage I granodiorites have high Zr and Sr, whereas Stage II leucogranites have low Zr and Sr. The yellow arrow on this, and all subsequent diagrams, indicates the direction of fractional crystallization.

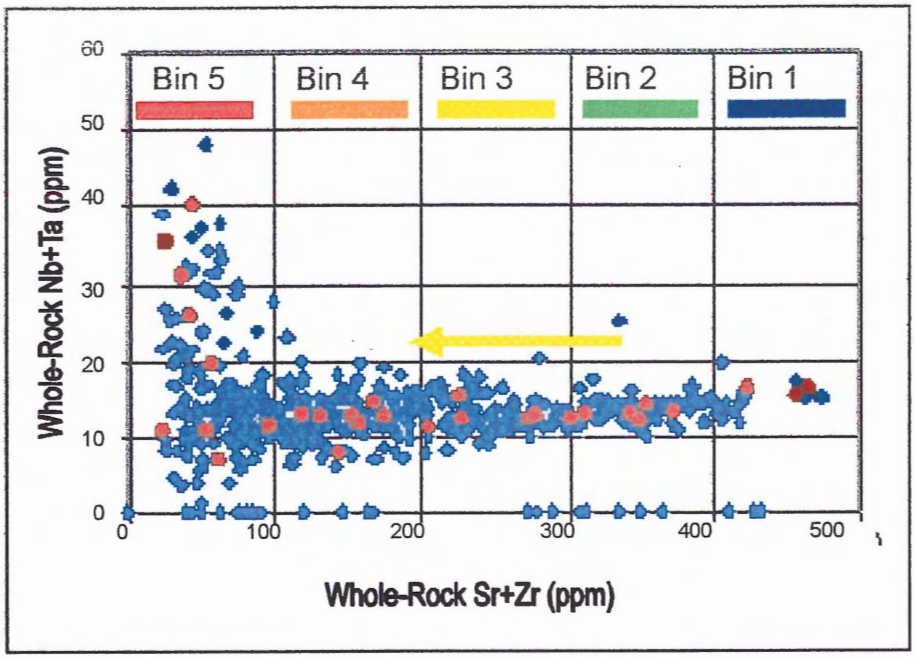

Figure 3.2: Sample distribution plot. The values of Sr+Zr are arbitrarily separated into five bins of equal size and labelled and numbered as a function of Nb+Ta, with blue representing the early stages of evolution, and red representing the more differentiated rocks. The samples marked in red are those selected for detailed examination.

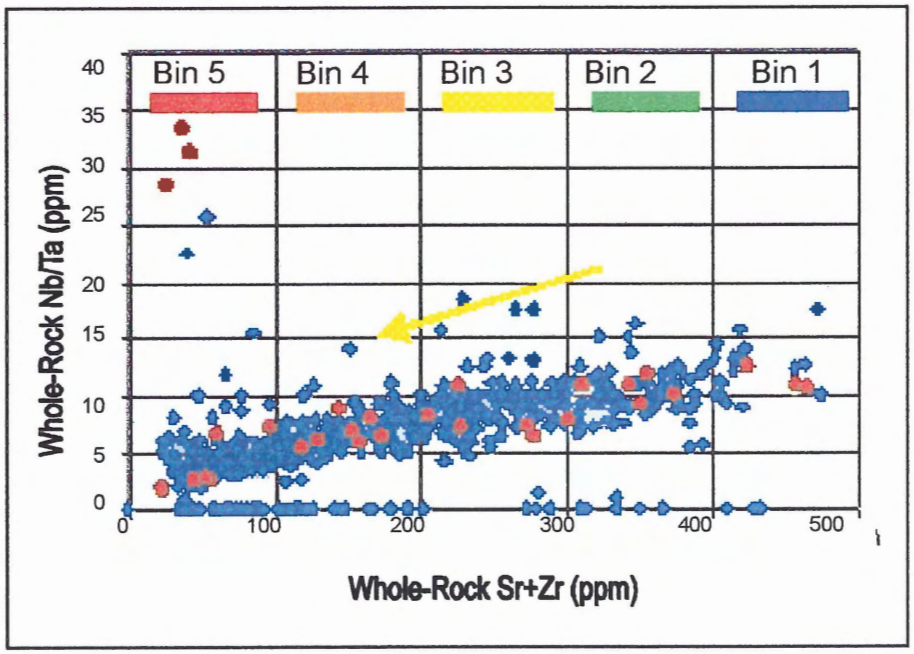

Figure 3.3: Sample distribution plot as a function of Nb/Ta. This variation diagram more clearly shows the concept of fractionation of the batholith. If the geochemical behaviour of niobium and tantalum were exactly the same, this trend line would plot horizontally. An overall decrease in Nb/Ta occurs within the batholith. In the later stages of the evolution, some ratios become very high.

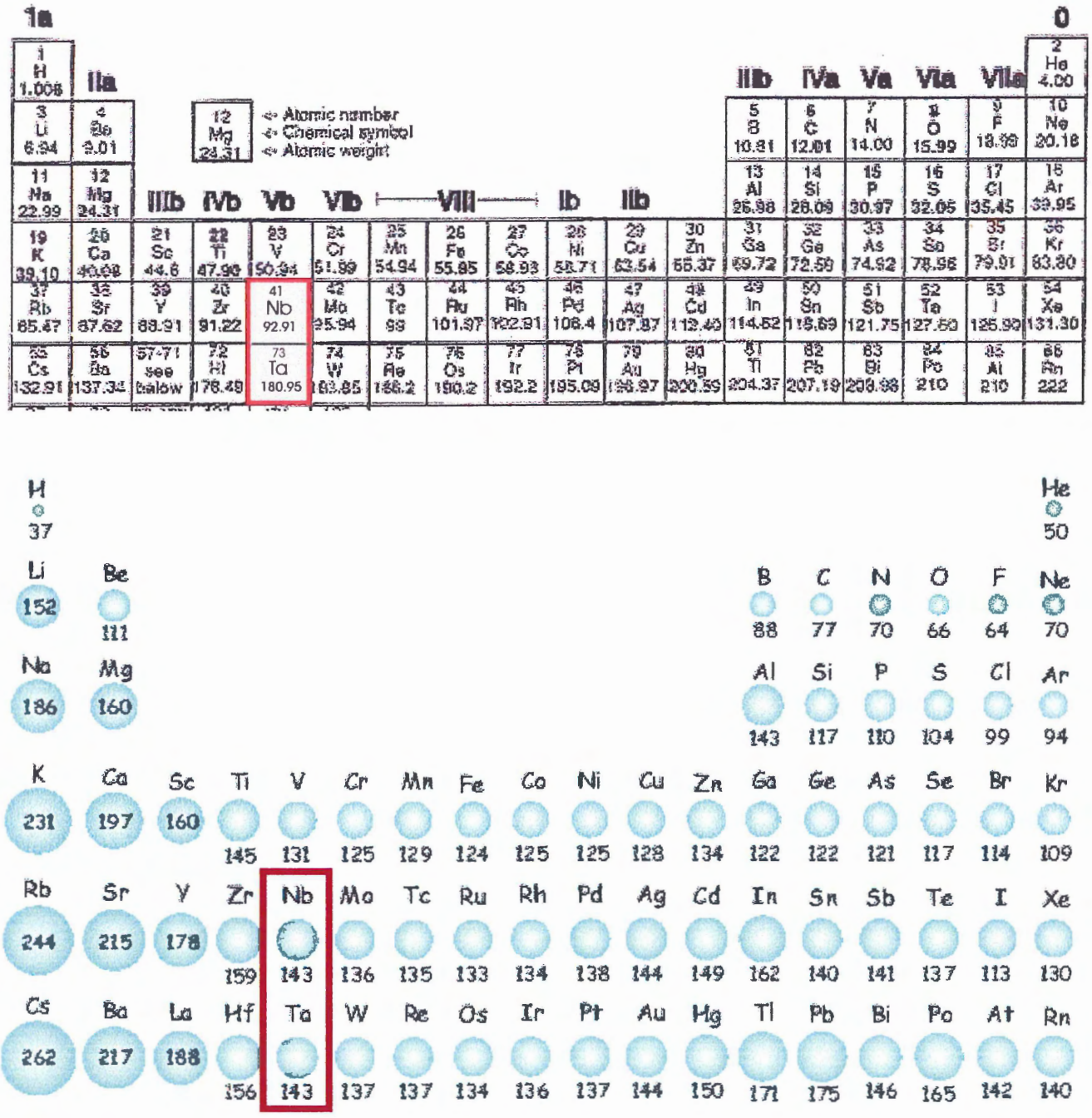

Figure 3.4: Similarities between niobium and tantalum. Niobium and tantalum are similar elements, with the same valence charge of +5, and atomic radii both measuring 143 pm (www.webelements.com).

selected 30 samples that best represent a full spectrum of chemical fractionation, representing approximately five samples from each bin. Gordon Brown, at Dalhousie University, prepared polished thin sections for examination by petrographic and electron microprobe methods.

3.3 Petrographic methods

The work of this thesis proceeded in two stages. First, I used standard petrographic techniques to locate grains and make maps of each thin section. Second, I used electron microprobe analysis to determine the chemical compositions of the grains located.

3.3.1 Transmitted light microscopy

Oxide minerals are opaque and, therefore, have no properties other than grain size and shape distinguishable in transmitted light. Even so, transmitted light microscopy is essential to determine the co-existing, and perhaps host, silicate minerals for the oxide phases.

3.3.2 Reflected light microscopy

Reflected light microscopy was used to distinguish between various opaque minerals. In reflected light, oxide minerals are white and gray, whereas silicates are darker, and sulphides are yellow or blue. The main criteria in the identification of oxide minerals in reflected light are shape, color, and reflectivity. The habit, shape, and host minerals of oxide grains on each thin section were carefully studied and marked for ease of location during probing.

3.4 Electron microprobe analysis

The Dalhousie Regional Electron Microprobe Laboratory is equipped with a JEOL JXA-8200 with five wavelength dispersive spectrometers (WDS) (1.5 kV, 15 nA, 1 μm spot size, and 20-40-second counting times) using the following geological and metallic standards: rutile for Ti; magnetite for Fe; Nb_2CoO_6 for Nb; Ta_2O_5 for Ta; and MnO_2 for Mn. The WDS is capable of analyzing elements from boron to uranium. The

instrument produces high quality (1280x1024) backscattered and secondary images. The operating system is Solaris (Unix) (MacKay 2002).

3.4.1 Quantitative Analysis

Quantitative chemical analysis on the electron microprobe utilizes the principle that atoms in the sample excited by a high-energy beam of electrons emit characteristic X-rays as they return to their stable states. The intensity of the X-rays is proportional to the concentration of that element in the sample.

Reduction of the complete set of analyses included removal of those with totals less than 85%. Within the ilmenite analyses, points eliminated included those with TiO_2 totals below 45% and above 75%, whereas within the rutile analyses rejected points include those with TiO_2 totals below 75%.

3.4.2 Imaging

The electron microprobe is used to create high quality (1280x1024) backscattered images. Backscattered electrons are high-energy electrons that rebound from a sample with a smooth surface. The difference in brightness of each grain is a function of the average atomic number of the mineral, and allows for distinct differences visible in the images. For example rutile appears slightly darker than ilmenite because rutile has an average atomic number of 18.0, whereas ilmenite has an average atomic number of 19.2. The images created by the electron microprobe show the shape, texture, habit, and reflectivity of grains, allowing for better comparison and description of opaque oxide minerals.

3.5 Summary

Sample selection was based on chemical, not spatial relationships. Reflected and transmitted light microscopy made it possible to determine location of oxide grains and their textural association with silicates. The JEOL 8200 microprobe created backscattered electron images, and provided quantitative chemical analyses that allow for a more complete understanding of oxide minerals and their textures and relationships.

CHAPTER 4: RESULTS

4.1 Introduction

The textures and compositions of minerals contain important information about their origins. This chapter describes the textures and compositions of ilmenite and rutile in the South Mountain Batholith.

4.2 Textural observations

Oxide minerals are opaque to transmitted light; therefore, most petrographic observations are in reflected light. Nevertheless, I used standard techniques of transmitted light microscopy to identify the silicate host minerals for the oxides (Table 4.1). The predominant oxide mineral phases that occur within the 30 samples are ilmenite and rutile. In general, the majority of the oxide grains occur as inclusions in biotite, feldspar, quartz, or muscovite.

4.2.1 Ilmenite

Grains of ilmenite (Table 4.2) appear as elongated prismatic grains when cut parallel to the crystallographic c-axis, or as blocky euhedral grains cut along basal planes. The grains range from 0.05 to 1.50 mm in maximum dimensions, and occur largely as inclusions in biotite, but may also occur as inclusions in plagioclase, K-feldspar, or quartz. Also, larger, irregular-shaped grains occur along grain boundaries between biotite, plagioclase, and K-feldspars (Fig. 4.1 a-d).

4.2.2 Rutile

Rutile occurs as three distinct types within the South Mountain Batholith. The characteristics of these rutile grains (Table 4.3) are as follows:

Type 1 rutile (Fig. 4.2 a-d):
Size: 0.08-0.90 mm
Shape: 25% euhedral grains, 45% subhedral grains, 30% anhedral grains
Location: discrete isolated grains

Table 4.1: Overall Petrographic Results - Samples shown in gray have no oxide phases, most opaque minerals are sulphides. Rock types (and locations) (MacDonald 2001) are as follows: BGD - Biotite granodiorite; BMG - Biotite monzogranite; MLG - Muscovite leucogranite; FGLMG - Fine-grained leucomonzogranite; and CGLMG - Coarse-grained leucomonzogranite. Ratio of Rutile/(Rutile+Ilmenite) is a modal approximation based on points analyzed.

Bin #	Sample Number	Location	Abbrev.	Rock Type	Sr+Zr	Ilmenite	Rutile	Rut/(Rut+Ilm)	Ilmenite Hosts	Rutile Hosts
1	A15-0081	Cloud Lake Pluton	CLP	BGD	465	yes	yes	0.50	feldspar	biotite
	D13-2090	Big Indian Lk P	BIP	CGLMG	458	no	yes	1.00	N/A	biotite, chlorite, feldspar
	D13-2095-1a	Big Indian Lk P	BIP	CGLMG	424	yes	yes	0.07	quartz, feldspar	quartz, feldspar
2	A16-1268	Salmontail Lk P	STP	BMG	374	yes	no	0.00	biotite, feldspar	N/A
	A11-2267	Scrag Lk Pluton	SGP	BGD	355	yes	no	0.00	biotite, feldspar	N/A
	A10-3086	Scrag Lk Pluton	SGP	BGD	350	no	no	N/A	N/A	N/A
	D12-0134-C	Halifax Pluton	HP	BGD	343	no	no	N/A	N/A	N/A
	D12-0028	Halifax Pluton	HP	BMGs	311	yes	yes	0.63	quartz, feldspar, biotite	quartz, biotite, feldspar
	A11-2286	Scrag Lk Pluton	SGP	BMG	302	yes	yes	0.08	biotite	biotite
3	A06-3015	Scrag Lk Pluton	SGP	BMG	279	no	no	N/A	N/A	N/A
	A11-2300	Little Round Lk P	LRP	BMG	274	no	no	N/A	N/A	N/A
	A15-1320	Salmontail Lk P	STP	BMG	228	yes	yes	0.10	biotite, feldspar, quartz	feldspar, muscovite
	A14-0007	West Dalhousie P	WDP	CGLMG	226	yes	no	0.00	feldspar, quartz	N/A
	D05-0016	Halifax Pluton	HP	BMGp	206	yes	yes	0.00	biotite, chlorite, feldspar	biotite, quartz
4	D12-0081	Halifax Pluton	HP	CGLMG	175	no	yes	1.00	biotite, feldspar	biotite, chlorite

	A15-0111	Scrag Lk Pluton	SGP	FGLMG	167	no	no	N/A	N/A	N/A
	A11-2259	West Dalhousie P	WDP	CGLMG	159	yes	yes	0.20	biotite, chlorite, feldspar, quartz	muscovite, feldspar
	A16-3024	New Ross P	NRP	FGLMG	154	no	yes	1.00	N/A	biotite
	D13-2095-01	Big Indian Lk P	BIP	CGLMG	144	no	yes	1.00	N/A	biotite
	A15-0101	East Dalhousie P	EDP	CGLMG	131	yes	yes	0.87	biotite, chlorite, feldspar	biotite
	A11-2262	Scrag Lk Pluton	SGP	FGLMG	119	yes	yes	0.26	biotite, chlorite, feldspar, quartz	muscovite, biotite, chlorite
5	D13-2086	?	?	?	97	no	yes	1.00	N/A	biotite, chlorite, feldspar
	A16-1159	Big Indian Lk P	BIP	CGLMG	62	no	yes	1.00	N/A	biotite, chlorite
	A15-0044	East Dalhousie P	EDP	FGLMG	57	no	yes	1.00	N/A	biotite, feldspar, muscovite
	A09-2193	New Ross P	NRP	FGLMG	54	no	yes	1.00	N/A	muscovite, biotite, chlorite
	A15-0068	East Dalhousie P	EDP	MLG	45	no	yes	1.00	N/A	N/A
	A16-1224	New Ross P	NRP	FGLMG	43	no	yes	1.00	N/A	N/A
	A15-0008	East Dalhousie P	EDP	MLG	37	no	no	N/A	N/A	N/A
	A16-1238	New Ross P	NRP	FGLMG	26	yes	yes	0.88	biotite, feldspar, chlorite	biotite, chlorite, feldspar
	A11-2272	Scrag Lk Pluton	SGP	FGLMG	23	yes	yes	0.72	quartz	chlorite, biotite, feldspar, muscovite

Table 4.2 Ilmenite crystal morphology

Sample Number	Bin #	Sr+Zr	% Euhedral	% Subhedral	% Anhedral
A15-0081	1	465	0	35	65
D13-2095-1A	1	424	30	50	20
A16-1268	2	374	0	20	80
A11-2267	2	355	50	0	50
D12-0028	2	311	70	30	0
A11-2286	2	302	0	50	50
A15-1320	3	228	10	50	40
A14-0007	3	226	35	40	25
D05-0016	3	206	40	35	25
A11-2259	4	159	0	65	35
A15-0101	4	131	10	80	10
A11-2262	4	119	10	20	70
A16-1238	5	26	50	50	0
A11-2272	5	23	25	0	75

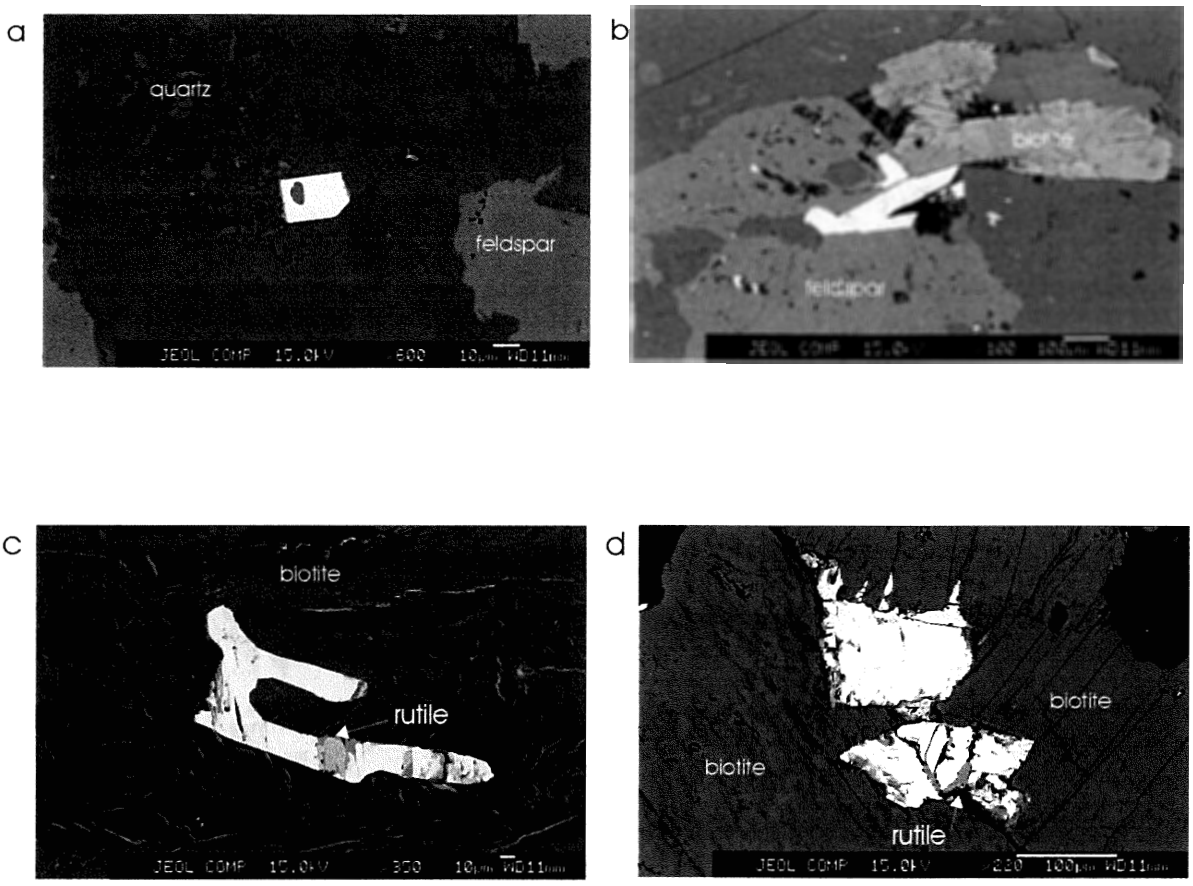

Figure 4.1: Ilmenite grains in the SMB.
a) A small euhedral ilmenite grain in quartz
b) A larger euhedral ilmenite grain associated with feldspar and biotite
c) An anhedral ilmenite grain with one of the highest concentrations of MnO (~23.0%)
d) Ilmenite grains that are zoned with higher concentrations of MnO in the rim (not visible)

Table 4.3: Rutile crystal morphology

Sample Number	Bin #	Sr+Zr	% Euhedral	% Subhedral	% Anhedral
A15-0081	1	465	10	60	30
D13-2090	1	458	0	80	20
D13-2095-1A	1	424	0	55	45
D12-0028	2	311	0	0	100
A11-2286	2	302	20	40	40
A15-1320	3	228	20	60	20
D05-0016	3	206	0	50	50
D12-0081	4	175	0	0	100
A11-2259	4	159	50	0	50
A16-3024	4	154	20	50	30
D13-2095-01	4	144	15	70	15
A15-0101	4	131	0	60	40
A11-2262	4	119	15	25	60
D13-2086	5	97	40	20	40
A16-1159	5	62	0	40	60
A15-0044	5	57	0	70	30
A09-2193	5	54	20	50	30
A15-0068	5	45	0	100	0
A16-1224	5	43	0	100	0
A16-1238	5	26	5	45	50
A11-2272	5	23	20	30	50

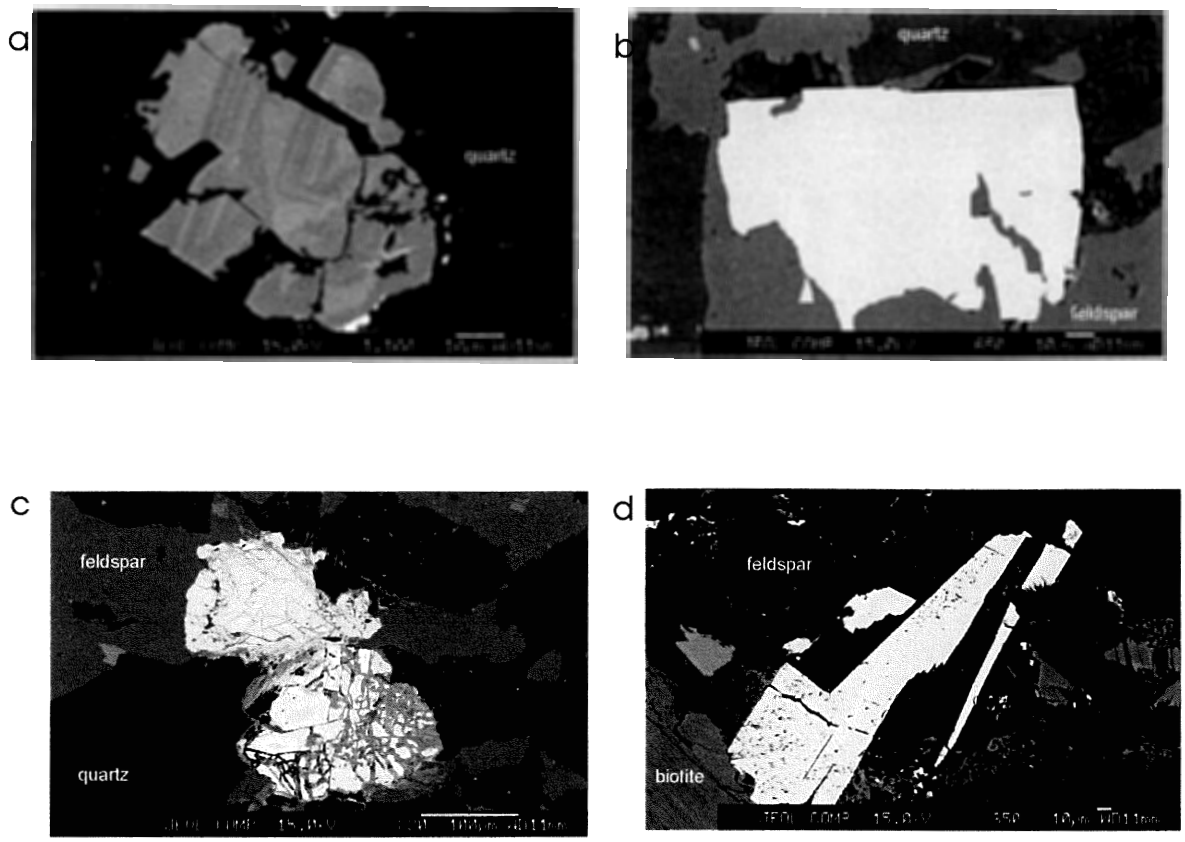

Figure 4.2: Type 1 Rutiles.
a) An oscillatory zoned rutile occurring within grains of quartz (lighter bands contain higher concentrations of Nb and Ta)
b) A large, subhedral, more homogenous, rutile occurring along a quartz and feldspar grain boundary
c) A large, anhedral, highly fractured rutile along quartz and feldspar grain boundaries
d) A large, euhedral, rutile associated with biotite and feldspar

Inclusions: of silicate / iron-rich phases in <5% of grains

Type 2 rutile (Fig. 4.3 a-d):

Size: 0.05-0.80 mm

Shape: 10% euhedral grains, 35% subhedral grains, 55% anhedral grains

Location: within grains of biotite

Inclusions: of silicate / iron-rich phases in 35% of grains

Type 3 rutile (Fig. 4.4 a-d):

Size: 0.05-0.40 mm

Shape: 5% euhedral grains, 45% subhedral grains, 50% anhedral grains

Location: within grains of ilmenite

Inclusions: of silicate / iron-rich phases in 50% of grains

4.3 Mineral chemical data

Table 4.4 shows the average ilmenite chemical compositions, and Table 4.5 similarly shows average rutile chemical compositions.

4.3.1 Ilmenite-Pyrophanite

In the South Mountain Batholith, the whole-rock concentrations of FeO range from 0.31 wt% to 5.72 wt%, and MnO from 0.02 wt% to 0.50 wt%. The chemical compositions of ilmenite range from 24% to 46% FeO, and 2% to 23% MnO. Most ilmenite grains are chemically zoned, with cores lower in MnO (3 to 15%) than rims (5 to 25%). Rim-core differences in MnO range from 2% to 8%, generally with larger differences in the more fractionated rocks. Appendix A contains all analyses of ilmenite.

4.3.2 Niobian Rutile

The whole-rock compositions of the South Mountain Batholith show that the concentrations of TiO_2 range from 0.01-0.94 wt%, whereas the rutile grains have concentrations of 94 to 99% TiO_2. Within the batholith the concentration of FeO_t ranges

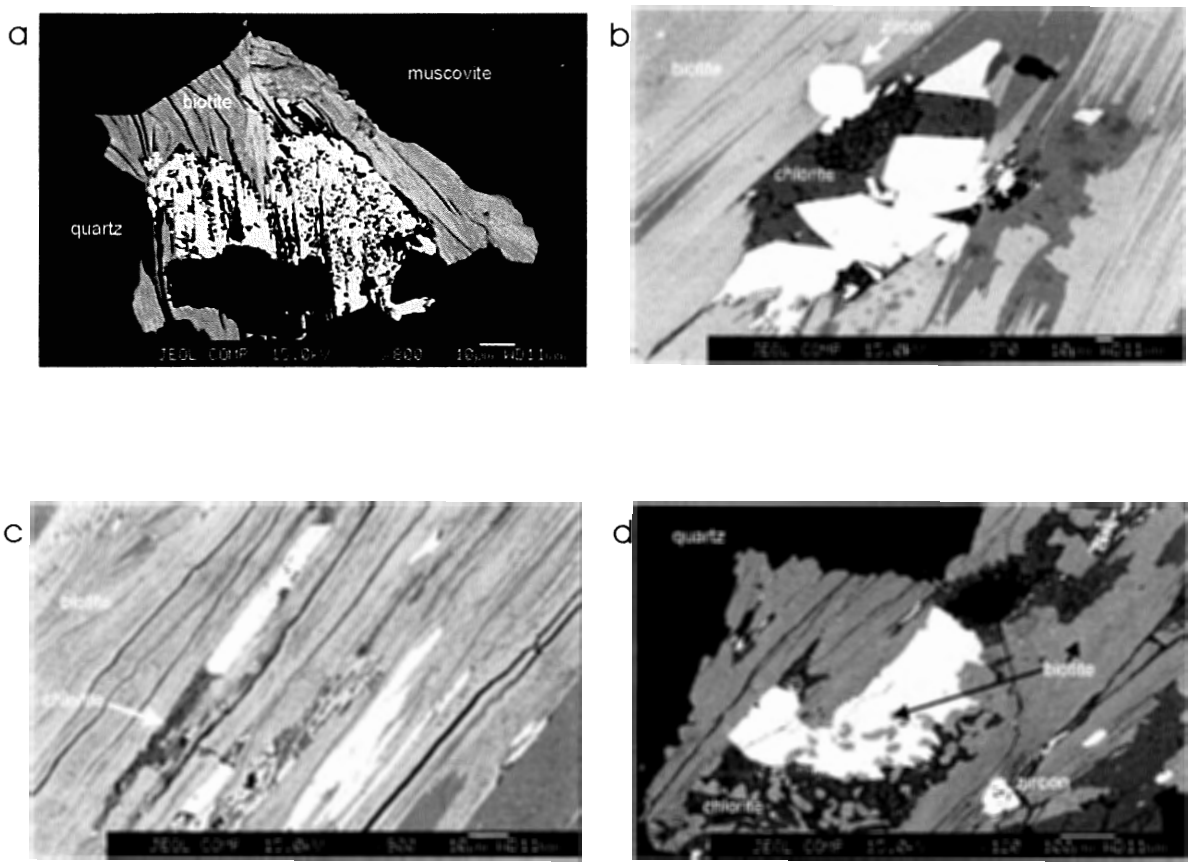

Figure 4.3: Type 2 Rutiles.
a) Small irregular rutile grains within a grain of biotite occurring with muscovite and quartz
b) Large, euhedral homogeneous grains of rutile associated with chlorite and zircon, within a large grain of biotite
c) Small, anhedral grains of rutile associated with chlorite, within a large grain of biotite
d) A large, subhedral, fractured rutile within a grain of biotite, occurring with chlorite and quartz

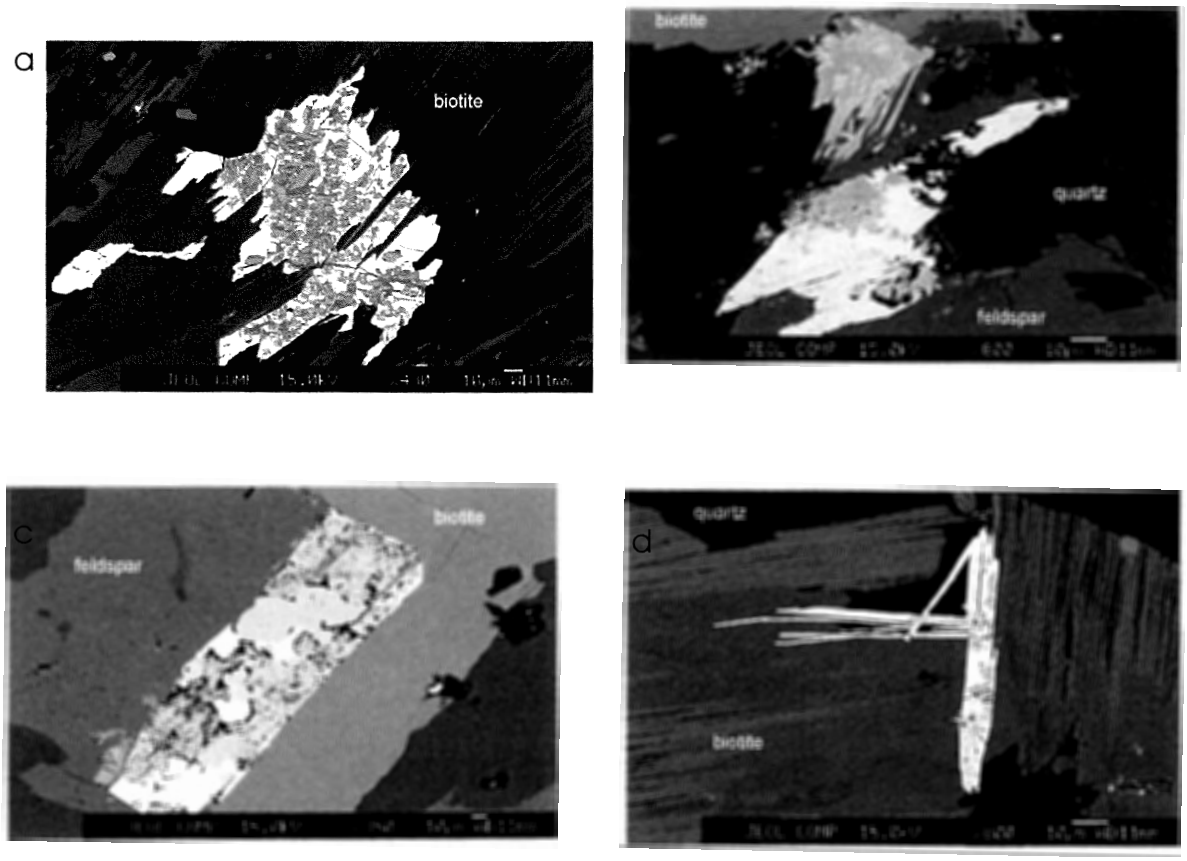

Figure 4.4: Type 3 Rutiles.
a) Small, irregular rutile grains occurring within a grain of ilmenite, associated with biotite
b) Small, altered, subhedral rutile grain, occurring with quartz, feldspar, and biotite
c) Small, anhedral rutile grains occurring with subhedral grains of ilmenite, both are associated with biotite and feldspar
d) Small, irregular rutile grains occurring within acicular grains of ilmenite that are parallel to cleavage in biotite and along grain boundaries

Table 4.4: Ilmenite average chemical compositions

Sample Number	A15-0081	D13-2095-1A	A16-1268	A11-2267	D12-0028	A11-2286	A15-1320
Bin #	1	1	2	2	2	2	3
Sr+Zr	465	424	374	355	311	302	228
n	3	14	9	4	3	11	9
TiO_2 (wt%)	52.80	52.84	52.66	51.39	51.96	52.20	52.66
FeO (wt%)	29.01	36.40	40.63	39.12	36.45	41.67	37.49
MnO (wt%)	10.67	9.76	7.71	8.65	11.76	5.18	10.86
Nb_2O_5 (wt%)	0.29	0.05	0.14	0.16	0.15	0.12	0.21
Ta_2O_5 (wt%)	0.02	0.11	0.37	0.33	0.00	0.15	0.36
Nb metal	0.20	0.03	0.10	0.11	0.10	0.08	0.15
Ta metal	0.02	0.09	0.30	0.27	0.00	0.12	0.29
Nb/Ta	11.29	0.39	0.34	0.40	31.34	0.68	0.50
Nb+Ta	0.22	0.13	0.40	0.39	0.11	0.21	0.44
Total	94.25	99.50	101.88	99.75	100.76	99.95	102.00

Cations per formula unit (based on 3 oxygens)

Sample Number	A15-0081	D13-2095-1A	A16-1268	A11-2267	D12-0028	A11-2286	A15-1320
Ti	1.05	1.01	0.99	0.98	0.99	1.00	0.99
Fe^{2+}	0.64	0.77	0.85	0.83	0.77	0.89	0.78
Mn	0.24	0.21	0.16	0.19	0.25	0.11	0.23
Nb	0.00	0.00	0.00	0.00	0.00	0.00	0.00
Ta	0.00	0.00	0.00	0.00	0.00	0.00	0.00
Total	1.94	1.99	2.00	2.01	2.01	2.00	2.00

Table 4.4 (continued): Ilmenite average chemical compositions

Sample Number	A14-0007	D05-0016	A11-2259	A15-0101	A11-2262	A16-1238	A11-2272
Bin #	3	3	4	4	4	5	5
Sr+Zr	226	206	159	131	119	26	23
n	9	9	16	2	23	2	5
TiO_2 (wt%)	51.70	54.14	53.66	56.54	55.92	51.35	52.11
FeO (wt%)	42.49	32.07	31.18	26.74	32.82	42.30	41.79
MnO (wt%)	5.33	12.66	13.33	1.11	5.99	4.02	4.35
Nb_2O_5 (wt%)	0.21	0.21	0.36	0.17	0.49	0.41	0.29
Ta_2O_5 (wt%)	0.01	0.51	0.32	0.35	0.25	0.00	0.22
Nb metal	0.15	0.15	0.25	0.12	0.34	0.28	0.20
Ta metal	0.01	0.42	0.26	0.29	0.20	0.00	0.18
Nb/Ta	14.90	0.36	0.96	0.40	1.67	0.00	1.13
Nb+Ta	0.16	0.56	0.51	0.40	0.55	0.28	0.38
Total	100.10	99.91	99.32	88.81	96.33	98.64	98.99

Cations per formula unit (based on 3 oxygens)

Sample Number	A14-0007	D05-0016	A11-2259	A15-0101	A11-2262	A16-1238	A11-2272
Ti	0.99	1.02	1.02	1.17	1.08	0.99	1.00
Fe^{2+}	0.90	0.67	0.66	0.62	0.70	0.91	0.89
Mn	0.11	0.27	0.29	0.03	0.13	0.09	0.09
Nb	0.00	0.00	0.00	0.00	0.01	0.00	0.00
Ta	0.00	0.00	0.00	0.00	0.00	0.00	0.00
Total	2.01	1.97	1.97	1.82	1.91	2.00	1.99

Table 4.5: Rutile average chemical compositions

Sample Number	A15-0081	D13-2090	D13-2095-1A	D12-0028	A11-2286	A15-1320	D05-0016	D12-0081	A11-2259	A16-3024
Bin #	1	1	1	2	2	3	3	4	4	4
Sr+Zr	465	458	424	311	302	228	206	175	159	154
n	13	17	1	5	1	6	2	7	5	12
TiO_2 (wt%)	97.84	98.27	97.41	96.54	96.84	97.66	98.83	96.98	92.53	96.68
Nb_2O_5 (wt%)	0.54	0.43	0.33	0.33	0.81	0.48	0.32	0.77	0.70	0.65
Ta_2O_5 (wt%)	0.07	0.19	0.00	0.26	0.16	0.07	0.00	0.33	0.11	0.02
FeO (wt%)	0.43	0.44	0.64	1.22	0.73	0.82	0.63	0.90	1.42	0.89
MnO (wt%)	0.03	0.05	0.17	0.05	0.04	0.01	0.01	0.04	0.03	0.07
Nb metal	0.38	0.30	0.23	0.23	0.57	0.34	0.22	0.54	0.49	0.45
Ta metal	0.06	0.16	0.00	0.21	0.13	0.06	0.00	0.27	0.09	0.02
Nb/Ta	6.58	1.93	0.00	1.08	4.32	5.85	0.00	1.99	5.43	27.74
Nb+Ta	0.43	0.46	0.23	0.45	0.70	0.39	0.22	0.80	0.58	0.47
Nb_20_5/Ta_2O_5	6.47	11.48	0.00	0.06	5.02	9.92	0.00	5.57	41.35	5.56
$Nb_2O_5+Ta_2O_5$	0.61	0.62	0.33	0.59	0.98	0.55	0.32	1.09	0.81	0.67
Total	100.19	100.32	99.38	100.09	98.96	100.07	100.74	100.03	97.65	99.65

Cations per formula unit (based on 3 oxygens)

Sample Number	A15-0081	D13-2090	D13-2095-1A	D12-0028	A11-2286	A15-1320	D05-0016	D12-0081	A11-2259	A16-3024
Ti	0.99	0.99	0.99	0.99	0.99	0.99	0.99	0.99	0.99	0.99
Nb	0.00	0.00	0.00	0.00	0.00	0.00	0.00	0.00	0.00	0.00
Ta	0.00	0.00	0.00	0.00	0.00	0.00	0.00	0.00	0.00	0.00
Fe^{2+}	0.00	0.00	0.01	0.01	0.01	0.01	0.01	0.01	0.02	0.01
Mn	0.00	0.00	0.00	0.00	0.00	0.00	0.00	0.00	0.00	0.00
Total	1.00	1.00	1.01	1.00	1.00	1.00	1.00	1.01	1.00	1.00

Table 4.5 (continued): Rutile average chemical compositions

Sample Number	D13-2095-01	A15-0101	A11-2262	D13-2086	A16-1159	A15-0044	A09-2193	A15-0068	A16-1224	A16-1238	A11-2272
Bin #	4	4	4	5	5	5	5	5	5	5	5
Sr+Zr	144	131	119	97	62	57	54	45	43	26	23
n	8	12	8	27	19	13	24	6	2	23	24
TiO_2 (wt%)	95.91	94.34	96.97	95.71	96.95	96.33	95.21	85.03	93.95	96.64	96.23
Nb_2O_5 (wt%)	1.00	1.81	1.21	0.96	0.89	1.12	1.94	8.43	1.14	1.44	0.90
Ta_2O_5 (wt%)	0.33	0.14	0.27	0.20	0.12	0.06	0.60	1.81	1.55	0.23	0.35
FeO (wt%)	0.37	1.47	0.48	1.37	0.74	1.01	1.07	3.29	1.55	0.92	1.31
MnO (wt%)	0.02	0.04	0.03	0.02	0.03	0.03	0.04	0.02	0.16	0.03	0.03
Nb metal	0.70	1.27	0.85	0.67	0.62	0.78	1.36	5.89	0.80	1.01	0.63
Ta metal	0.27	0.11	0.22	0.16	0.10	0.05	0.49	1.48	1.27	0.19	0.29
Nb/Ta	2.59	11.03	3.82	4.10	6.33	15.93	2.76	3.98	0.63	5.34	2.19
Nb+Ta	0.97	1.38	1.07	0.84	0.72	0.83	1.84	7.38	2.06	1.19	0.91
Nb_20_5/Ta_2O_5	4.47	2.44	9.60	9.60	8.64	59.25	6.50	12.69	0.73	12.18	4.77
$Nb_2O_5+Ta_2O_5$	1.33	1.95	1.49	1.17	1.01	1.18	2.54	10.25	2.69	1.67	1.24
Total	99.23	99.04	100.09	99.24	100.02	99.54	100.03	99.60	101.32	100.48	99.59

Cations per formula unit (based on 3 oxygens)

Sample Number	D13-2095-01	A15-0101	A11-2262	D13-2086	A16-1159	A15-0044	A09-2193	A15-0068	A16-1224	A16-1238	A11-2272
Ti	0.99	0.98	0.99	0.98	0.99	0.99	0.98	0.90	0.97	0.98	0.98
Nb	0.01	0.01	0.01	0.01	0.01	0.01	0.01	0.05	0.01	0.01	0.01
Ta	0.00	0.00	0.00	0.00	0.00	0.00	0.00	0.01	0.01	0.00	0.00
Fe^{2+}	0.00	0.02	0.01	0.02	0.01	0.01	0.01	0.04	0.02	0.01	0.01
Mn	0.00	0.00	0.00	0.00	0.00	0.00	0.00	0.00	0.00	0.00	0.00
Total	1.00	1.01	1.00	1.01	1.00	1.00	1.00	1.01	1.01	1.00	1.01

from 0.3 to 5.7 wt%, and within the rutile grains the total FeO ranges from 0.04 to 6.82 wt%. The whole-rock Nb concentrations within the South Mountain Batholith range from 3 to 34 ppm, and the whole-rock Ta concentrations range from 0.5 to 14 ppm. Type 1 rutile grains have Nb concentrations ranging from 0.20 to 8.11 wt%, and Ta concentrations from 0.01 to 3.42 wt%. Type 2 rutile grains have Nb concentrations ranging from 0.07 to 2.00 wt%, and Ta concentrations from 0.01-1.25 wt%. Type 3 rutile grains have Nb concentrations ranging from 0.25 to 0.91 wt%, and Ta concentrations from 0.03 to 0.24 wt%. The low-Nb+Ta grains belong to low bin numbers (least fractionated rocks), and the high-Nb+Ta rutile grains belong to higher bin numbers (more highly fractionated rocks).

4.4 Summary

Ilmenite in the South Mountain Batholith occurs as prismatic or blocky grains ranging in size from 0.05-1.50 mm. These grains, as well as larger irregular-shaped grains, are associated with biotite and/or feldspar. The SMB has three types of rutile, each having distinct physical and chemical characteristics. Type 1 rutiles are large discrete grains with the highest concentrations of Nb and Ta. Type 2 rutiles are acicular, smaller than Type 1 rutile, occur within grains of biotite, and have moderate concentrations of Nb and Ta. Type 3 rutiles are the smallest of the three types, occur within grains of ilmenite, and have the lowest concentrations of Nb and Ta. The more fractionated late-stage rutile grains contain higher concentrations of Nb and Ta compared to early-stage less fractionated rocks.

CHAPTER 5: DISCUSSION

5.1 Introduction

Several trends, both physical and chemical, occur within ilmenite and rutile as a function of evolution of the South Mountain Batholith. Primary grain shapes indicate the precise moment the batholith crystallizes, and give information about the melt conditions in which they grew, or in the case of secondary minerals the grains shapes indicate the type of alteration. In addition, chemical exchanges take place between the melt and the growing crystals, documented by the electron microprobe data. Many plots created from this data set hold critical information regarding these trends of fractionation.

5.2 Ilmenite

5.2.1 Ilmenite crystal morphology

Ilmenites in the South Mountain Batholith show several types of grain shapes (Table 4.2). Euhedral shapes account for 20% of the ilmenite grains, whereas anhedral shapes occur in 30% of the grains. The remaining 50% of the ilmenite grains are subhedral in shape.

The euhedral (prismatic and blocky) grains (Fig. 4.1 a,b) occur as inclusions in biotite and quartz, or they occur as discrete grains along quartz and feldspar grain boundaries. If these euhedral grains owe their shapes to unrestricted growth in the melt, they have a primary magmatic origin.

The subhedral-anhedral grain shapes (Fig. 4 c,d) have several possible origins:
Primary Magmatic:

A: Euhedral primary magmatic grains, growing in the melt, eventually come in contact with other grains. This physical interaction may result in the interruption of the growth of perfect crystal faces, and the former euhedral shape of these grains becomes lost, leading to the development of interstitial subhedral-anhedral grains.

B: At a peritectic point, one mineral that has been growing from the melt will develop a reaction relationship with that melt and undergo resorption. The South Mountain Batholith, however, appears to have been saturated in ilmenite throughout its crystallization history, because anhedral magmatic grains of ilmenite occur in every Bin. Euhedral ilmenite occurs throughout; therefore, no peritectic relationship involving

ilmenite was encountered, and no primary magmatic grains appear to have lost their euhedral shape as a result of such a relationship.

C: Under conditions of significant undercooling of magma, primary magmatic grains may grow too rapidly to develop all their crystal faces and, as a result, have skeletal anhedral shapes. Conditions for significant undercooling normally, however, do not occur in plutonic environments, and no minerals of any kind exhibit skeletal or quenched textures; therefore, the anhedral ilmenite shapes are not likely the result of rapid growth.

Non-Magmatic:

A: Anhedral grains of ilmenite with rutile inclusions occur in the Meguma Supergroup (Haysom et al. 1997). Similar grains of ilmenite occur in the South Mountain Batholith (Fig. 4.1 c), suggesting the partial assimilation of xenocrystic grains from the Meguma (Section 2.2). As in any case of xenocrystic grains, these grains of must be out of equilibrium with the granitic melt; therefore, these newly introduced ilmenite grains cannot have the same composition as those already forming in the South Mountain Batholith. Reaction relationships, such as resorption, between the melt and the xenocrystic ilmenite crystals can produce anhedral ilmenite.

B: Ilmenite within the South Mountain Batholith is not spatially associated with any type of alteration. There appears to be no phase for which ilmenite is a breakdown product of a secondary reaction; therefore, ilmenite does not have an origin by secondary hydrothermal alteration.

C: Within the South Mountain Batholith there appears to be no phase for which ilmenite could occur as an exsolution product from another mineral, such as titaniferous-magnetite. Spiess et al. (2000), and Druppel et al. (2001) showed several cases of polycrystalline magnetite that contains ilmenite exsolution lamellae in the Kunene Intrusive Complex, NW Namibia, but no such textures occur in the SMB ilmenites.

5.2.2 Ilmenite chemical substitutions

Ilmenite belongs to the trigonal crystal system and has a rhombohedrally-centered lattice (Fig. 5.1). Solid solution exists among ilmenite ($FeTiO_3$), pyrophanite ($MnTiO_3$), and geikielite ($MgTiO_3$) (Feenstra and Peters 1996). Geikielite and pyrophanite

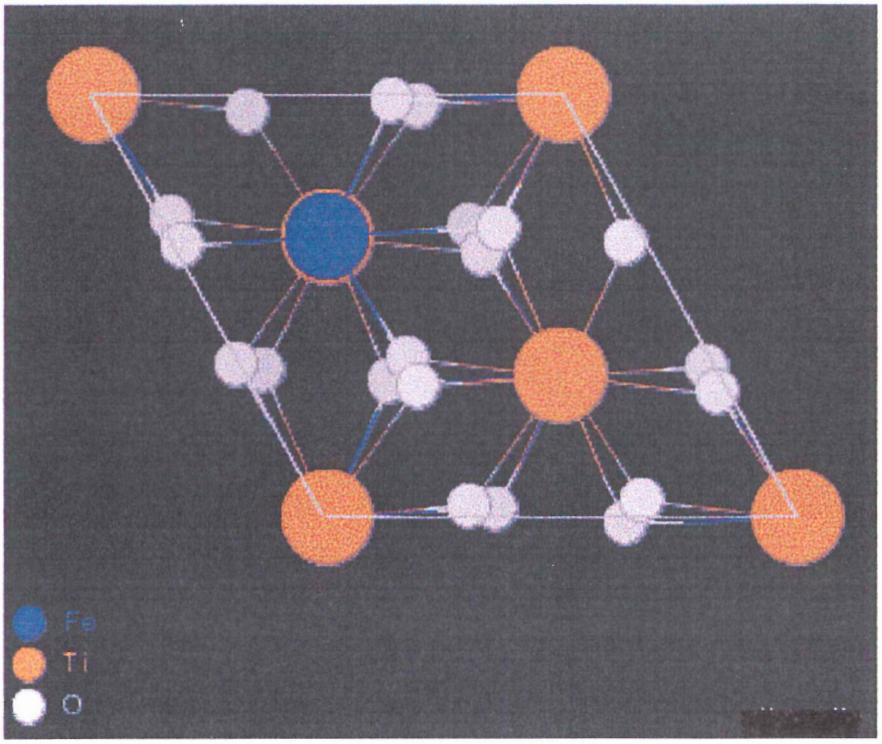

Figure 5.1: Ilmenite crystal lattice. Ilmenite belongs to the trigonal crystal system and has a rhombohedrally-centered lattice. Ilmenite is in solid solution with pyrophanite, as Mn^{2+} replaces Fe^{2+}.

commonly occur as minor components in ilmenite. Magnesian ilmenite commonly occurs in kimberlites, and manganoan ilmenite is characteristic of alkaline rocks, carbonatites, and granites (Mitchell 1978) (http://www.unb.ca/courses/geo l2142/LEC-32.html). Pyrophanite has a slightly larger cell size because Mn^{2+} (80 pm) replaces Fe^{2+} (77pm) (www.webelements.com). Craig et al. (1985) stated that pyrophanite is a product of high-grade metamorphism, and that it commonly occurs in areas of high Mn and Ti with lower oxygen fugacity. Elsdon (1975) proposed two hypotheses to account for the concentrations of manganese in ilmenite (Cerny 1986). The first hypothesis is that ilmenite crystallizes from melts that may be enriched in Mn relative to Fe resulting from differences in ionic radii (Czamanske and Mihalik 1972), and the second hypothesis is that oxidation reactions during or after crystallization account for the enrichment in manganese (Snetsinger 1969).

Ilmenite in the South Mountain Batholith exhibits zoning, where each grain has higher manganese in the rim than in the core. If the ilmenites are magmatic in origin, Fe^{2+} is preferentially removed from the melt relative to Mn^{2+}, because according to Goldschmidt's rules (1937), when two elements compete for a single site in a mineral, the smaller of the two enters the crystal lattice preferentially, also Mn/Fe in the melt must increase with fractionation (Feenstra and Peters 1996). Octahedral site preference energy, which is the difference between the crystal field stabilization energies for an octahedral complex, accounts for this site preference (http://chemiris.labs.brocku.ca/~chemweb/courses/chem232/CHEM2P32_ Lecture_12.html). At the final stages of crystallization, the Mn/Fe in the melt is high, and the outer rims of the ilmenite grains contain higher pyrophanite contents. This reverse zoning occurs, therefore, as a result of disequilibrium crystallization, and strong fractionation of manganese and iron between the melt and the ilmenite grains. The rate of crystallization appears to have been rapid enough that iron and manganese underwent fractionation; however, crystallization was slow enough that the grains do not exhibit quenched textures, such as skeletal or feathery-shaped crystals.

This same type of manganese enrichment in rims occurs in magmatic garnets in the South Mountain Batholith. Allan and Clarke (1981) described two types of garnets in the SMB: (i) normally zoned relict metamorphic grains with Mn-rich cores; and (ii)

reversely zoned magmatic grains with Mn-rich rims. Allan and Clarke (1981) believed that falling temperatures during crystal growth caused the manganese content of garnet to rise during the last stages of crystallization, resulting in these reversely zoned garnets.

5.2.3 Ilmenite compositional variation diagrams

Figure 5.2a shows the replacement of manganese for iron in the ilmenite grains during the fractionation of the batholith. The extent of zoning within the ilmenite grains is greater in the later stages of evolution of the South Mountain Batholith, with rim-core differences ranging from 2 to 12 wt% MnO, except in Bin 5, where few ilmenite grains occur. The outlying grains belong to Bin 2, and may be preferentially removed from the trend line as a result of late-stage manganese and iron leaching. Figure 5.2b illustrates the range of manganese in each sample (constant value on the x-axis). Within the South Mountain Batholith, the maximum MnO variation in a single ilmenite grain is from 11 to 23%. The maximum range of MnO in ilmenites from a single sample is from 3 to 24%, and within one bin, the maximum range of MnO in ilmenites is from 2 to 24%. Clarke and Chatterjee (1985) suggested that high TiO_2 and MnO values in the Meguma Supergroup, and the stoped metasedimentary enclaves, could have had a large influence on the final compositions of the SMB.

The primary ilmenite in the Tibchi granite, exposed at Kalato, in the Tibchi ring-complex, northern Nigeria is slightly enriched in Mn (Sakoma and Martin 2002). These grains are presumed to have crystallized later in the history of the melt when it has become slightly more fractionated. The secondary ilmenite occurring in the Tibchi granite has increased Mn content that is closer to the composition of pyrophanite that formed at the expense of primary ilmenite along fractures and microfissures. The excess Mn in the later stages of evolution may have come from hydrothermal transfer of Mn along fissures (Sakoma and Martin 2002). Feenstra and Peters (1996) divided the ilmenite in experimental samples into primary and secondary categories based on textural criteria. Primary ilmenite occurred as discrete homogeneous grains, and secondary ilmenite occurred as lamellae or blebs in or around Fe-(Ti)-oxides, such as magnetite.

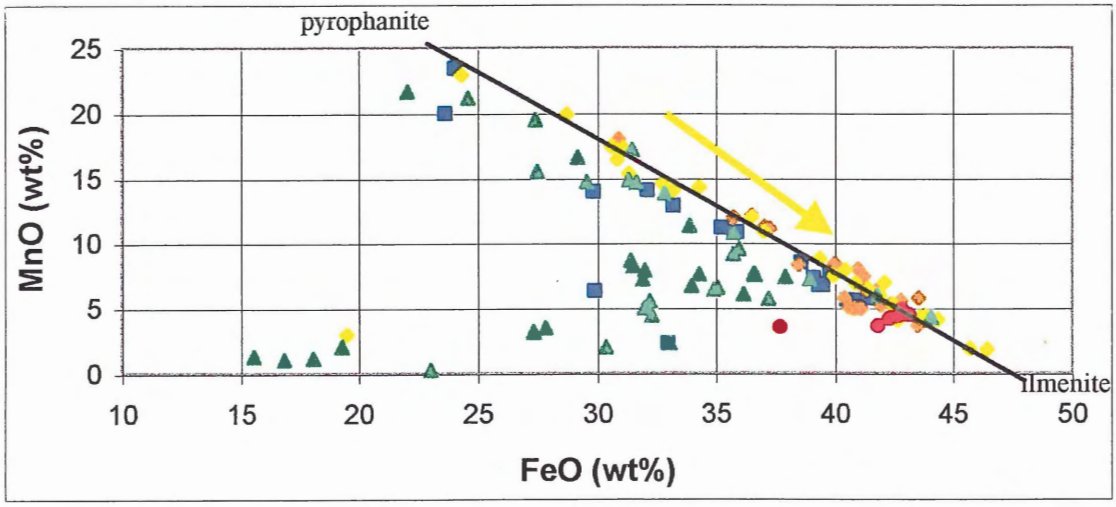

Figure 5.2a: FeO-MnO relations in the SMB ilmenites. Note the most differentiated samples towards the bottom of the trend line. The cause of preferential removal of Bin 2 ilmenites from the trend line is most likely a result of the leaching of Mn and Fe from these samples.

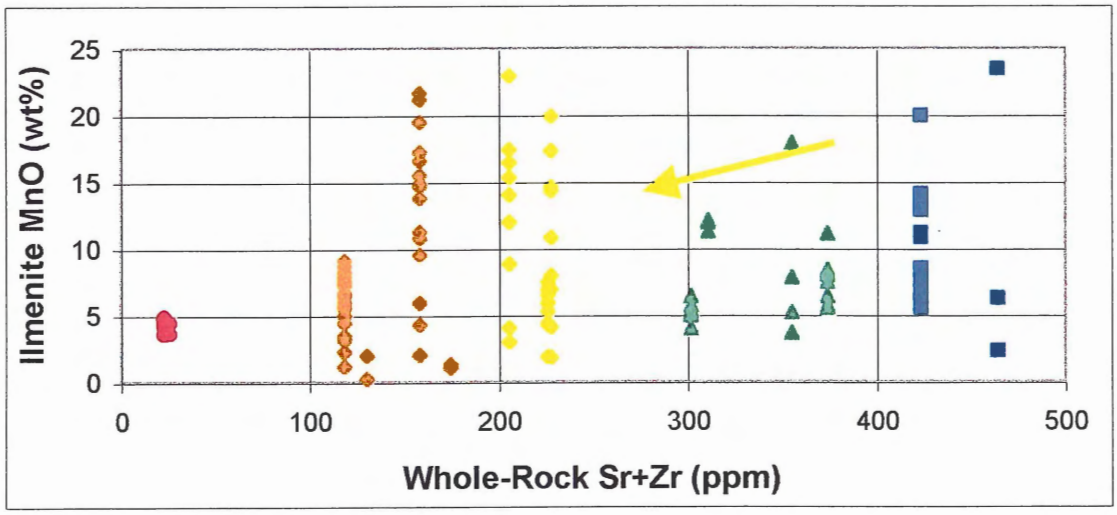

Figure 5.2b: Ilmenite MnO contents as a function of evolution of the SMB. Each sample chosen was based on these same x-axis values, and therefore plot as stacks of data. In any one sample the concentrations of manganese in ilmenite can range from 3 to 24%.

5.3 Rutile

5.3.1 Rutile crystal morphology

Table 4.3 presents several of the rutile grain shapes that occur within the South Mountain Batholith. Euhedral grains account for 20% of the rutile shapes, whereas anhedral shapes occur in 40% of the grains. Subhedral shapes account for the remaining 40% of the rutile grains. Anhedral and subhedral grain shapes occur over the entire range of the evolution of the South Mountain Batholith. The euhedral grains, however, are more likely to occur in the later stages of evolution.

The euhedral grains are included in biotite or muscovite, or they occur along grain boundaries. These grain shapes appear to be the result of undisturbed crystal growth in the melt and, therefore, probably have a primary magmatic origin.

As with the ilmenites, the subhedral-anhedral rutile grain shapes have several possible origins:

Primary Magmatic:

A: The same physical interactions occur with the euhedral rutile grains, as previously noted for the euhedral ilmenite grains. Crystal interference at the final stages of crystallization resulted in the interstitial development of subhedral-anhedral grains. Some of these primary magmatic grains exhibit oscillatory zoning (Fig. 4.2 a), similar to the niobian rutiles from Ilmen Mountain, Russia (Cerny and Chapman 2001). Oscillatory-zoning in these primary rutile grains may be caused by growth in a system during varying P-T-X conditions.

B: The South Mountain Batholith appears to have been saturated in rutile throughout its crystallization history, just as it was saturated in ilmenite. Primary rutile occurs in every Bin and therefore throughout the crystallization history; therefore, the melt never left the ilmenite-rutile cotectic, and no resorption occurred.

C: Conditions for significant undercooling normally do not occur in plutonic environments, and the rutile grains do not exhibit skeletal or quenched textures; therefore, the anhedral shapes are probably not the result of rapid growth.

Non-magmatic:

A: Inclusions of rutile occur within 25% of the ilmenite grains in the Meguma Supergroup (Haysom et al. 1997), whereas rutile is included in 10% of the ilmenite grains from the South Mountain Batholith. The incorporation of xenocrysts from the nearby Meguma Supergroup may have occurred, as noted for the partial resorption of the xenocrystic ilmenite grains. Three possible origins for rutile grains within ilmenite are as follows:

- the ilmenite grains with rutile inclusions originated in the Meguma Supergroup and were emplaced in the SMB by stoping;
- the ilmenite grains are xenolithic, and subsequently altered within the SMB resulting in the rutile inclusions; or
- the ilmenite grains are primary magmatic, originated in the SMB, and are altered by late stage hydrothermal alteration.

B: Anhedral rutile could be the result of the hydrothermal alteration of biotite. Shaw and Penczak (1996) noted that octahedrally coordinated Ti^{4+} is readily incorporated into the structure of biotite. If biotite, which in the case of the South Mountain Batholith is rich is Ti, is hydrothermally altered, chlorite forms (Mueller 1966). Chlorite, however, has no cation site that can readily accept Ti^{4+}, therefore; rutile forms as a byproduct of this reaction (Bhattacharyya 1965). Using data from natural minerals in the SMB (sample A16-1238), a possible chemical reaction is as follows:

$$2K_{1.9}Na_{0.1}(Mg_{1.5}Fe_{2.8}Al_{0.7}Ti_{0.5})(OH)_4 + 6H_2O \rightarrow$$

titaniferous biotite

$$TiO_2 + (Mg_{3.3}Fe_{5.3}Mn_{0.3}Al_{2.9})(OH)_{16} + K + Na\ (aq)$$

rutile chlorite

In addition to this reaction, rutile may also be the product of the hydrothermal alteration of ilmenite (Southwick 1968). As noted by Waerenborgh et al. (2002), ilmenite in the Beja-Acebuches Ophiolite Complex (SE Portugal) broke down via oxidation resulting in the formation of Ti-hematite and rutile. Sakoma and Martin (2002) also noted that altered grains of ilmenite contain Fe-oxide with patches of rutile in the Tibchi granite, exposed at Kalato, in the Tibchi ring-complex, northern Nigeria. In addition, Ramdohr

and Cevales (1980) documented the replacement of ilmenite by rutile via hydrothermal processes, in granitic pegmatites in Adamello, Italy by the following oxidation reaction:

$$2FeTiO_3 + {}^1/_2O_2 = Fe_2O_3 + 2TiO_2$$

ilmenite hematite rutile

C: Exsolution may account for the origin of the grains of rutile included in ilmenite. However, no known significant $(Fe,Mn)TiO_3$-TiO_2 solid solution exists (Fig. 5. 3); therefore, there can be no low temperature exsolution to produce these multi-phase grains.

The euhedral grains may, therefore, be the result of unrestricted growth in the melt (Type 1). Some subhedral-anhedral grains may be space filling, whereas others probably occur as a product of the hydrothermal alteration of biotite (Type 2). Finally, the rutile grains that occur within grains of ilmenite appear to be xenocrystic grains originating in the Meguma Supergroup, and/or the product of hydrothermal alteration of ilmenite (Type 3).

Three general categories separate the chemical composition of the rutile grains that are based on the types given earlier. Type 1 rutile grains are primary magmatic and have concentrations ranging from 0.20 to 8.11 wt% Nb_2O_5, and from 0.02 to 2.60 wt% Ta_2O_5. Type 2 rutile grains are the product of the breakdown of biotite during hydrothermal alteration and have the lowest concentrations of Nb_2O_5 (0.07-2.00 wt%), and Ta_2O_5 (0.01-1.25 wt%). The origin of Type 3 rutile grains may be from the hydrothermal alteration of ilmenite, and/or they may have come from xenocrystic material derived from the Meguma country rocks. The concentrations of Nb_2O_5 (0.25-0.91 wt%), and Ta_2O_5 (0.03-0.24 wt%), are moderate compared to Type 1, and Type 2 rutiles (Fig. 5.4). The concentrations of niobium and tantalum within the three different Types of rutile are those measured, and not necessarily a good discriminator of Type.

5.3.2 Rutile chemical substitutions

Rutile belongs to the tetragonal crystal system, and the titanium is in octahedral coordination (Fig. 5.5). Niobium (143 pm) or tantalum (143 pm) replaces titanium (145 pm) (Fig 3.4) (www.webelements.com), plus one vacany in order to achieve electrostatic balance in the following exchange reaction: $5Ti^{4+} \rightarrow 4(Nb,Ta)^{5+} + \square$, where

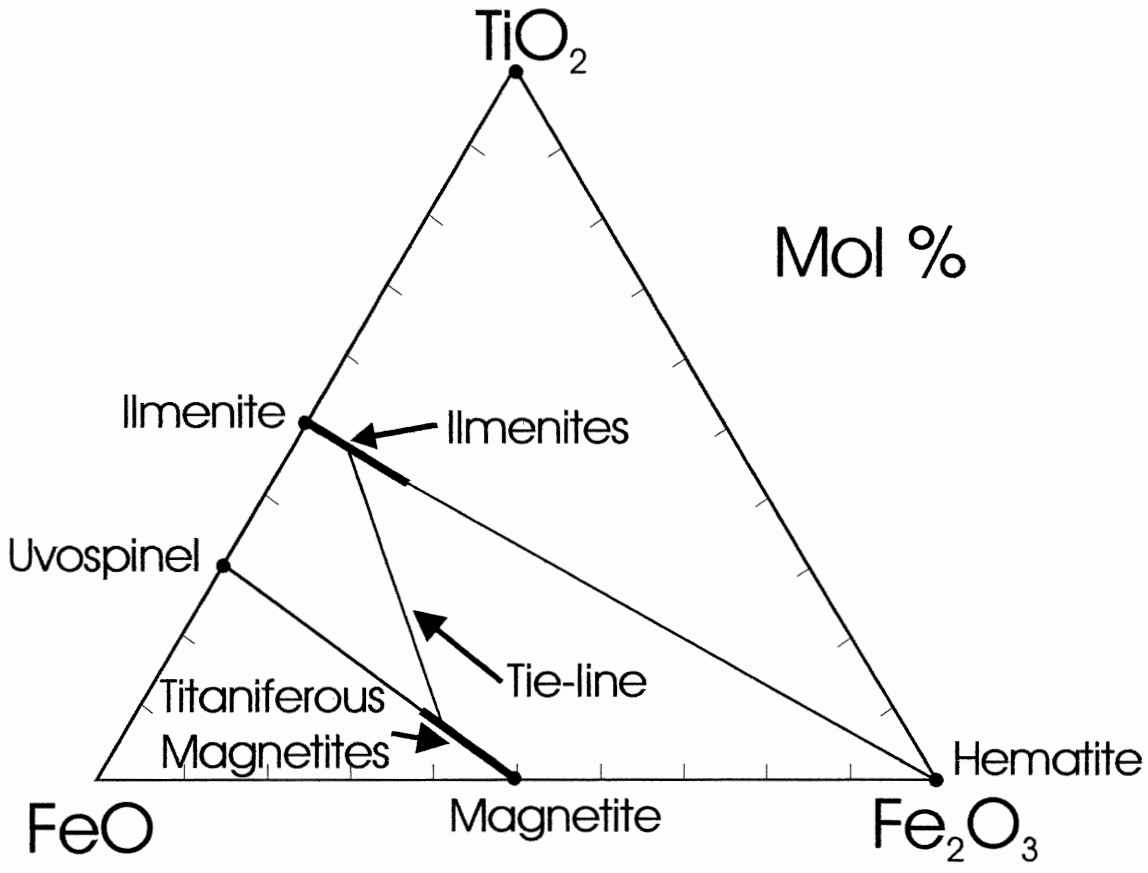

Figure 5.3: Triangular TiO_2-FeO-Fe_2O_3 diagram. This diagram illustrates the relationship between ilmenite and rutile. There is no known solid-solution between these minerals; therefore, rutile is not likely to occur as exsolution in ilmenite grains (Waerenborgh et al. 2002).

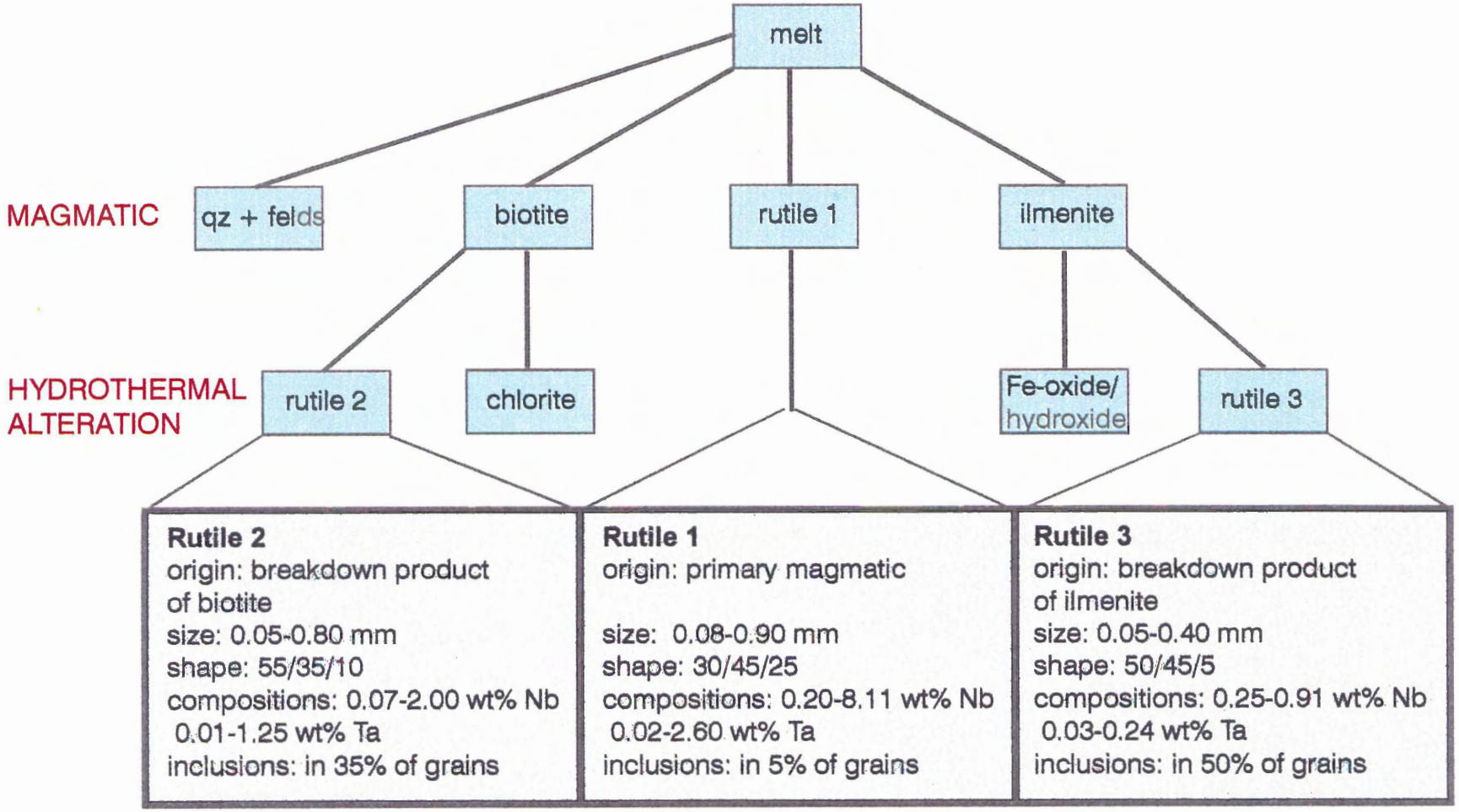

Figure 5.4: Flowchart of rutile formation. Three types of rutile occur in the SMB. Type 1 rutile has a primary magmatic origin. Type 2 rutile is the product of the breakdown of biotite during hydrothermal alteration. Type 3 rutile is the product of the breakdown of ilmenite also during hydrothermal alteration either from primary SMB ilmenite grains or from xenolithic ilmenite grains that were altered within the Meguma Supergroup prior to incorporation into the melt.

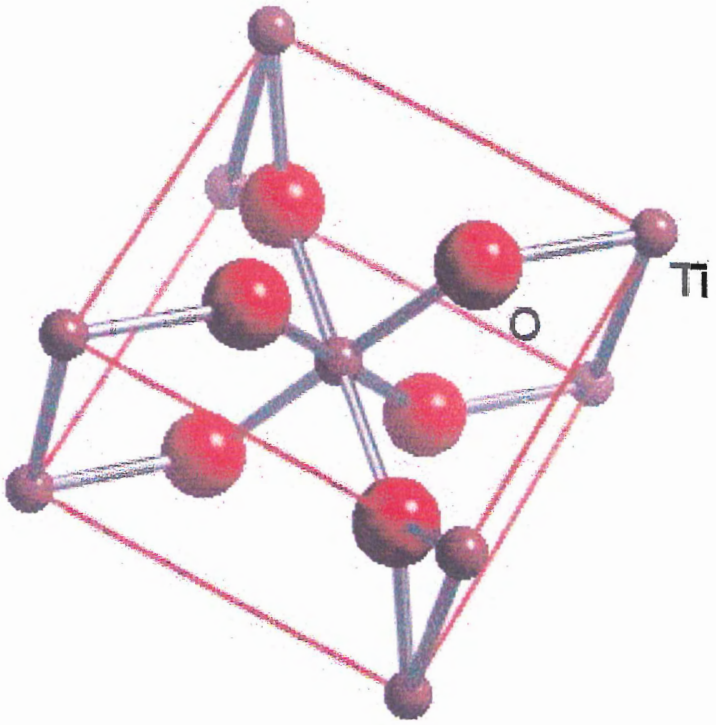

Figure 5.5: Rutile crystal lattice. Titanium is in octahedral coordination in each of the smaller sites. Nb^{5+} or Ta^{5+} replaces Ti^{4+} resulting in one vacancy in order to achieve electrostatic balance.

□ represents one octahedral vacancy. Hanson et al. (1998) noted a similar relationship between Ti and Nb and Ta, suggesting either Nb or Ta may substitute for Ti when it is in octahedral coordination.

5.3.4 Rutile compositional variation diagrams

Figure 5.6 (a) shows the substitution of niobium or tantalum oxides for titanium in the rutile grains during the fractionation of the batholith. The line shown on the plot represents compositions produced by the $5Ti^{4+} \rightarrow 4(Nb,Ta)^{5+} + \square$ substitution. The analyses from the least evolved rocks, shown in blue, concentrate towards the lower right side of the cluster, where the TiO_2 wt% totals are closest to 100. The most evolved rocks are shown in red and have the highest concentrations of $Nb_2O_5+Ta_2O_5$ wt%. Several analyses, also belonging to the higher bins, lie off of the trend line, as a result of an increase of iron concentrations in these rutiles (Horng et al. 1999), with only a few exceptions.

Figure 5.6 (b) shows a similar trend to that of the ilmenite grains (Fig 5.2b), except in this case the plot shows niobium plus tantalum metal concentrations. The maximum variation of Nb+Ta within a single grain is from 1.8 to 2.6%, whereas within a given sample the largest variation is from 0.5 to 5.0%. The South Mountain Batholith, as a whole, has a maximum whole-rock Nb+Ta variation from 0.1 to 42.2 ppm.

Figure 5.6 (c) shows the relationship between niobium and tantalum during the evolution of the batholith. In the later stages of evolution of the batholith, the totals of both niobium and tantalum in rutile increase up to 3.4 wt%, and 2.1 wt% respectively. The two lines on the plot represent ratios of Nb/Ta=1, and Nb/Ta=4. The least evolved samples plot close to the origin of the graph, because at this stage Nb and Ta behave similarly in the melt. The most evolved rocks are those that experience the most decoupling, which must be some function of temperature, pressure, and geochemical conditions including H_2O saturation, oxygen fugacity, and pH levels (Cawthorn 1983).

Figure 5.6 (d) shows similar characteristics to the plots used for sample selection. As the total niobium and tantalum increases, the ratio of niobium to tantalum appears to decrease as well. Figure 5.6 (c) shows an increase of niobium and tantalum over the evolution of the batholith and, therefore, the decrease of the ratio of niobium to tantalum

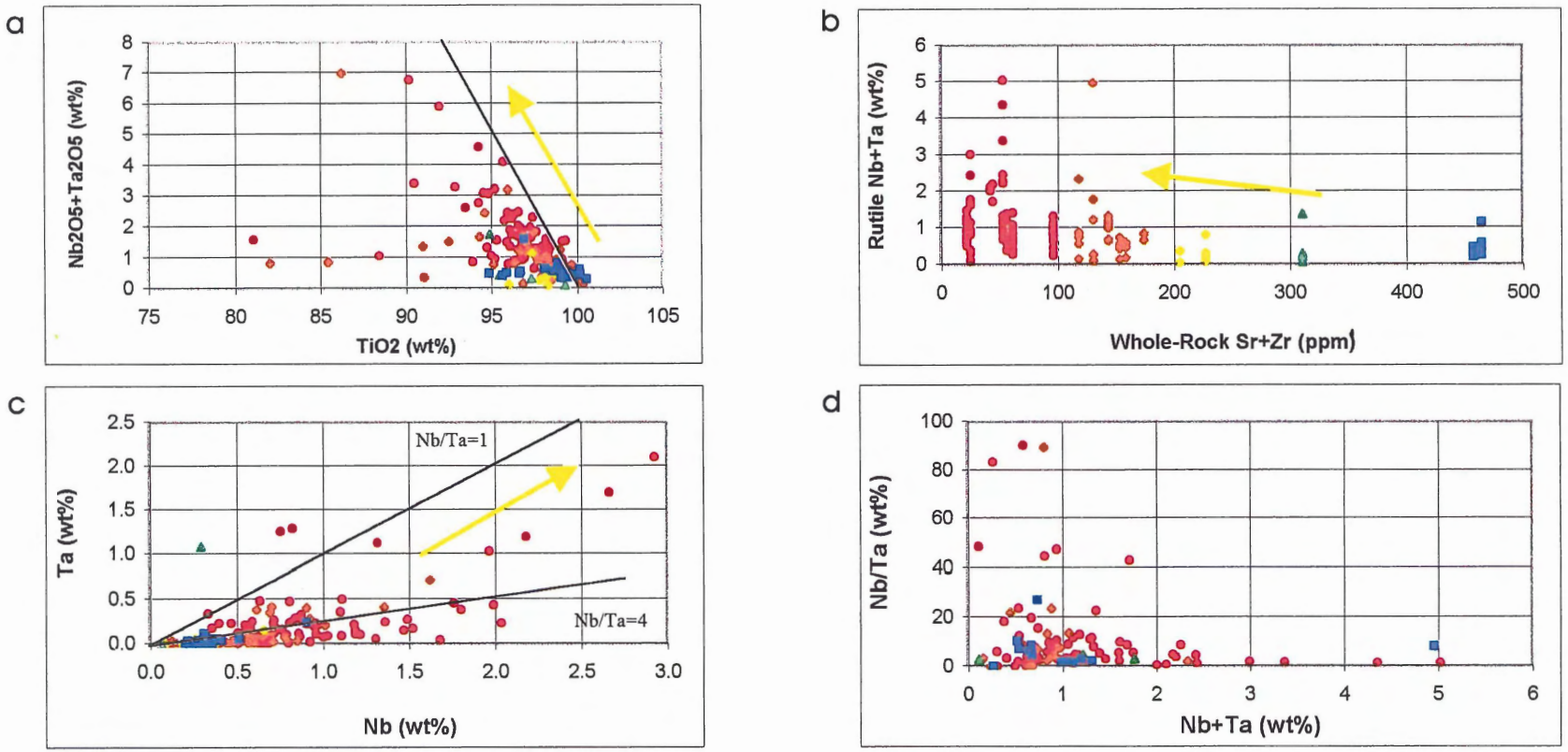

Figure 5.6: Rutile plots.

a) Replacements of niobium or tantalum for titanium in the rutile grains. The more evolved samples (red) are those which have higher concentrations of niobium and tantalum.

b) This plot shows a similar trend to that of the ilmenite grains, except in this case there are niobium and tantalum totals of between 0.1 and 5.0 within the same sample, also note that there are very few rutile grains in the early history of the batholith.

c) The decoupling of niobium and tantalum is some function of temperature, pressure and geochemical conditions, and is more pronounced in the later stages of evolution.

d) As the total niobium and tantalum decreases in the rutile grains, the ratio of niobium to tantalum appears to increase, the same characteristic shown on the sample distribution plots seen in Chapter 2.

does not appear to be the result of low Ta values. As on the other plots the most evolved rocks are the points that have the highest concentrations of Nb and Ta, and the greatest amount of decoupling of these two elements.

5.4 Evolution of titanium minerals in the batholith

The ratio of rutile/(rutile+ilmenite) illustrates the modal abundances of these minerals in the batholith in Table 4.1 and Figure 5.7 (a). During the crystallization history of the batholith the relative modal abundance of rutile increases, whereas the relative modal abundance of ilmenite decreases.

In the early stages of the evolution of the batholith, when Fe+Mn concentrations are high and Nb+Ta concentrations are low, the Ti available in the melt forms ilmenite (Fig 5.7 b). In the later stages of crystallization when Fe+Mn concentrations are low, and Nb+Ta concentrations are relatively high, Ti forms rutile (Fig. 5.7 c).

5.5 Niobium and Tantalum variations within the SMB and other granites

In Section 3.2, sample distribution plots show the relationship between Nb and Ta in the SMB. Bins 1 through 5, created arbitrarily by dividing the totals of whole-rock Sr+Zr (ppm) into 5 equal parts, illustrate fractionation over the chemical evolution of the batholith. Figure 3.2 shows whole-rock Sr+Zr versus whole-rock Nb+Ta. In the later stages of evolution of the batholith, the totals of niobium and tantalum can become very high in some rocks (48 ppm), and very low in others (1 ppm). Figure 3.3 has the same x-axis values, but better illustrates the concept of fractionation. As the batholith becomes more fractionated the ratio of whole-rock Nb/Ta (ppm) decreases (also noted by Dostal and Chatterjee 2000), and some ratios become very high (34).

Mineral fractionation can account for evolutionary trends in major, trace elements, and REEs in the SMB (Tate and Clarke 1997). Linnen and Keppler (1997) determined that the solubility of MnO, Nb_2O_5, and Ta_2O_5 increases slightly with aluminum content in peraluminous granites, and peraluminous granites have decreasing ratios of Nb/Ta with increasing fractionation. As previously discussed in Section 3.2, niobium and tantalum are identical in ionic charge and ionic size. Figure 5.6 (c) shows that, despite their geochemical similarities, Nb and Ta fractionate relative to one another

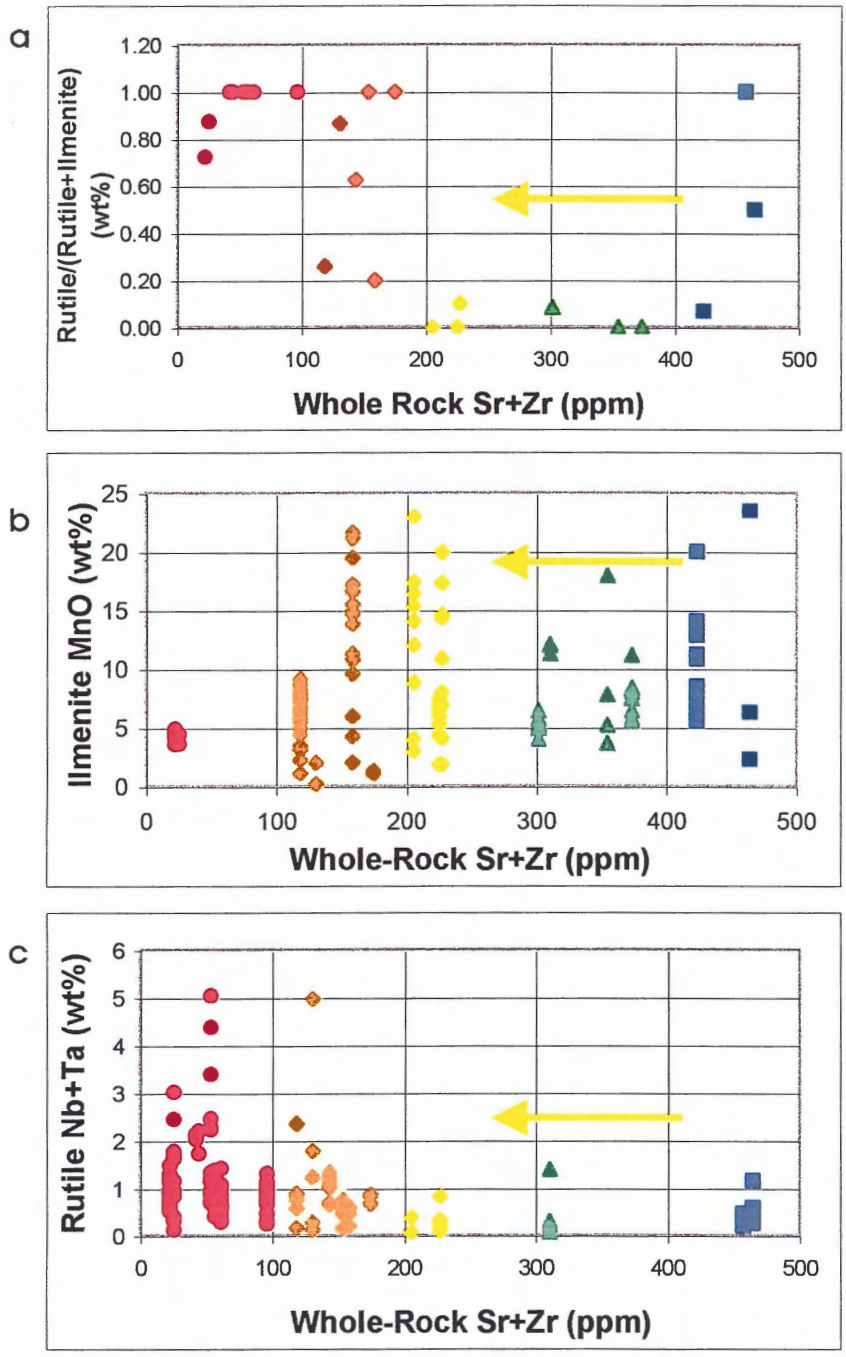

Figure 5.7: Evolution of titanium minerals in the batholith. Plot (a) shows the estimated modal abundances of ilmenite and rutile over the crystallization history of the SMB. Plot (b) illustrates all the grains of ilmenite data analyzed, and (c) illustrates all the rutile grains analyzed.

at late stages of crystallization of the batholith. Dostal and Chatterjee (2000) discussed the contrasting behaviour of Nb/Ta in the South Mountain Batholith, and stated that although these elements exhibit similar behaviour in the granitic melt, the ratios of Nb/Ta vary significantly in the continental crust (Green 1995). The ratio of Nb/Ta has a positive correlation with Ti, Zr, and Ba, and Dostal and Chatterjee (2000) suggest that this relationship is a result of fractional crystallization involving both major and accessory phases (Uher et al. 1998; Tindle and Breaks 1998).

Novak and Cerny (1998) noted decreasing Nb/Ta ratios in the niobium-tantalum oxide minerals from complex granitic pegmatites in the Moldanubicum, Czech Republic. Primary phases in the Moldanubicum pegmatites have the same Nb and Ta proportions as the secondary replacement phases (Novak and Cerny 1998), and some of the secondary rutile in the SMB also has notable concentrations of Nb and Ta. Cerny et al. (1998) noted the same correlation between primary and secondary phases, in titanian ixiolite and titanian columbite-tantalite. Green (1995) stated that variations in Nb/Ta may indicate crystal / melt fractionation for Ti-rich minerals, and in some more varied cases the ratio may be an important indicator of fluid-related fractionation processes. Linnen and Keppler (1997) disagreed with Green (1995) and explained there is no need to invoke fluid phase fractionation to explain the low Nb/Ta in some granitic rocks. It is only necessary to fractionate a small amount of rutile (Nb/Ta > melt) to decrease the Nb/Ta in the remaining melt, to create the decrease in the trend line in Figure 3.3. The trend line in Figure 3.2 shows no strong fractionation of niobium and tantalum, except where late stage fluids are important. Therefore, this increase in Nb+Ta need not necessarily mean a mineral deposit is near, as totals would need to be significantly higher. Delayed fractionation of Ta over Nb was noted by Abdalla et al. (1998), in the columbite-tantalite-bearing granitoids of the Eastern Desert province of Egypt, and Linnen and Keppler (1997) stated that melt compositions control the solubility of columbite or tantalite, as well as the fractionation of Nb/Ta and Fe/Mn (Aurisicchio et al. 2002).

Cerny (1986) noted similar characteristics of ilmenite to those in the SMB, and Green (1995) stated that ilmenite in gabbros controls the ratio of Nb/Ta because it fractionates these elements. In addition, rutile can play a major role in the behaviour of Nb and Ta (Linnen and Keppler 1997), who also noted the partitioning of Nb and Ta

between rutile and the silicate melt in the final stages of magmatic crystallization agreed with Logothetis (1984) who stated that late stage rutile resulted in the enrichment of Nb and Ta in the SMB.

5.6 South Mountain Batholith mineral deposits

During the crystallization of the batholith, every element eventually finds a place within a mineral. For reasons of ionic size and/or charge, incompatible elements do not have suitable mineral hosts early in the crystallization and, therefore, become concentrated in the remaining melt. These elements create the more chemically exotic minerals occurring in the last stages of crystallization. Within the Tibchi granite in northern Nigeria, the ilmenite is enriched in Mn, Nb, and Ta, and contributes to the economic potential of the area (Sakoma and Martin 2002). Fractional crystallization in the Yichun granite complex (SE China) resulted in a moderate increase of Ta/(Ta+Nb) ratios and a strong increase of Mn/(Mn+Fe) ratios within the granites (Belkasmi et al. 2000). Logothetis (1984) described the behaviour of tantalum during magmatic differentiation, where Ta tends to concentrate in independent minerals in pegmatites, aplites, and greisens. Within the SMB, the concentrations of Ta range from 2 ppm in granodiorites, up to 7 ppm in leucomonzogranites, increasing with differentiation (Logothetis 1984). MacDonald (2001) described the mineral deposits in the SMB, and concluded that mineral deposits enriched in Rb, Cs, Li, Nb, Ta, Sn, W, U, and F are most likely to occur in muscovite-topaz leucogranite, and in leucomonzogranite. Both greisen- and pegmatite-type mineral deposits occur in leucomonzogranites and leucogranites, whereas breccia-type deposits occur in leucomonzogranites. Vein-type mineral deposits are most likely to occur in biotite monzogranite or biotite granodiorite (MacDonald 2001).

Within the South Mountain Batholith, several mineral deposits containing significant niobium and tantalum concentrations occur. Table 5.1 shows several analyses of the samples taken from these mineral deposits (O'Reilly 2001). Niobium-tantalum oxides are excellent indicators of chemical evolution and fractionation (Tindle and Breaks 1998).

Table 5.1: Ta Mineral Deposit, Keddy-Lantz Mo-Nb-Ta Pegmatite, New Ross (O'Reilly 2001)

Sample #	Grain	TiO_2	FeO	MnO	WO_3	Ta_2O_5	Nb_2O_5	Nb:Ta	Total	Comments
A9C-7508	1	2.87	15.53	3.19	2.48	18.17	56.49	3.11	98.73	Tantalite?
	2	3.24	15.30	3.15	2.31	19.19	55.29	2.88	98.48	
	3	1.59	15.94	3.35	2.86	11.74	54.44	4.64	89.92	
A9C-7514	1	3.26	15.70	3.19	2.66	15.20	56.54	3.72	96.55	Tantalite?
	2	1.17	13.40	3.97	1.45	11.52	38.25	3.32	69.76	
A9C-7517	1	Silicate interference of a Nb-Ta mineral (Nb:Ta = 1.58:1)						1.58		Tantalite?
	2	2.20	13.97	2.51	1.72	12.87	44.69	3.47	77.96	
	3	Silicate interference of a Nb-Ta mineral (Nb:Ta = 1.79:1)						1.79		
A9C-7516	1	1.77	12.92	2.59	2.16	37.87	36.27	0.96	93.58	Tantalite?
	2	Silicate interference of a Nb-Ta mineral (Nb:Ta = 2.80:1)						2.8		
	3	1.85	15.77	3.06	2.37	19.23	51.30	2.67	93.58	
A9C-7509	1	1.25	14.79	2.55	2.77	19.92	55.36	2.78	96.64	Unknown mineral
	2	Analysis failed.								
	3	0.82	14.21	4.13	N.D.	16.93	51.39	3.04	87.48	
	4	3.39	15.82	3.00	4.45	14.99	57.80	3.86	99.45	
	5	6.17	10.85	2.35	2.20	20.05	52.02	2.59	93.64	
A9C-7518	1	Silicate interference of a Nb-Ta mineral (Nb:Ta = 2.94:1)						2.94		Tantalite?
	2	0.66	14.98	3.75	2.02	16.07	52.28	3.25	89.76	
	3	Silicate interference of a Nb-Ta mineral (Nb:Ta = 4.45:1)						4.45		
A9C-7521	1	Silicate interference of a Nb-Ta mineral (Nb:Ta = 2.54:1)						2.54		Large amblygonite?
	2	Silicate interference of a Nb-Ta mineral (Nb:Ta = 2.42:1)						2.42		
	3	Silicate interference of a Nb-Ta mineral (Nb:Ta = 4.13:1)						4.13		
	4	Silicate interference of a Nb-Ta mineral (Nb:Ta = 2.23:1)						2.23		

To date, only greisen- and vein-type deposits have proven to be economically viable, however, exploration including the other types of deposits appears promising for future exploration (MacDonald 2001). The trends discovered in this study may allow for further study of rutile in the SMB. A sample containing elevated levels of Nb and Ta may indicate proximity to niobium and tantalum deposits.

5.7 Shubenacadie Ti-sands

In the near future, attempts will be made to remove titanium from the sands in the Shubenacadie River in central Nova Scotia. A junior mining company is in the process of completing a $700,000 pilot project, in hopes of finding the most environmentally conscientious method of removing the titanium-bearing heavy mineral sands from the 114 km long river.

Ilmenite and magnetite are the principal mineralogical hosts for the titanium within the Ti-rich sands. Table 5.2 shows several analyses of ilmenite grains collected from the river, approximately 100 meters south (upstream) of the South Maitland Bridge.

Comparisons of mineral assemblages from each possible source are as follows:

- Shubenacadie River: ilmenite (Mn absent), magnetite, titanomagnetite, rutile, zircon, pyrite
- South Mountain Batholith: ilmenite/pyrophanite, rutile
- North Mountain Basalt: ilmenite (Mn absent), titanomagnetite, rutile
- Meguma Supergroup: ilmenite (with Mn), rutile

Comparison of ilmenite only from three surrounding areas (Fig. 2.1) permits determination of the source of this potentially economically viable titanium deposit. Appendix A contains chemical analyses of ilmenite grains from the South Mountain Batholith. Table 5.3 presents chemical analyses of ilmenite grains from the North Mountain Basalt. Finally, Table 5.4 presents the chemical analyses of ilmenite from the Meguma Supergroup. Table 5.5 presents the similarities and differences among the ilmenite grains from the three possible sources, and Figure 5.8 shows backscattered electron images of representative oxide minerals from each possible source with the exception of the SMB (Fig. 4.1).

Table 5.2: Representative electron microprobe analyses of oxides from the Shubenacadie River

Sample #	TiO_2	FeO_t	Al_2O_3	MnO	Total
1	0.08	93.47	0.06	0.10	93.80
2	53.82	33.06	0.04	6.60	93.68
3	53.51	35.90	0.04	4.09	93.91
4	0.27	93.56	0.06	0.00	93.88
5	49.68	46.42	0.01	3.48	99.71
6	48.87	48.31	0.00	3.09	100.35
7	0.08	92.39	0.04	0.07	92.64
8	51.97	27.32	0.11	12.63	92.52
9	49.44	49.64	0.01	1.74	100.99
10	51.53	41.86	0.13	0.64	94.64

Table 5.3: Representative electron microprobe analyses of oxides from the North Mountain Basalt (Kontak and Dostal 1992)

Sample #	TiO_2	FeO_t	Al_2O_3	MnO	Total
ZL-2001-3c	21.46	67.02	1.05	2.63	93.20
ZL-2001-3c	17.93	69.51	1.36	2.25	91.69
ZL-2001-43	26.53	62.64	1.73	1.04	92.62
ZL-2001-43	26.18	61.17	1.74	0.91	91.46
ZL-2001-44	26.79	63.01	1.86	1.19	93.65
ZL-2001-44	27.28	60.41	1.89	1.02	91.34
ZL-2001-45	26.93	63.07	1.91	0.90	93.31
ZL-2001-45	24.08	64.21	1.90	0.95	93.06
ZL-2001-3	23.26	67.03	1.14	0.60	92.60
ZL-2001-3	23.23	66.48	1.18	1.08	92.43
ZL-2001-3e	23.26	67.02	1.13	0.59	92.26
ZL-2001-3e	23.22	66.48	1.18	1.08	92.10
ZL-2001-1B	26.98	64.49	1.08	1.96	94.51
ZL-2001-1B	27.66	62.17	1.27	2.07	93.16
ZL-2001-47	53.19	35.97	0.17	0.99	95.97
ZL-2001-47	16.10	71.29	2.77	0.58	91.76
ZL-2000-A	23.28	67.21	0.85	2.05	93.44
ZL-2000-A	24.71	64.22	0.72	2.21	91.92
ZL-2001-35D	24.79	64.04	1.69	1.17	91.70
ZL-2001-35D	27.02	63.08	1.83	1.34	93.27

Table 5.4: Representative electron microprobe analyses of ilmenite from the Meguma Supergroup (Haysom et al. 1997)

Sample #	SiO_2	TiO_2	FeO_t	MnO	Total
MS1030	0.13	52.67	29.87	16.62	99.29
MS1030	0.14	52.87	26.45	20.49	99.95
MS1023	0.24	51.92	38.54	7.68	98.38
MS1029	-	52.94	41.71	5.33	99.98
MS1019	0.35	52.04	34.87	11.64	98.90
MS1014b	0.26	51.13	33.86	14.17	99.42

Table 5.5: Comparison of possible sources of Ti in sands

Characteristic	SR	MSG	SMB	NMB
Ilmenite:Rutile:Magnetite	15:10:75	>80:15:<5	80:20:00	30:15:55
Mn content in ilmenite	0.6-12.6%	5-20%	2-25%	0.6-2.6%
Rutile Nb_2O_5	0.2-1.32%	no rutile analyzed	0.01-3% (avg 1.8%)	no rutile analyzed
Rutile Ta_2O_5	no Ta detected	no rutile analyzed	0.01-1.15% (avg 0.6%)	no rutile analyzed
Magnetite TiO_2	15-28%	no Ti detected	magnetite absent	25-30%
Grain Size (elongate)	0.4-2 mm	0.5-5 mm	0.3-2.0 mm	0.5-4 mm
Characteristics of Grains	inclusions (Fe,Si), exsolution (ilm,mt)	inclusions(?)	inclusions (Fe,Si),	inclusions (?), exsolution (ilm,mt)

Legend

SR = Shubenacadie River

SMB = South Mountain Batholith

NMB = North Mountain Basalt (Kontak and Dostal 1992)

MSG = Meguma Supergroup (Haysom et al. 1997)

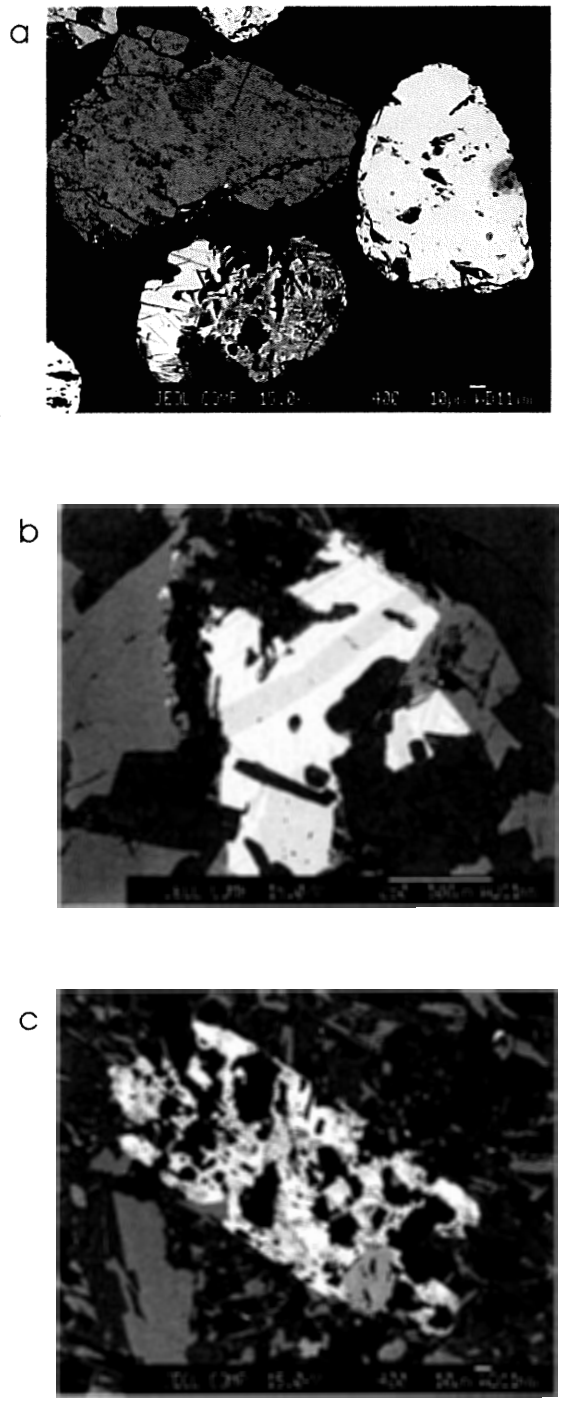

Figure 5.8: Oxide grains from possible sources of the Ti in the Shubenacadie River.
a) Titanomagnetite and magnetite sand grains from the Shubenacadie River,
b) Titanomagnetite with ilmenite exsolution from the North Mountain Basalt,
c) Altered, fractured, Mn-ilmenite grain occurring with rutile and sphene, from the Meguma Supergroup.

Based on comparison of mineral assemblages, the source of the titanium is most likely the North Mountain Basalt because of the presence of Mn-poor ilmenite, and titanomagnetite. However, based on ilmenite compositions the most likely source appears to be a combination of several of the possible sources. A more detailed study is needed to definitively determine the source.

5.8 Summary

The grain shapes and chemical compositions of the ilmenite and rutile permit several conclusions regarding the fractionation of the South Mountain Batholith. Plots created from the chemical data collected from the electron microprobe give us further information that is not necessarily visible in thin section. New information regarding the oxide minerals in the SMB includes the following:

- Ilmenite is in solid solution with pyrophanite and the grains are chemically zoned with manganese-enriched rims. These relationships suggest disequilibrium crystallization, and a strong fractionation of manganese and iron between the melt and the ilmenite grains;
- Type 1 rutile grain shapes and compositions suggest primary magmatic origin. Some of these grains exhibit zoning and have niobium and tantalum enriched rims. These rutile grains occur as relatively larger discrete grains of all shapes, which have no inclusions, and the highest concentrations of niobium and tantalum. Oscillatory zoning in these grains is a result of growth within a system during varying P-T-X conditions.
- Type 2 rutile grain shapes and compositions suggest they are the product of the hydrothermal alteration of biotite. These rutile grains occur as relatively medium-sized inclusions in biotite. Some grains have inclusions, most are anhedral, and have low concentrations of niobium and tantalum.
- Type 3 rutile grain shapes and compositions suggest they are the product of the hydrothermal alteration of ilmenite. These rutile grains occur as relatively small grains associated with ilmenite. Most grains have inclusions, are anhedral, and have moderate concentrations of niobium and tantalum.

- In the early stages of evolution of the SMB ilmenite ties up most of the titanium available in the melt, whereas late in the crystallization history rutile sequesters most of the titanium available and acts as a host to niobium and tantalum.

CHAPTER 6: CONCLUSIONS

6.1 Conclusions

6.1.1 Ilmenite

The grain shapes of most ilmenites in the SMB suggest a primary magmatic origin, whereas other ilmenite grains could have a xenocrystic origin, originally formed in the Meguma Supergroup. Blocks of the Meguma country rock broke off and dropped into the granitic melt, and the stoped block became either partially, or fully assimilated into the melt. Manganese replaces iron in ilmenite grains, most of which have manganese-enriched rims, and some grains are depleted in manganese and iron possibly as a result of leaching. And finally, the iron-manganese zoning suggests disequilibrium crystallization, and strong fractionation of manganese and iron between the melt and the ilmenite grains.

6.1.2 Rutile

Three types of rutile occur in the South Mountain Batholith. Type 1 rutiles have a primary magmatic origin, occur as discrete grains of all shapes with no inclusions, have the highest concentrations of niobium and tantalum, and occur in every Bin. Type 2 rutiles are the product of the hydrothermal alteration of biotite. These anhedral or acicular rutile grains have moderate concentrations of niobium and tantalum, occur within grains of biotite, are associated with chlorite, and have moderate numbers of inclusions. Type 3 rutiles are the product of the breakdown of ilmenite and, therefore, occur within grains of ilmenite. These rutile grains have the lowest concentrations of niobium and tantalum, are mostly anhedral, and have inclusions in approximately 50% of the grains. Type 3 rutile grains may have a xenocrystic origin, just as the ilmenite may have originated in the Meguma.

6.1.3 General conclusions

Rutile, and to some extent ilmenite, are good indicator minerals of chemical evolution of the South Mountain Batholith. Highly variable niobium to tantalum ratios in rutile illustrates fractionation of niobium relative to tantalum. In the early stages of the evolution of the batholith, ilmenite ties up most of the titanium available in the melt,

whereas in the later stages rutile sequesters most of the titanium available and acts as a host to niobium and tantalum. Analyses of unknown rutile and ilmenite from the SMB could be plotted on graphs similar to those in Chapter 2 and Chapter 5. This comparison could potentially lead to the discovery of new niobium-tantalum deposits, by indicating the stage at which the unknown rutile or ilmenite crystallized, and subsequently their proximity to the most fractionated rocks, where mineral deposits are most likely to occur.

6.2 Recommendation for future work

In order to resolve several problems arising from this project further work may be required. Issues that should be addressed include the following:

- examine the possibility of two trends in the data on Figure 3.1;
- determine the rock types of each sample, and obtain sample location maps from the Department of Natural Resources; and
- obtain further analyses from the possible sources of the Ti-rich sands from the Shubenacadie River in order to definitively determine their source.

More chemical analyses might confirm trends in fractionation in the South Mountain Batholith. More thin sections could be cut of the samples that did not contain any oxide phases in hopes of finding more rutile and ilmenite to analyze. In most cases the samples chosen could be crushed, and mineral separation techniques could isolate the heavy fractions concentrating any oxide phases. Crushing, separation, and mounting could be an alternative method of sample preparation, possibly allowing for more oxide analyses. With this information, additional conclusions regarding the oxide phases may be possible.

REFERENCES

Abdalla H. M., Helba H. A., and Mohamed F. H. 1998. Chemistry of columbite-tantalite minerals in rare metal granitoids, Eastern Desert, Egypt. Mineralogical Magazine, 62; 6: 821-836.

Allan B.D., and Clarke D.B. 1981. Occurrence and origin of garnets in the South Mountain Batholith, Nova Scotia. Canadian Mineralogist, 19: 19-24.

Aurisicchio C., De-Vito C., Ferrini V., and Orlandi P. 2002. Nb and Ta oxide minerals in the Fonte del Prete granitic pegmatite dike, Island of Elba, Italy. The Canadian Mineralogist. 40; 3: 799-814.

Belkasmi M., Cuney M., Pollard P. J., and Bastoul A. 2000. Chemistry of the Ta-Nb-Sn-W oxide minerals from the Yichun rare metal granite (SE China); genetic implications and comparison with Moroccan and French Hercynian examples. Mineralogical Magazine. 64; 3(424): 507-523.

Bhattacharyya C. 1965. Genesis of some linear structures in mica from Gopannavalasa, Dt. Srikakulam, Andhra Pradesh. Quarterly Journal of the Geological, Mining and Metallurgical Society of India. 37; 4: 185.

Carruzzo S. 2003. Granite-Hosted Mineral Deposits of the New Ross Area, South Mountain Batholith, *in prep.* PhD. Thesis, Dalhousie University.

Cawthorn G. R. 1983. Magma addition and possible decoupling of major- and trace-element behaviour in the Bushveld Complex, South Africa. Chemical Geology. 39; 3-4: 335-345.

Cerny P. 1986. Exploration strategy and methods for pegmatite deposits of tantalum. *In*: Lanthanides, tantalum and niobium;: mineralogy, geochemistry, characteristics of primary ore deposits, prospecting, processing and applications. *Edited by*: Moeller P., Cerny P., and Saupe F. Special Publication of the Society for Geology Applied to Mineral Deposits. 7: 274-302.

Cerny P., and Chapman R. 2001. Exsolution and breakdown of scandian and tungstenian Nb-Ta-Ti-Fe-Mn phases in niobian rutile. The Canadian Mineralogist. 39; 1: 93-101.

Cerny P., Chapman R., Uher P., and Simmons W. B. 1998. Exsolution in niobian rutile; new processes and new phases. *In*: Quebec 1998; recueil des resumes; Carrefour des sciences de la terre--Quebec 1998; abstract volume; Crossroads of Earth sciences. Program with Abstracts - Geological Association of Canada; Mineralogical Association of Canada; Canadian Geophysical Union, Joint Annual Meeting. 23: A29.

Chatterjee A. K., and Strong D. F. 1985. Review of some chemical and mineralogical characteristics of granitoid rocks hosting Sn, W, U, Mo deposits in Newfoundland and Nova Scotia. *In*: High heat production (HHP) granites, hydrothermal circulation and ore genesis. *Chairperson*: Halls C. 489-516.

Clarke D. B. 1992. Granitoid Rocks. Topics in the Earth Sciences. *Series Editors:* van Andel T. H. *Publisher:* Chapman & Hall.

Clarke D. B., and Chatterjee A. K. 1985. Physical and chemical processes in the South Mountain Batholith. *In*: Granite-related mineral deposits; geology, petrogenesis and tectonic setting; extended abstracts of papers presented at the CIM conference. *Edited by*: Taylor R. P., and Strong D. F. 58-62.

Clarke D. B., and Muecke G. K. 1985. Review of the petrochemistry and origin of the South Mountain Batholith and associated plutons, Nova Scotia, Canada. *In*: High heat production (HHP) granites, hydrothermal circulation and ore genesis. *Chairperson*: Halls C. 41-54.

Clarke D. B., Henry A. S., and White M. A. 1998. Exploding xenoliths and the absence of "elephants' graveyards" in granite batholiths. *In*: Extraction, transport and emplacement of granitic magmas. *Edited by*: Benn K., Cruden A. R., Sawyer E. W., and Evans J. P. Journal of Structural Geology. 20; 9-10: 1325-1343.

Clarke D.B., MacDonald M.A., Reynolds P.H., and Longstaffe F.J. 1993. Leucogranites from the eastern part of the South Mountain Batholith, Nova Scotia. Journal of petrology, 34; 4: 653-679.

Craig J. R., Sandhaus D. J., and Guy R. E. 1995. Pyrophanite, MnTiO (sub 3), from Sterling Hill, New Jersey. The Canadian Mineralogist. 23, 3; Pages 491-494.

Czamanske G. K., and Mihalik P. 1972. Oxidation During Magmatic Differentiation, Finnmarka Complex, Oslo Area, Norway; Part 1, The Opaque Oxides. Journal of Petrology. 13; 3: 493-509.

Dostal J., and Chatterjee A. K. 1995. Origin of topaz-bearing and related peraluminous granites of the Late Devonian Davis Lake Pluton, Nova Scotia, Canada; crystal versus fluid fractionation. Chemical Geology. 123; 1-4: 67-88.

Dostal J., and Chatterjee A.K. 2000. Contrasting behaviour of Nb/Ta and Zr/Hf ratios in a peraluminous granitic pluton (Nova Scotia, Canada). Chemical Geology, 163: 207-218.

Druppel K., von Seckendorff V., and Okrusch M. 2001. Subsolidus reaction textures in the anorthositic rocks of the southern part of the Kunene Intrusive Complex, NW Namibia. European Journal of Mineralogy. 13; 2: 289-309.

Dunning G. R., Barr S. M., Giles P. S., McGregor D. C., Pe-Piper G., and Piper D. J. W. 2002. Chronology of Devonian to Early Carboniferous rifting and igneous activity in southern Magdalen Basin based on U-Pb (zircon) dating. Canadian Journal of Earth Sciences. 39; 8: 1219-1237.

Elsdon R. 1975. Manganoan ilmenite from the Leinster Granite, Ireland. Mineralogical Magazine and Journal of the Mineralogical Society. 40; 312: 419-421.

Farley, E. 1978. Mineralization at the Turner and Walker deposits, South Mountain Batholith. Masters thesis, Dalhousie University.

Feenstra A., and Peters T. 1996. Experimental determination of activities in $FeTiO_3$ - $MnTiO_3$ ilmenite solid solution by redox reversals. Contributions to Mineralogy and Petrology. 126; 1-2: 109-120.

Goldschmidt V.M. 1937. The principles of distribution of chemical elements in minerals and rocks. J. Chem. Soc., 655-672.

Green T. H. 1995. Experimental versus natural two-mineral partition coefficients; a "high-tech" controversy. International Geology Review. 37; 10: 851-865.

Haggerty S.E. 1976. Opaque Mineral Oxides in Terrestrial Igneous Rocks. *In* Oxide Minerals. *Edited by* D. Rumble III. Mineralogical Society of America Short Course Notes, 3: Hg101-Hg277.

Haggerty S.E. 1991. Oxide textures – A mini-atlas. *In* Oxide Minerals: Petrological and Magnetic Significance. *Edited by* Lindsley D.H. Reviews in Mineralogy, 25: 129-137.

Hanson S. L., Simmons W. B. Jr., and Falster A. U. 1998. Nb-Ta-Ti oxides in granitic pegmatites from the Topsham pegmatite district, southern Maine. *In*: Granitic pegmatites; the Cerny-Foord volume. *Prefacers*: Anderson A. J., Simmons W. B. Jr., Groat L. A. The Canadian Mineralogist. 36; 2: 601-608.

Haysom S. J., Horne R. J., and Pe-Piper G. 1997. The opaque mineralogy of metasedimentary rocks of the Meguma Group, Beaverbank-Rawdon area, Nova Scotia. *In:* Geology and mineralogy of the Meguma Group and their importance to environmental problems in Nova Scotia. *Edited by*: Zentilli M., and Fox D. Atlantic Geology. 33; 2: 105-120.

Hicks R. J., Jamieson R. A., and Reynolds P. H. 1999. Detrital and metamorphic $^{40}Ar/^{39}Ar$ ages from muscovite and whole-rock samples, Meguma Supergroup, southern Nova Scotia. Canadian Journal of Earth Sciences. 36; 1: 23-32.

Horng W. S., Hess P. C., and Gan H. 1999. The interactions between M^{+5} cations Nb^{+5}, Ta^{+5}, or P^{+5} and anhydrous haplogranite melts. Geochimica et Cosmochimica Acta. 63;

16: 2419-2428.

Ishihara S., and Wang P. A. 1999. The ilmenite-series and magnetite-series classification of the Yanshanian granitoids of South China. Bulletin of the Geological Survey of Japan. 50; 10: 661-670.

Klein C., and Hurlbut C.S., Jr. 1985. Systematic mineralogy; Part II: Oxides, Hydroxides, and Halides. *In* Manual of Mineralogy, pp 295.
Kontak D. J, and Dostal J. 1992. The East Kemptville tin deposit, Yarmouth County, southwestern Nova Scotia; a lithogeochemical study of wallrock metasedimentary rocks. Atlantic Geology. 28; 1: 63-83.

Linnen R. L., and Keppler H. 1997. Columbite solubility in granitic melts; consequences for the enrichment and fractionation of Nb and Ta in the Earth's crust. Contributions to Mineralogy and Petrology. 128; 2-3: 213-227.

Logothetis J. 1985. Contrasting types of hydrothermal alteration associated with the late-magmatic stages of the South Mountain Batholith. *In:* Transactions of the Atlantic Geoscience Society Colloquium on current research in the Atlantic Provinces; abstracts. *Converner:* Ferguson L. Maritime Sediments and Atlantic Geology. 20; 2: 114.

MacDonald M. A. 2001. Geology of the South Mountain Batholith, southwestern Nova Scotia. Nova Scotia Department of Natural Resources. *[Open File Report ME 2001-2 is accompanied by Map ME 1994-1, "Geological Map of the South Mountain Batholith (1: 250 000)".]*

MacDonald M.A., Corey M.C., Ham L.J., Horne R.J., and Chatterjee A.K. 1992. New insights into the generation, emplacement, and magmatic evolution of the South Mountain Batholith, Nova Scotia. *In:* Devono-Carboniferous magmatism, deformation, metamorphism and related mineralization in the Atlantic Provinces; 1992 colloquium; Current research in the Atlantic Provinces. Atlantic Geology, 28;2: 203-304.

MacKay R. 2002. Handout "The Electron Microprobe"

McKenzie C. B., and Clarke D. B. 1974. Petrology of the South Mountain Batholith, Nova Scotia. Nova Scotia Department of Natural Resources.

McKenzie C.B., and Clarke D.B. 1975. Petrology of the South Mountain Batholith, Nova Scotia. Canadian Journal of Earth Sciences, 12: 1209-1218.

Mitchell R. H. 1978. Manganoan magnesian ilmenite and titanian clinohumite from the Jacupiranga carbonatite, Sao Paulo, Brazil. American Mineralogist. 63; 5-6: 544-547.

Muecke G.K., and Clarke D.B. 1981. Geochemical evolution of the South Mountain Batholith, Nova Scotia; rare-earth-element evidence. *In:* Peraluminous granites. *Edited by:* Clarke D.B. The Canadian Mineralogist. 19: 133-145.

Mueller G. 1966. Die Beziehungen zwischen der chemischen Zusammensetzung, Lichtbrechung und Dichte einiger koexistierender Biotite, Muskowite und Chlorite aus granitischen Tiefengesteinen. Translated Title: Relations between chemical composition, refractive index, and density of coexisting biotite, muscovite, and chlorite from granitic plutonic rocks. Contributions to Mineralogy and Petrology. 12; 2: 173-191.

Novak M., and Cerny P. 1998. Niobium-tantalum oxide minerals from complex granitic pegmatites in the Moldanubicum, Czech Republic; primary versus secondary compositional trends. *In:* Granitic pegmatites; the Cerny-Foord volume. *Prefacers*: Anderson A. J., Simmons W. B. Jr., Groat L. A. The Canadian Mineralogist. 36; 2: 659-672.

O'Reilly G. 2001. Mineral Inventory studies in mainland Nova Scotia for 2001. *In:* Minerals and Energy Branch Report of Activities 2001, *Edited by:* D. R. MacDonald. Nova Scotia Department of Natural Resources. *Report ME 2002-1*

Press F., and Siever R. 2001. Understanding Earth. Third edition. *Publisher:* W.H. Freeman

Ramdohr P., and Cevales G. 1980. Eine durch Tiefensteinskontakt veraenderte Uranlagerstaette. Translated Title: A deep-seated, altered uranium deposit. Mineralium Deposita. 15; 3: 383-390.

Sakoma E. M., and Martin R. E. 2002. Oxidation-induced postmagmatic modifications of primary ilmenite, NYG-related aplite dyke, Tibchi Complex, Kalato, Nigeria. Mineralogical Magazine. 66; 4: 591-604.

Schenk P. 1995. Meguma Zone (chapter 3). *In:* Geology of the Appalachian-Caledonian Orogen in Canada and Greenland. *Edited by:* Williams H. Geological Survey of Canada. Geology of Canada. 6: 367-383.

Shaw C. S. J., and Penczak R. S. 1996. Barium and titanium-rich biotite and phlogopite from the western and eastern gabbro, Coldwell alkaline complex, northwestern Ontario. The Canadian Mineralogist. 34, 5: 967-975.

Snetsinger K. G. 1969. Manganoan minerals in a Sierran adamellite. Eos, Transactions, American Geophysical Union. 50; 4: 329.

Southwick D. L. 1968. Mineralogy of a rutile- and apatite-bearing ultramafic chlorite rock, Harford County, Maryland. U. S. Geological Survey Professional Paper. C38-C44.

Spiess R., Bertolo B., Borghi A., Chinellato M., and Tinor C. M. 2000. Microtextures of opaque inclusions; their use as indicators for hiatuses during garnet porphyroblast growth. Journal of Metamorphic Geology. 18; 5: 591-603.

Tate M. C. 1994. The nature and origin of enclaves in four peraluminous granitoid intrusions from the Meguma Zone, Nova Scotia. Atlantic Geology. 30; 3, Pages 205-215.

Tate M. C., and Clarke D. B. 1997. Compositional diversity among Late Devonian peraluminous granitoid intrusions in the Meguma Zone of Nova Scotia, Canada. Lithos. 39; 3-4:179-194.

Tindle A. G., and Breaks F. W. 1998. Oxide minerals of the separation rapids rare-element granitic pegmatite group, northwestern Ontario. *In*: Granitic pegmatites; the Cerny-Foord volume. *Prefacers*: Anderson A. J., Simmons W. B. Jr., Groat L. A. The Canadian Mineralogist. 36; 2: 609-635.

Uher P., Cerny P., Chapman R, Hatar J., and Miko O. 1998. Evolution of Nb,Ta-oxide minerals in the Prasiva granitic pegmatites, Slovakia; II, External hydrothermal Pb,Sb overprint. *In*: Granitic pegmatites; the Cerny-Foord volume. *Prefacers*: Anderson A. J., Simmons W. B. Jr., Groat L. A. The Canadian Mineralogist. 36; 2: 535-545.

Waerenborgh J. C., Figueiras J., Mateus A., and Goncalves M. 2002. Nature and mechanism of ilmenite alteration; a Mossbauer and X-ray diffraction study of oxidized ilmenite from the Beja-Acebuches ophiolite complex (SE Portugal). Mineralogical Magazine. 66; 3: 421-430.

Waychunas G.A. 1991. Crystal Chemistry of Oxides and Oxyhydroxides. *In* Oxide Minerals: Petrological and Magnetic Significance. *Edited by* Lindsley D.H. Reviews in Mineralogy, 25: 11-61.

Winter J.D. 2001. Chemical Petrology I: Major and Minor Elements. *In* An Introduction to igneous and metamorphic petrology, pp 128-160.

WORLD WIDE WEB REFERENCES

aae.www.ecn.purdue.edu/AAE/Career/Military.html. Uses of titanium for Figure 1.3a. Accessed on October 1, 2002 at 4:15 p.m.

chemiris.labs.brocku.ca/ ~chemweb/courses/chem232/CHEM2P32_ lecture_12.html. Octahedral site preference energy. Accessed on January 16, 2002 at 5:00 p.m.

helios.gsfc.nasa.gov/ ace_spacecraft.html. Uses of tantalum for Figure 1.2b. Accessed on October 1, 2002 at 4:11 p.m.

www.bioanalytical.com/ products/md/sik.html. Uses of titanium for Figure 1.3b. Accessed on November 17, 2002 at 8:39 a.m.

www.dewalt.com/us/images/ articles/blades_02.jpg. Uses of tantalum for Figure 1.2d. Accessed on November 17, at 8:50 a.m.

www.hd.org/Damon/photos/electronics/. Uses of tantalum for Figure 1.2a. Accessed on October 1, 2002 at 4:44 p.m.

www.healthenterprises.com/contentmgr/ showdetails.php. Uses of niobium for Figure 1.1d. Accessed on October 1, 2002 at 4:23 p.m.

www.jeo.com/nmr/mag_view/magnet_destruction.html. Uses of niobium for Figure 1.1b. Accessed on October 1, 2002 at 4:38 p.m.

www.luxury-line.com/diamonds/engagement/ashford-metals.htm. Uses of titanium for Figure 1.3c. Accessed on October 12, 2002 at 8:45 p.m.

www.mahavirminerals.com/ profile.html. Uses of titanium for Figure 1.3d. Accessed on October 12, 2002 at 9:00 p.m.

www.nonferrous-metal.com/ new-page/titanium07.htm. Uses of niobium for Figure 1.1a. Accessed on October 1, 2002 at 4:00 p.m.

www.out-there.com. Length of the Shubenacadie River. Accessed on February 12, 2002 at 8:15 a.m.

www.pearl1.lanl.gov/gov/periodic/elements/22.html. Uses of titanium. Accessed on March 18, 2002 at 8:01 p.m.

www.sl66.com/sl66_lens_details/oberkochen.htm. Uses of niobium for Figure 1.1c. Accessed on December 3, 2002 at 12:30 p.m.

www.twi.co.uk/j32k/getFile/ elec_medical.html. Uses of tantalum for Figure 1.2c. Accessed on October 12, 2002 at 10:15 p.m.

www.unb.ca/courses/geo l2142/LEC-32.html. Characteristics of manganoan ilmenite. Accessed on September 28, 2002 at 12:00 p.m.

www.webminerals.com. Atomic radii used in each exchange reaction. Accessed on February 20, 2002 at 5:07 p.m.

Appendix A - Ilmenite analyses

Sample Number	Sr+Zr	Bin #	TiO2	FeO	MnO	FeO+MnO	MgO	Nb2O5	Ta2O5	Nb metal	Ta metal	Nb+Ta	Nb/Ta	Total
A15-0081	465	1	52.56	24.09	23.43	47.52	0.09	0.47	0.00	0.33	0.00	0.33	0.00	101.02
A15-0081	465	1	47.75	33.02	2.29	35.32	0.04	0.17	0.07	0.12	0.05	0.17	2.16	86.48
A15-0081	465	1	58.08	29.92	6.28	36.20	0.08	0.23	0.00	0.16	0.00	0.16	0.00	95.24
Average			52.80	29.01	10.67	39.68	0.07	0.29	0.02	0.20	0.02	0.22	0.72	94.25
D13-2095-1A	424	1	49.69	23.70	19.96	43.66	0.12	0.00	0.27	0.00	0.22	0.22	0.00	99.07
D13-2095-1A	424	1	52.56	35.92	10.83	46.75	0.00	0.00	0.00	0.00	0.00	0.00	0.00	99.52
D13-2095-1A	424	1	53.35	39.36	6.72	46.08	0.00	0.05	0.00	0.03	0.00	0.03	0.00	99.79
D13-2095-1A	424	1	54.50	29.88	13.94	43.82	0.15	0.17	0.00	0.12	0.00	0.12	0.00	99.09
D13-2095-1A	424	1	51.64	32.15	14.05	46.20	0.27	0.00	0.29	0.00	0.23	0.23	0.00	99.92
D13-2095-1A	424	1	54.13	33.24	12.85	46.09	0.00	0.00	0.00	0.00	0.00	0.00	0.00	100.78
D13-2095-1A	424	1	52.47	35.25	11.18	46.44	0.08	0.14	0.04	0.10	0.04	0.13	2.73	99.38
D13-2095-1A	424	1	52.97	38.60	8.48	47.08	0.06	0.00	0.00	0.00	0.00	0.00	0.00	100.38
D13-2095-1A	424	1	52.55	39.14	7.31	46.46	0.09	0.09	0.00	0.06	0.00	0.06	0.00	99.64
D13-2095-1A	424	1	53.59	39.50	6.72	46.23	0.02	0.10	0.00	0.07	0.00	0.07	0.00	100.09
D13-2095-1A	424	1	52.48	39.82	7.71	47.53	0.04	0.12	0.58	0.08	0.47	0.56	0.17	100.85
D13-2095-1A	424	1	52.70	41.04	5.54	46.57	0.07	0.00	0.00	0.00	0.00	0.00	0.00	99.73
D13-2095-1A	424	1	52.90	41.42	5.77	47.19	0.00	0.06	0.00	0.04	0.00	0.04	0.00	100.69
D13-2095-1A	424	1	54.25	40.53	5.61	46.14	0.07	0.04	0.36	0.03	0.29	0.10	0.32	101.43
Average			52.84	36.40	9.76	46.16	0.07	0.05	0.11	0.04	0.09	0.11	0.23	100.03
A16-1268	374	2	51.99	37.29	11.12	48.41	0.00	0.05	0.00	0.04	0.00	0.04	0.00	100.85
A16-1268	374	2	51.49	38.48	8.33	46.81	0.13	0.13	0.45	0.09	0.37	0.46	0.26	100.03
A16-1268	374	2	52.70	40.00	8.39	48.38	0.02	0.09	0.83	0.06	0.68	0.75	0.09	102.19
A16-1268	374	2	53.06	40.99	7.97	48.96	0.00	0.35	0.43	0.25	0.35	0.60	0.70	102.90
A16-1268	374	2	53.06	41.22	7.45	48.67	0.00	0.09	0.91	0.07	0.74	0.81	0.09	102.82
A16-1268	374	2	52.16	41.33	6.39	47.72	0.01	0.00	0.20	0.00	0.16	0.16	0.00	100.54
A16-1268	374	2	53.50	43.57	5.75	49.31	0.05	0.33	0.00	0.23	0.00	0.23	0.00	103.42
A16-1268	374	2	52.54	40.01	8.40	48.41	0.01	0.01	0.00	0.01	0.00	0.01	0.00	101.48
A16-1268	374	2	53.46	42.81	5.56	48.37	0.09	0.23	0.48	0.16	0.40	0.56	0.41	102.71

Average			52.66	40.63	7.71	48.34	0.04	0.14	0.37	0.10	0.30	0.40	0.17	101.88
A11-2267	355	2	51.69	30.92	17.94	48.86	0.03	0.00	0.08	0.00	0.07	0.07	0.00	100.77
A11-2267	355	2	51.57	41.99	5.21	47.20	0.00	0.17	0.51	0.12	0.42	0.54	0.28	99.44
A11-2267	355	2	51.01	40.03	7.78	47.81	0.00	0.41	0.49	0.29	0.40	0.69	0.71	99.76
A11-2267	355	2	51.31	43.55	3.67	47.22	0.00	0.06	0.25	0.04	0.21	0.25	0.19	99.03
Average			51.39	39.12	8.65	47.77	0.01	0.16	0.33	0.11	0.27	0.39	0.29	99.75
D12-0028	311	2	51.73	36.52	12.08	48.60	0.11	0.10	0.01	0.07	0.01	0.08	7.43	100.85
D12-0028	311	2	51.82	37.06	11.25	48.31	0.00	0.22	0.00	0.15	0.00	0.15	0.00	100.85
D12-0028	311	2	52.34	35.78	11.95	47.73	0.00	0.12	0.00	0.08	0.00	0.08	0.00	100.59
Average			51.96	36.45	11.76	48.21	0.04	0.15	0.00	0.10	0.00	0.11	2.48	100.76
A11-2286	302	2	51.19	41.81	6.42	48.23	0.00	0.11	0.00	0.08	0.00	0.08	0.00	100.07
A11-2286	302	2	52.07	42.67	5.22	47.89	0.00	0.19	0.00	0.13	0.00	0.13	0.00	100.76
A11-2286	302	2	51.69	42.74	5.34	48.09	0.04	0.06	0.11	0.04	0.09	0.13	0.46	100.16
A11-2286	302	2	50.55	40.42	5.75	46.17	0.02	0.10	0.35	0.07	0.28	0.35	0.25	98.16
A11-2286	302	2	51.71	42.41	5.33	47.74	0.06	0.09	0.17	0.06	0.14	0.20	0.44	99.96
A11-2286	302	2	52.26	43.84	4.00	47.84	0.11	0.12	0.00	0.09	0.00	0.09	0.00	100.70
A11-2286	302	2	52.86	41.11	4.96	46.07	0.04	0.12	0.13	0.09	0.10	0.19	0.82	99.82
A11-2286	302	2	53.05	40.61	5.05	45.66	0.04	0.11	0.23	0.08	0.19	0.27	0.42	99.97
A11-2286	302	2	53.76	40.80	4.94	45.74	0.04	0.11	0.22	0.08	0.18	0.26	0.43	100.74
A11-2286	302	2	52.63	40.85	4.95	45.80	0.04	0.14	0.15	0.10	0.13	0.22	0.76	99.46
A11-2286	302	2	52.46	41.14	4.95	46.09	0.03	0.12	0.24	0.08	0.19	0.43	0.28	99.69
Average			52.20	41.67	5.18	46.85	0.04	0.12	0.15	0.06	0.12	0.21	0.35	99.95
A15-1320	228	3	52.06	31.12	17.29	48.41	0.09	0.40	0.11	0.28	0.09	0.37	3.10	101.90
A15-1320	228	3	53.53	32.77	14.58	47.35	0.04	0.21	0.39	0.15	0.32	0.47	0.46	101.65
A15-1320	228	3	53.11	42.13	6.94	49.06	0.09	0.20	0.00	0.14	0.00	0.14	0.00	102.73
A15-1320	228	3	52.31	28.76	19.92	48.68	0.14	0.39	0.38	0.28	0.31	0.59	0.89	102.33
A15-1320	228	3	52.07	34.33	14.29	48.62	0.13	0.37	0.79	0.26	0.65	0.91	0.40	102.00
A15-1320	228	3	52.45	37.03	10.85	47.88	0.12	0.03	0.56	0.02	0.46	0.48	0.05	101.13
A15-1320	228	3	52.68	40.44	7.95	48.39	0.08	0.00	0.00	0.00	0.00	0.00	0.00	101.50
A15-1320	228	3	52.73	44.39	4.11	48.50	0.10	0.19	0.99	0.13	0.81	0.94	0.16	102.66

A15-1320	228	3	52.97	46.47	1.85	48.32	0.14	0.10	0.00	0.07	0.00	0.07	0.00	102.11
Average			52.66	37.49	10.86	48.36	0.10	0.21	0.36	0.15	0.29	0.44	0.56	102.00
A14-0007	226	3	51.96	42.51	5.31	47.82	0.03	0.42	0.00	0.29	0.00	0.29	0.00	100.56
A14-0007	226	3	51.80	43.84	4.40	48.23	0.03	0.11	0.01	0.08	0.00	0.08	15.59	100.37
A14-0007	226	3	50.86	39.97	7.48	47.45	0.00	0.11	0.00	0.08	0.00	0.08	28.94	98.70
A14-0007	226	3	51.91	41.43	6.48	47.91	0.10	0.07	0.00	0.05	0.00	0.05	0.00	100.32
A14-0007	226	3	51.92	43.64	4.31	47.95	0.19	0.21	0.00	0.14	0.00	0.14	0.00	100.63
A14-0007	226	3	51.66	40.88	6.89	47.77	0.00	0.00	0.10	0.00	0.08	0.08	0.00	99.81
A14-0007	226	3	52.30	41.94	5.94	47.87	0.00	0.51	0.00	0.35	0.00	0.35	0.00	101.07
A14-0007	226	3	51.57	42.48	5.30	47.78	0.00	0.28	0.00	0.20	0.00	0.20	0.00	99.93
A14-0007	226	3	51.31	45.75	1.86	47.61	0.03	0.18	0.00	0.13	0.00	0.13	0.00	99.56
Average			51.70	42.49	5.33	47.82	0.04	0.21	0.01	0.15	0.01	0.16	4.95	100.10
D05-0016	206	3	51.90	30.87	16.41	47.28	0.13	0.26	0.03	0.18	0.02	0.20	7.40	100.04
D05-0016	206	3	52.30	36.53	12.01	48.55	0.08	0.15	0.85	0.11	0.70	0.81	0.15	102.04
D05-0016	206	3	68.88	19.56	2.98	22.54	0.04	0.22	0.80	0.15	0.66	0.81	0.23	93.00
D05-0016	206	3	52.37	33.25	14.04	47.29	0.10	0.40	0.32	0.28	0.27	0.54	1.05	100.57
D05-0016	206	3	51.96	39.38	8.80	48.18	0.06	0.25	0.60	0.17	0.49	0.66	0.35	101.18
D05-0016	206	3	51.74	42.69	4.05	46.75	0.07	0.12	0.01	0.08	0.01	0.09	10.55	98.82
D05-0016	206	3	52.48	24.35	22.94	47.29	0.00	0.04	1.21	0.03	0.99	1.02	0.03	101.26
D05-0016	206	3	52.30	30.63	17.41	48.04	0.09	0.12	0.43	0.08	0.35	0.43	0.23	101.09
D05-0016	206	3	53.30	31.35	15.32	46.66	0.06	0.35	0.31	0.24	0.25	0.49	0.97	101.16
Average			54.14	32.07	12.66	44.73	0.07	0.21	0.51	0.15	0.42	0.56	2.33	99.91
D12-0081	175	4	75.20	15.60	1.31	16.91	0.01	0.21	0.02	0.14	0.02	0.16	7.33	94.39
D12-0081	175	4	73.86	16.87	1.06	17.94	0.00	0.17	0.00	0.12	0.00	0.12	0.00	93.65
Average			74.53	16.24	1.19	17.43	0.01	0.19	0.01	0.13	0.01	0.14	3.66	94.02
A11-2259	159	4	53.01	27.43	19.47	46.89	0.08	0.23	0.84	0.16	0.69	0.84	0.23	101.14
A11-2259	159	4	51.85	29.21	16.57	45.78	0.02	0.82	0.41	0.57	0.34	0.91	1.70	98.95
A11-2259	159	4	51.26	31.35	14.81	46.16	0.00	0.24	0.01	0.17	0.01	0.18	14.50	97.99
A11-2259	159	4	54.35	35.74	10.78	46.52	0.01	0.48	1.32	0.33	1.08	1.42	0.31	103.14
A11-2259	159	4	52.37	41.83	5.94	47.78	0.09	0.28	0.13	0.19	0.11	0.30	1.82	100.75

A11-2259	159	4	52.83	24.65	21.13	45.77	0.01	0.29	0.00	0.20	0.00	0.20	0.00	98.93
A11-2259	159	4	53.41	31.50	17.19	48.69	0.02	0.35	0.00	0.25	0.00	0.25	0.00	102.49
A11-2259	159	4	67.37	19.34	2.01	21.35	0.09	0.39	0.81	0.27	0.66	0.94	0.41	90.34
A11-2259	159	4	52.48	27.51	15.46	42.98	0.00	0.53	0.01	0.37	0.01	0.38	33.05	97.40
A11-2259	159	4	50.90	31.67	14.64	46.31	0.12	0.17	0.00	0.12	0.00	0.12	0.00	98.54
A11-2259	159	4	52.21	32.88	13.80	46.67	0.03	0.41	0.86	0.29	0.70	0.99	0.41	100.39
A11-2259	159	4	52.71	33.92	11.29	45.21	0.25	0.47	0.29	0.33	0.23	0.56	1.40	100.23
A11-2259	159	4	53.09	35.99	9.53	45.52	0.04	0.52	0.00	0.36	0.00	0.36	0.00	99.37
A11-2259	159	4	53.49	44.11	4.27	48.38	0.08	0.11	0.41	0.08	0.33	0.41	0.24	102.59
A11-2259	159	4	53.79	29.59	14.71	44.30	0.00	0.26	0.04	0.18	0.04	5.10	0.22	98.88
A11-2259	159	4	53.44	22.10	21.62	43.71	0.02	0.28	-	0.20	0.00	0.00	0.20	97.95
Average			53.66	31.18	13.33	44.50	0.05	0.36	0.32	0.25	0.26	0.81	3.41	99.32
A15-0101	131	4	58.75	23.08	0.23	23.31	0.02	0.01	0.31	0.00	0.26	0.26	0.02	87.13
A15-0101	131	4	54.33	30.40	1.99	32.39	0.00	0.33	0.39	0.23	0.32	0.55	0.71	90.48
Average			56.54	26.74	1.11	27.85	0.01	0.17	0.35	0.12	0.29	0.40	0.36	88.81
A11-2262	119	4	54.66	33.99	6.69	40.68	0.05	0.21	0.07	0.14	0.05	0.20	2.63	97.86
A11-2262	119	4	54.89	36.65	7.52	44.17	0.00	0.84	0.00	0.59	0.00	0.59	893.91	99.95
A11-2262	119	4	54.89	36.18	6.03	42.21	0.00	0.90	0.07	0.63	0.06	0.69	11.03	98.23
A11-2262	119	4	54.93	37.93	7.37	45.29	0.01	0.37	0.16	0.26	0.13	0.39	1.99	100.90
A11-2262	119	4	55.16	34.31	7.57	41.88	0.06	0.12	0.00	0.09	0.00	0.09	0.00	97.65
A11-2262	119	4	67.21	18.12	1.13	19.25	0.11	0.25	0.00	0.18	0.00	0.18	0.00	89.04
A11-2262	119	4	59.14	27.35	3.20	30.55	0.11	0.60	0.62	0.42	0.50	0.92	0.83	91.52
A11-2262	119	4	61.64	27.37	3.11	30.48	0.03	0.10	0.13	0.07	0.10	0.17	0.66	93.16
A11-2262	119	4	61.35	27.87	3.46	31.33	0.12	0.58	0.00	0.40	0.00	0.40	0.00	95.79
A11-2262	119	4	56.64	32.01	4.95	36.96	0.07	0.67	0.99	0.47	0.81	1.29	0.58	95.50
A11-2262	119	4	54.98	35.09	6.55	41.64	0.02	0.31	0.05	0.22	0.04	0.26	5.06	97.28
A11-2262	119	4	53.14	35.74	9.13	44.87	0.06	0.28	0.00	0.20	0.00	0.20	0.00	98.67
A11-2262	119	4	53.15	36.61	7.62	44.24	0.10	0.34	0.29	0.24	0.24	0.47	0.99	98.24
A11-2262	119	4	52.47	37.22	5.71	42.93	0.00	0.42	0.16	0.29	0.13	0.42	2.25	97.39
A11-2262	119	4	56.92	32.32	4.43	36.75	0.07	0.96	0.96	0.67	0.79	1.46	0.85	96.09
A11-2262	119	4	57.06	33.10	2.26	35.36	0.05	1.02	0.27	0.71	0.22	0.93	3.26	94.41
A11-2262	119	4	52.45	38.94	7.21	46.15	0.04	0.51	0.02	0.36	0.02	0.37	20.48	99.37

A11-2262	119	4	53.22	31.44	8.65	40.09	0.06	0.27	0.23	0.19	0.19	1.02	0.38	95.24
A11-2262	119	4	54.50	34.93	6.42	41.35	0.01	0.27	0.35	0.19	0.29	0.64	0.47	97.18
A11-2262	119	4	54.19	32.03	7.91	39.94	0.02	0.72	0.48	0.50	0.39	1.28	0.89	96.35
A11-2262	119	4	54.33	32.26	5.49	37.74	0.01	0.95	0.31	0.67	0.25	2.65	0.92	94.66
A11-2262	119	4	54.82	31.95	7.21	39.16	0.03	0.35	0.32	0.25	0.26	0.96	0.51	95.32
A11-2262	119	4	54.54	31.56	8.25	39.81	0.02	0.32	0.33	0.22	0.27	0.83	0.49	95.86
Average			55.92	32.82	5.99	38.82	0.05	0.49	0.25	0.35	0.21	0.71	41.23	96.33
A16-1238	26	5	52.22	41.86	3.61	45.47	0.00	0.39	0.00	0.27	0.00	0.27	0.00	98.34
A16-1238	26	5	50.48	42.75	4.43	47.18	0.09	0.42	0.00	0.29	0.00	0.29	0.00	98.94
Average			51.35	42.30	4.02	46.32	0.04	0.41	0.00	0.28	0.00	0.28	0.00	98.64
A11-2272	23	5	51.38	42.87	4.87	47.74	0.01	0.33	0.00	0.23	0.00	0.23	0.00	99.51
A11-2272	23	5	51.73	42.35	4.18	46.53	0.02	0.29	0.29	0.20	0.24	0.44	0.84	98.99
A11-2272	23	5	51.88	43.16	4.45	47.60	0.04	0.22	0.05	0.16	0.04	0.20	3.79	99.85
A11-2272	23	5	52.09	42.88	4.68	47.56	0.00	0.33	0.48	0.23	0.40	0.63	0.58	100.48
A11-2272	23	5	53.46	37.71	3.55	41.25	0.06	0.26	0.26	0.18	0.21	0.86	0.39	96.12
Average			52.11	41.79	4.35	46.14	0.02	0.29	0.22	0.20	0.18	0.47	1.12	98.99

Appendix B - Rutile analyses

Sample Number	Sr+Zr	Bin #	TiO2	Nb2O5	Ta2O5	FeO	MnO	Total	Nb metal	Ta metal	Nb/Ta	Nb+Ta	Nb2O5/Ta2O5	Nb2O5+Ta2O5
A15-0081	465	1	97.44	0.57	0.00	0.23	0.04	98.79	0.40	0.00	0.00	0.40	0.00	0.57
A15-0081	465	1	97.89	0.49	0.34	0.29	0.14	99.39	0.35	0.28	1.24	0.62	1.45	0.84
A15-0081	465	1	97.79	0.52	0.00	0.51	0.02	99.42	0.36	0.00	0.00	0.36	0.00	0.52
A15-0081	465	1	96.75	0.51	0.03	0.23	0.01	99.49	0.36	0.02	14.98	0.38	17.55	0.54
A15-0081	465	1	100.24	0.41	0.05	0.25	0.00	101.81	0.28	0.04	7.55	0.32	8.85	0.45
A15-0081	465	1	98.94	0.74	0.07	0.41	0.02	101.22	0.52	0.06	9.18	0.58	10.75	0.81
A15-0081	465	1	99.78	0.32	0.04	0.25	0.01	101.34	0.23	0.03	7.23	0.26	8.47	0.36
A15-0081	465	1	95.94	0.48	0.03	0.39	0.02	99.12	0.33	0.02	14.48	0.35	16.96	0.50
A15-0081	465	1	96.97	1.30	0.29	1.54	0.08	101.10	0.91	0.24	3.77	1.15	4.42	1.59
A15-0081	465	1	99.99	0.42	0.03	0.12	0.00	101.45	0.30	0.02	13.37	0.32	15.67	0.45
A15-0081	465	1	95.71	0.42	0.00	0.55	0.05	99.39	0.29	0.00	0.00	0.29	0.00	0.42
A15-0081	465	1	94.94	0.48	0.00	0.38	0.05	98.74	0.33	0.00	0.00	0.33	0.00	0.48
A15-0081	465	1	99.53	0.37	0.00	0.39	0.00	101.22	0.26	0.00	0.00	0.26	0.00	0.37
Average			97.84	0.54	0.07	0.43	0.03	100.19	0.38	0.05	5.52	0.43	6.47	0.61
D13-2090	458	1	97.89	0.60	0.74	0.12	0.12	99.86	0.42	0.61	0.69	1.03	0.81	1.34
D13-2090	458	1	96.78	0.17	0.00	0.52	0.08	98.60	0.12	0.00	0.00	0.12	0.00	0.17
D13-2090	458	1	96.50	0.56	0.66	0.56	0.10	99.28	0.39	0.54	0.72	0.94	0.85	1.22
D13-2090	458	1	97.14	0.43	0.00	0.66	0.17	99.72	0.30	0.00	0.00	0.30	0.00	0.43
D13-2090	458	1	96.64	0.41	0.54	0.74	0.07	99.05	0.28	0.44	0.64	0.73	0.75	0.95
D13-2090	458	1	97.18	0.39	0.08	0.89	0.05	99.15	0.27	0.06	4.43	0.34	5.19	0.47
D13-2090	458	1	98.60	0.41	0.60	0.04	0.08	99.83	0.29	0.49	0.59	0.78	0.69	1.01
D13-2090	458	1	98.79	0.31	0.27	0.07	0.03	100.16	0.22	0.22	1.00	0.44	1.18	0.58
D13-2090	458	1	98.65	0.47	0.10	0.05	0.05	100.51	0.33	0.08	4.20	0.40	4.92	0.56
D13-2090	458	1	99.04	0.45	0.14	0.05	0.03	100.85	0.31	0.11	2.79	0.43	3.27	0.59
D13-2090	458	1	96.69	0.49	0.01	0.50	0.09	99.23	0.34	0.00	69.27	0.35	81.17	0.49
D13-2090	458	1	99.13	0.32	0.02	0.74	0.01	101.32	0.22	0.02	12.26	0.24	14.36	0.34
D13-2090	458	1	98.17	0.59	0.05	0.72	0.00	100.90	0.42	0.04	9.57	0.46	11.21	0.65
D13-2090	458	1	100.19	0.54	0.06	0.43	0.00	102.12	0.38	0.05	7.25	0.43	8.50	0.61
D13-2090	458	1	99.14	0.37	0.01	0.62	0.01	101.24	0.26	0.00	53.20	0.27	62.33	0.38
D13-2090	458	1	100.62	0.29	0.00	0.37	0.01	102.22	0.20	0.00	0.00	0.20	0.00	0.29

D13-2090	458	1	99.49	0.52	0.00	0.40	0.00	101.33	0.36	0.00	0.00	0.36	0.00	0.52
Average			98.27	0.43	0.19	0.44	0.05	100.32	0.30	0.16	9.80	0.46	11.48	0.62
D13-2095-1A	424	1	97.41	0.33	0.00	0.64	0.17	99.38	0.23	0.00	0.00	0.23	0.00	0.33
Average			97.41	0.33	0.00	0.64	0.17	99.38	0.23	0.00	0.00	0.23	0.00	0.33
D12-0028	311	2	95.48	0.38	0.00	1.21	0.00	98.23	0.27	0.00	0.00	0.27	0.00	0.38
D12-0028	311	2	94.95	0.43	1.32	2.58	0.21	102.70	0.30	1.08	0.28	1.38	0.32	1.75
D12-0028	311	2	95.52	0.43	0.00	1.05	0.03	98.76	0.30	0.00	0.00	0.30	0.00	0.43
D12-0028	311	2	99.34	0.10	0.00	0.47	0.00	100.82	0.07	0.00	0.00	0.07	0.00	0.10
D12-0028	311	2	97.40	0.31	0.00	0.80	0.00	99.95	0.22	0.00	0.00	0.22	0.00	0.31
Average			96.54	0.33	0.26	1.22	0.05	100.09	0.23	0.22	0.06	0.45	0.06	0.59
A11-2286	302	2	96.84	0.81	0.16	0.73	0.04	98.96	0.57	0.13	4.28	0.70	5.02	0.98
Average			96.84	0.81	0.16	0.73	0.04	98.96	0.57	0.13	4.28	0.70	5.02	0.98
A15-1320	228	3	97.42	0.78	0.14	0.95	0.00	99.61	0.54	0.12	4.67	0.66	5.47	0.92
A15-1320	228	3	98.82	0.38	0.07	0.71	0.03	100.97	0.27	0.06	4.41	0.33	5.16	0.46
A15-1320	228	3	96.10	0.13	0.00	1.23	0.03	99.35	0.09	0.00	37.55	0.09	44.00	0.14
A15-1320	228	3	97.45	0.95	0.19	0.76	0.01	100.23	0.66	0.16	4.17	0.82	4.88	1.14
A15-1320	228	3	97.90	0.27	0.00	0.90	0.00	100.19	0.19	0.00	0.00	0.19	0.00	0.27
A15-1320	228	3	98.26	0.38	0.00	0.37	0.02	100.06	0.27	0.00	0.00	0.27	0.00	0.38
Average			97.66	0.48	0.07	0.82	0.01	100.07	0.34	0.06	8.47	0.39	9.92	0.55
D05-0016	206	3	99.30	0.54	0.00	0.94	0.01	101.75	0.38	0.00	0.00	0.38	0.00	0.54
D05-0016	206	3	98.36	0.10	0.00	0.32	0.01	99.72	0.07	0.00	0.00	0.07	0.00	0.10
Average			98.83	0.32	0.00	0.63	0.01	100.74	0.22	0.00	0.00	0.22	0.00	0.32
D12-0081	175	4	97.67	1.12	0.09	0.98	0.01	100.95	0.78	0.08	10.35	0.86	12.13	1.21
D12-0081	175	4	97.91	0.84	0.09	0.70	0.00	100.70	0.59	0.07	7.89	0.66	9.24	0.93
D12-0081	175	4	97.15	1.01	0.16	1.13	0.05	100.81	0.70	0.13	5.26	0.84	6.17	1.17
D12-0081	175	4	98.41	0.83	0.11	0.88	0.03	101.25	0.58	0.09	6.21	0.67	7.28	0.94
D12-0081	175	4	96.54	0.66	0.88	0.63	0.20	99.94	0.46	0.72	0.64	1.18	0.75	1.53

D12-0081	175	4	94.47	0.58	0.20	0.83	0.00	97.37	0.41	0.16	2.52	0.57	2.96	0.78
D12-0081	175	4	96.70	0.34	0.74	1.14	0.00	99.20	0.24	0.61	0.39	0.85	0.46	1.09
Average			96.98	0.77	0.33	0.90	0.04	100.03	0.54	0.27	4.75	0.80	5.57	1.09
A11-2259	159	4	97.90	0.83	0.55	0.76	0.04	100.26	0.58	0.45	1.29	1.03	1.52	1.38
A11-2259	159	4	82.10	0.82	0.00	2.87	0.04	92.91	0.57	0.00	175.18	0.58	205.25	0.83
A11-2259	159	4	85.51	0.86	0.00	2.93	0.06	94.31	0.60	0.00	0.00	0.60	0.00	0.86
A11-2259	159	4	98.56	0.29	0.00	0.48	0.01	100.49	0.20	0.00	0.00	0.20	0.00	0.29
A11-2259	159	4	98.59	0.67	0.00	0.05	0.00	100.29	0.47	0.00	0.00	0.47	0.00	0.67
Average			92.53	0.70	0.11	1.42	0.03	97.65	0.49	0.09	35.29	0.58	41.35	0.81
A16-3024	154	4	95.12	0.81	0.00	0.41	0.14	97.59	0.56	0.00	0.00	0.56	0.00	0.81
A16-3024	154	4	96.63	0.65	0.00	0.53	0.09	98.47	0.46	0.00	0.00	0.46	0.00	0.65
A16-3024	154	4	95.22	0.37	0.00	0.58	0.15	98.57	0.26	0.00	0.00	0.26	0.00	0.37
A16-3024	154	4	95.02	0.16	0.03	0.89	0.06	98.04	0.11	0.02	4.87	0.14	5.71	0.19
A16-3024	154	4	95.67	0.74	0.00	1.02	0.15	99.16	0.52	0.00	0.00	0.52	0.00	0.74
A16-3024	154	4	98.26	1.02	0.03	0.70	0.05	101.19	0.72	0.03	27.28	0.74	31.97	1.06
A16-3024	154	4	95.18	0.70	0.08	0.86	0.01	98.66	0.49	0.07	7.34	0.55	8.60	0.78
A16-3024	154	4	99.74	0.70	0.06	0.50	0.02	102.04	0.49	0.05	10.59	0.53	12.41	0.75
A16-3024	154	4	99.16	0.58	0.07	0.58	0.03	101.60	0.41	0.06	6.90	0.47	8.08	0.65
A16-3024	154	4	98.34	0.64	0.00	0.50	0.02	100.82	0.45	0.00	0.00	0.45	0.00	0.64
A16-3024	154	4	100.37	0.22	0.00	0.48	0.02	102.30	0.15	0.00	0.00	0.15	0.00	0.22
A16-3024	154	4	91.43	1.19	0.00	3.59	0.10	97.36	0.83	0.00	0.00	0.83	0.00	1.19
Average			96.68	0.65	0.02	0.89	0.07	99.65	0.45	0.02	4.75	0.47	5.56	0.67
D13-2095-01	144	4	97.60	1.30	0.50	0.11	0.02	101.15	0.91	0.41	2.23	1.32	2.61	1.80
D13-2095-01	144	4	98.86	0.87	0.09	0.11	0.01	101.22	0.61	0.07	8.57	0.68	10.05	0.96
D13-2095-01	144	4	94.38	1.33	0.35	0.81	0.02	98.37	0.93	0.29	3.23	1.22	3.78	1.68
D13-2095-01	144	4	97.75	0.81	0.11	0.18	0.01	100.71	0.56	0.09	6.31	0.65	7.39	0.92
D13-2095-01	144	4	97.86	0.82	0.14	0.12	0.00	100.61	0.57	0.12	4.93	0.69	5.77	0.96
D13-2095-01	144	4	92.58	1.01	0.51	0.56	0.02	96.33	0.71	0.42	1.68	1.13	1.96	1.52
D13-2095-01	144	4	97.19	1.00	0.43	0.22	0.02	100.46	0.70	0.35	1.97	1.05	2.31	1.43
D13-2095-01	144	4	91.03	0.89	0.47	0.83	0.04	94.97	0.62	0.38	1.61	1.00	1.89	1.36
Average			95.91	1.00	0.33	0.37	0.02	99.23	0.70	0.27	3.82	0.97	4.47	1.33

A15-0101	131	4	96.95	1.46	0.26	1.19	0.02	101.04	1.02	0.21	4.84	1.23	5.67	1.71
A15-0101	131	4	94.69	1.95	0.51	3.32	0.07	101.46	1.36	0.41	3.28	1.78	3.85	2.45
A15-0101	131	4	96.92	0.13	0.04	0.56	0.03	99.14	0.09	0.03	3.06	0.12	3.58	0.17
A15-0101	131	4	86.31	6.35	0.65	2.33	0.05	98.91	4.44	0.53	8.39	4.97	9.83	6.99
A15-0101	131	4	97.99	0.40	0.00	0.85	0.04	100.51	0.28	0.00	0.00	0.28	0.00	0.40
A15-0101	131	4	96.20	0.54	0.00	0.64	0.12	98.22	0.37	0.00	0.00	0.37	0.00	0.54
A15-0101	131	4	94.38	0.27	0.00	0.72	0.00	97.18	0.19	0.00	0.00	0.19	0.00	0.27
A15-0101	131	4	96.25	0.30	0.00	0.99	0.00	98.07	0.21	0.00	0.00	0.21	0.00	0.30
A15-0101	131	4	95.72	1.15	0.00	1.00	0.00	98.65	0.80	0.00	0.00	0.80	0.00	1.15
A15-0101	131	4	95.99	1.44	0.00	1.23	0.05	99.36	1.00	0.00	0.00	1.00	0.00	1.44
A15-0101	131	4	86.86	5.88	0.00	2.35	0.00	97.05	4.11	0.00	0.00	4.11	0.00	5.88
A15-0101	131	4	93.80	1.85	0.29	2.50	0.06	98.93	1.29	0.24	5.40	1.53	6.33	2.14
Average			94.34	1.81	0.14	1.47	0.04	99.04	1.26	0.12	2.06	1.38	2.44	1.95
A11-2262	119	4	96.46	0.74	0.07	0.57	0.07	99.72	0.52	0.06	9.05	0.58	10.60	0.81
A11-2262	119	4	98.50	0.18	0.05	0.43	0.03	100.53	0.13	0.04	3.47	0.16	4.07	0.23
A11-2262	119	4	99.07	1.22	0.04	0.24	0.04	101.56	0.85	0.04	23.72	0.89	27.80	1.27
A11-2262	119	4	97.64	0.94	0.11	0.60	0.01	100.53	0.65	0.09	7.20	0.75	8.43	1.05
A11-2262	119	4	96.70	1.13	0.07	0.76	0.06	99.98	0.79	0.06	13.56	0.85	15.89	1.20
A11-2262	119	4	96.02	2.33	0.88	0.42	0.02	100.71	1.63	0.72	2.27	2.34	2.66	3.20
A11-2262	119	4	95.14	1.63	0.66	0.29	0.00	98.37	1.14	0.54	2.11	1.67	2.47	2.28
A11-2262	119	4	96.21	1.56	0.32	0.54	0.00	99.33	1.09	0.26	4.19	1.35	4.91	1.87
Average			96.97	1.21	0.27	0.48	0.03	100.09	0.85	0.22	8.20	1.07	9.60	1.49
D13-2086	97	5	98.31	0.60	0.14	0.00	0.04	99.25	0.42	0.11	3.79	0.53	4.44	0.74
D13-2086	97	5	96.97	1.26	1.15	0.19	0.02	100.03	0.88	0.94	0.94	1.82	1.10	2.41
D13-2086	97	5	95.93	0.85	0.26	0.30	0.00	97.84	0.60	0.21	2.85	0.81	3.34	1.11
D13-2086	97	5	97.23	0.84	0.56	0.37	0.00	99.11	0.59	0.46	1.28	1.04	1.50	1.40
D13-2086	97	5	97.58	0.41	0.00	0.79	0.12	99.24	0.29	0.00	0.00	0.29	0.00	0.41
D13-2086	97	5	96.35	0.82	0.37	0.97	0.08	99.16	0.58	0.31	1.89	0.88	2.21	1.20
D13-2086	97	5	95.19	1.98	0.30	1.06	0.01	98.81	1.38	0.24	5.69	1.63	6.67	2.28
D13-2086	97	5	95.69	0.97	0.40	1.09	0.11	98.74	0.68	0.33	2.07	1.00	2.42	1.37
D13-2086	97	5	95.00	1.03	0.27	1.49	0.06	98.88	0.72	0.22	3.29	0.94	3.85	1.30

D13-2086	97	5	95.38	0.56	0.56	1.64	0.03	98.46	0.39	0.46	0.84	0.85	0.98	1.12
D13-2086	97	5	90.78	1.19	0.06	2.55	0.00	95.89	0.83	0.05	17.60	0.88	20.62	1.25
D13-2086	97	5	97.74	1.71	0.13	1.09	0.02	101.62	1.19	0.11	11.21	1.30	13.14	1.84
D13-2086	97	5	81.16	1.48	0.11	0.30	0.00	85.00	1.03	0.09	11.68	1.12	13.69	1.59
D13-2086	97	5	97.83	0.90	0.09	0.91	0.00	100.75	0.63	0.08	8.18	0.71	9.59	1.00
D13-2086	97	5	99.37	1.44	0.09	0.55	0.01	102.46	1.01	0.07	13.82	1.08	16.19	1.53
D13-2086	97	5	97.49	1.10	0.19	1.07	0.00	101.28	0.77	0.16	4.85	0.92	5.68	1.29
D13-2086	97	5	96.79	0.85	0.30	1.92	0.00	101.03	0.59	0.25	2.38	0.84	2.79	1.15
D13-2086	97	5	96.94	1.05	0.21	1.76	0.00	101.08	0.73	0.17	4.26	0.90	4.99	1.26
D13-2086	97	5	96.90	0.80	0.12	1.71	0.00	100.76	0.56	0.10	5.51	0.66	6.46	0.93
D13-2086	97	5	97.21	1.15	0.01	1.52	0.00	101.10	0.81	0.01	89.38	0.81	104.73	1.16
D13-2086	97	5	97.04	1.24	0.14	1.94	0.02	101.67	0.86	0.12	7.48	0.98	8.77	1.38
D13-2086	97	5	97.58	0.62	0.02	1.70	0.00	100.81	0.43	0.02	22.12	0.45	25.92	0.65
D13-2086	97	5	99.17	0.95	0.00	0.30	0.00	101.38	0.66	0.00	0.00	0.66	0.00	0.95
D13-2086	97	5	97.85	0.98	0.00	0.89	0.01	101.05	0.68	0.00	0.00	0.68	0.00	0.98
D13-2086	97	5	99.71	0.43	0.00	0.99	0.00	102.01	0.30	0.00	0.00	0.30	0.00	0.43
D13-2086	97	5	91.12	0.35	0.00	4.05	0.04	98.35	0.24	0.00	0.00	0.24	0.00	0.35
D13-2086	97	5	86.00	0.44	0.00	5.95	0.05	94.75	0.31	0.00	0.00	0.31	0.00	0.44
Average			95.71	0.96	0.20	1.37	0.02	99.28	0.67	0.17	8.19	0.84	9.60	1.17
A16-1159	62	5	97.04	0.67	0.00	0.19	0.03	98.29	0.47	0.00	0.00	0.47	0.00	0.67
A16-1159	62	5	97.34	0.59	0.00	0.24	0.00	98.73	0.41	0.00	0.00	0.41	0.00	0.59
A16-1159	62	5	93.79	0.71	0.19	0.36	0.04	96.64	0.50	0.16	3.19	0.65	3.74	0.90
A16-1159	62	5	96.41	1.10	0.00	0.58	0.08	98.73	0.77	0.00	0.00	0.77	0.00	1.10
A16-1159	62	5	96.81	1.97	0.00	0.76	0.00	100.15	1.38	0.00	0.00	1.38	0.00	1.97
A16-1159	62	5	98.75	0.52	0.22	0.10	0.01	101.41	0.36	0.18	2.02	0.54	2.37	0.73
A16-1159	62	5	98.67	0.46	0.11	0.13	0.02	100.63	0.32	0.09	3.54	0.42	4.14	0.58
A16-1159	62	5	96.55	0.58	0.28	0.23	0.11	99.68	0.40	0.23	1.73	0.64	2.03	0.86
A16-1159	62	5	99.21	1.38	0.13	0.67	0.02	102.57	0.97	0.11	9.00	1.07	10.55	1.51
A16-1159	62	5	98.35	0.91	0.10	0.62	0.01	101.12	0.64	0.08	7.92	0.72	9.28	1.01
A16-1159	62	5	88.50	0.84	0.21	5.37	0.09	97.92	0.58	0.17	3.38	0.76	3.96	1.05
A16-1159	62	5	98.40	1.03	0.15	0.65	0.02	101.42	0.72	0.12	5.79	0.85	6.78	1.18
A16-1159	62	5	96.18	1.03	0.32	0.36	0.00	99.94	0.72	0.26	2.73	0.98	3.20	1.35
A16-1159	62	5	96.86	1.16	0.29	0.25	0.00	100.06	0.81	0.24	3.40	1.05	3.98	1.46

A16-1159	62	5	97.38	1.70	0.27	0.98	0.01	101.56	1.19	0.22	5.43	1.41	6.36	1.97
A16-1159	62	5	99.59	0.39	0.00	0.15	0.01	101.15	0.27	0.00	83.21	0.28	97.50	0.39
A16-1159	62	5	99.22	0.75	0.07	0.22	0.00	101.26	0.52	0.06	8.76	0.58	10.26	0.82
A16-1159	62	5	99.65	0.46	0.00	0.24	0.00	101.55	0.32	0.00	0.00	0.32	0.00	0.46
A16-1159	62	5	93.44	0.66	0.00	1.92	0.09	97.51	0.46	0.00	0.00	0.46	0.00	0.66
Average			96.95	0.89	0.12	0.74	0.03	100.02	0.62	0.10	7.37	0.72	8.64	1.01
A15-0044	57	5	96.64	0.94	0.00	0.17	0.00	98.47	0.65	0.00	0.00	0.65	0.00	0.94
A15-0044	57	5	95.28	0.84	0.00	0.45	0.02	97.84	0.58	0.00	0.00	0.58	0.00	0.84
A15-0044	57	5	94.56	2.46	0.19	0.86	0.06	98.50	1.72	0.16	10.76	1.88	12.61	2.65
A15-0044	57	5	95.76	0.71	0.00	1.16	0.03	98.24	0.49	0.00	0.00	0.49	0.00	0.71
A15-0044	57	5	95.31	0.84	0.14	1.30	0.10	97.90	0.59	0.11	5.24	0.70	6.14	0.98
A15-0044	57	5	97.49	0.41	0.00	1.30	0.00	99.53	0.29	0.00	0.00	0.29	0.00	0.41
A15-0044	57	5	96.61	1.59	0.10	1.84	0.00	100.97	1.11	0.09	13.04	1.20	15.28	1.69
A15-0044	57	5	96.18	1.71	0.18	2.25	0.00	101.22	1.19	0.15	8.08	1.34	9.47	1.89
A15-0044	57	5	97.01	0.93	0.04	0.47	0.02	100.48	0.65	0.03	19.80	0.68	23.20	0.97
A15-0044	57	5	98.13	0.57	0.00	0.39	0.01	100.53	0.40	0.00	487.34	0.40	571.00	0.57
A15-0044	57	5	96.80	1.88	0.07	0.94	0.02	100.57	1.31	0.06	22.86	1.37	26.79	1.95
A15-0044	57	5	93.96	0.85	0.01	1.68	0.08	98.86	0.59	0.01	90.26	0.60	105.75	0.85
A15-0044	57	5	98.50	0.89	0.00	0.36	0.01	100.90	0.62	0.00	0.00	0.62	0.00	0.89
Average			96.33	1.12	0.06	1.01	0.03	99.54	0.78	0.05	50.57	0.83	59.25	1.18
A09-2193	54	5	96.56	1.47	0.00	0.58	0.01	99.54	1.03	0.00	0.00	1.03	0.00	1.47
A09-2193	54	5	95.09	2.23	0.78	0.85	0.07	99.30	1.56	0.64	2.43	2.20	2.85	3.01
A09-2193	54	5	95.83	1.71	0.73	0.90	0.00	99.36	1.20	0.60	2.00	1.79	2.35	2.44
A09-2193	54	5	94.69	2.84	0.55	0.91	0.00	99.82	1.99	0.45	4.40	2.44	5.16	3.39
A09-2193	54	5	95.62	1.42	0.43	1.45	0.16	99.75	0.99	0.35	2.83	1.35	3.31	1.85
A09-2193	54	5	91.27	2.72	0.95	1.66	0.05	97.80	1.90	0.78	2.45	2.67	2.87	3.66
A09-2193	54	5	87.93	1.99	0.50	3.04	0.07	97.89	1.39	0.41	3.43	1.80	4.02	2.49
A09-2193	54	5	94.32	3.13	1.46	1.03	0.08	101.12	2.18	1.19	1.83	3.38	2.14	4.58
A09-2193	54	5	97.06	1.36	0.24	0.62	0.05	100.64	0.95	0.19	4.93	1.15	5.78	1.60
A09-2193	54	5	96.87	1.38	0.28	0.75	0.04	100.60	0.96	0.23	4.17	1.19	4.89	1.66
A09-2193	54	5	96.87	1.74	0.13	0.71	0.03	100.75	1.22	0.10	11.72	1.32	13.73	1.87
A09-2193	54	5	94.62	2.53	0.56	1.33	0.05	100.31	1.77	0.45	3.89	2.22	4.55	3.08

A09-2193	54	5	98.06	1.33	0.02	0.78	0.06	101.19	0.93	0.02	47.26	0.95	55.38	1.35
A09-2193	54	5	90.28	4.19	2.56	1.46	0.02	100.05	2.93	2.10	1.40	5.03	1.64	6.76
A09-2193	54	5	92.02	3.82	2.07	1.44	0.02	100.80	2.67	1.70	1.57	4.36	1.84	5.89
A09-2193	54	5	92.95	1.89	1.38	1.79	0.03	99.39	1.32	1.13	1.17	2.45	1.37	3.27
A09-2193	54	5	96.92	1.31	0.27	1.03	0.07	100.51	0.91	0.22	4.15	1.13	4.86	1.58
A09-2193	54	5	95.29	2.92	0.28	1.47	0.07	101.05	2.04	0.23	8.87	2.27	10.40	3.20
A09-2193	54	5	95.27	0.67	0.28	1.57	0.01	98.82	0.47	0.23	2.06	0.70	2.41	0.95
A09-2193	54	5	97.22	1.27	0.33	0.20	0.00	100.19	0.89	0.27	3.31	1.15	3.87	1.59
A09-2193	54	5	97.41	1.40	0.26	0.62	0.02	100.87	0.98	0.21	4.58	1.19	5.37	1.66
A09-2193	54	5	97.50	1.13	0.10	0.30	0.00	99.96	0.79	0.08	9.70	0.87	11.36	1.22
A09-2193	54	5	97.74	1.10	0.19	0.41	0.01	100.41	0.77	0.16	4.92	0.92	5.76	1.29
A09-2193	54	5	97.74	0.98	0.00	0.71	0.06	100.61	0.68	0.00	0.00	0.68	0.00	0.98
Average			95.21	1.94	0.60	1.07	0.04	100.03	1.35	0.49	5.54	1.84	6.50	2.54
A15-0068	45	5	79.28	11.61	3.17	4.42	0.06	100.10	8.12	2.60	3.13	10.71	3.66	14.78
A15-0068	45	5	96.01	2.41	0.05	0.46	0.02	99.85	1.68	0.04	42.83	1.72	50.19	2.46
A15-0068	45	5	94.92	2.59	0.46	0.75	0.02	100.26	1.81	0.38	4.79	2.19	5.61	3.05
A15-0068	45	5	79.77	11.41	2.84	4.13	0.00	98.76	7.97	2.33	3.43	10.30	4.02	14.25
A15-0068	45	5	85.53	7.90	0.94	4.19	0.00	99.15	5.52	0.77	7.15	6.29	8.37	8.84
A15-0068	45	5	74.70	14.69	3.42	5.77	0.00	99.50	10.27	2.80	3.66	13.07	4.29	18.11
Average			85.03	8.43	1.81	3.29	0.02	99.60	5.90	1.49	10.83	7.38	12.69	10.25
A16-1224	43	5	93.55	1.09	1.53	1.82	0.16	101.01	0.76	1.25	0.61	2.01	0.71	2.62
A16-1224	43	5	94.35	1.19	1.57	1.28	0.16	101.63	0.83	1.28	0.65	2.11	0.76	2.76
Average			93.95	1.14	1.55	1.55	0.16	101.32	0.79	1.27	0.63	2.06	0.73	2.69
A16-1238	26	5	96.79	0.21	0.00	0.28	0.00	98.48	0.15	0.00	0.00	0.15	0.00	0.21
A16-1238	26	5	95.27	1.77	0.47	0.41	0.05	98.39	1.24	0.38	3.24	1.62	3.80	2.23
A16-1238	26	5	95.31	0.53	0.00	0.44	0.06	98.22	0.37	0.00	0.00	0.37	0.00	0.53
A16-1238	26	5	96.57	0.95	0.08	0.46	0.00	98.75	0.67	0.07	10.19	0.73	11.93	1.03
A16-1238	26	5	97.75	0.92	0.18	0.52	0.06	99.97	0.65	0.15	4.37	0.79	5.13	1.10
A16-1238	26	5	96.26	1.84	0.06	1.10	0.04	99.73	1.29	0.05	27.12	1.34	31.78	1.90
A16-1238	26	5	99.71	1.92	0.44	1.15	0.06	103.79	1.34	0.36	3.71	1.70	4.34	2.36
A16-1238	26	5	93.64	1.32	0.10	1.98	0.00	97.50	0.92	0.08	10.91	1.01	12.79	1.42

A16-1238	26	5	90.96	1.97	0.00	2.22	0.00	98.44	1.38	0.00	0.00	1.38	0.00	1.97
A16-1238	26	5	100.43	0.17	0.00	0.32	0.02	102.20	0.12	0.00	48.65	0.12	57.00	0.17
A16-1238	26	5	98.11	1.13	0.12	0.51	0.01	100.96	0.79	0.10	8.07	0.89	9.45	1.25
A16-1238	26	5	97.51	2.11	0.18	0.47	0.02	101.32	1.47	0.15	10.06	1.62	11.79	2.29
A16-1238	26	5	96.28	1.96	0.30	0.53	0.02	100.19	1.37	0.24	5.60	1.61	6.56	2.25
A16-1238	26	5	98.29	1.32	0.27	0.59	0.02	101.62	0.92	0.22	4.15	1.15	4.86	1.59
A16-1238	26	5	90.54	2.86	0.53	1.78	0.05	98.25	2.00	0.44	4.58	2.43	5.37	3.39
A16-1238	26	5	96.68	2.14	0.33	1.32	0.02	101.76	1.50	0.27	5.59	1.76	6.54	2.47
A16-1238	26	5	98.48	0.54	0.03	1.20	0.03	101.63	0.37	0.02	18.26	0.39	21.40	0.56
A16-1238	26	5	96.41	2.19	0.21	1.31	0.03	101.52	1.53	0.17	8.93	1.70	10.46	2.40
A16-1238	26	5	99.36	0.39	0.05	0.75	0.02	101.58	0.27	0.04	6.12	0.31	7.17	0.44
A16-1238	26	5	95.84	1.59	0.61	1.39	0.03	101.95	1.11	0.50	2.22	1.62	2.60	2.21
A16-1238	26	5	95.78	2.82	1.26	0.94	0.04	101.98	1.97	1.03	1.91	3.00	2.24	4.08
A16-1238	26	5	98.14	1.15	0.02	0.59	0.03	101.09	0.80	0.02	44.65	0.82	52.32	1.17
A16-1238	26	5	98.55	1.24	0.10	0.92	0.02	101.83	0.87	0.08	10.83	0.95	12.69	1.34
Average			96.64	1.44	0.23	0.92	0.03	100.48	1.00	0.19	10.40	1.19	12.18	1.67
A11-2272	23	5	95.43	1.15	0.91	0.73	0.00	98.36	0.81	0.74	1.08	1.55	1.27	2.06
A11-2272	23	5	96.96	0.94	0.65	0.82	0.01	99.56	0.65	0.53	1.23	1.19	1.44	1.59
A11-2272	23	5	96.31	0.70	0.60	0.91	0.00	98.63	0.49	0.49	0.99	0.98	1.15	1.30
A11-2272	23	5	95.40	0.60	0.86	0.92	0.04	98.29	0.42	0.70	0.60	1.12	0.70	1.46
A11-2272	23	5	96.83	0.61	0.27	0.92	0.02	99.18	0.43	0.22	1.93	0.65	2.26	0.88
A11-2272	23	5	95.91	0.58	0.18	1.05	0.03	98.21	0.41	0.15	2.71	0.56	3.18	0.76
A11-2272	23	5	95.96	0.93	0.17	1.51	0.04	99.08	0.65	0.14	4.59	0.80	5.37	1.11
A11-2272	23	5	94.38	0.72	0.00	2.36	0.00	98.21	0.51	0.00	0.00	0.51	0.00	0.72
A11-2272	23	5	92.78	1.11	0.71	2.82	0.05	98.04	0.78	0.58	1.33	1.36	1.56	1.82
A11-2272	23	5	98.60	0.74	0.05	0.59	0.03	100.97	0.51	0.04	12.55	0.55	14.70	0.79
A11-2272	23	5	96.67	1.03	0.22	1.60	0.02	100.49	0.72	0.18	3.96	0.90	4.64	1.25
A11-2272	23	5	94.83	1.03	0.29	2.11	0.05	99.50	0.72	0.24	3.01	0.95	3.52	1.32
A11-2272	23	5	95.38	1.20	0.35	2.15	0.07	100.50	0.84	0.29	2.94	1.13	3.44	1.55
A11-2272	23	5	96.67	1.58	0.44	0.99	0.04	100.72	1.11	0.36	3.05	1.47	3.58	2.02
A11-2272	23	5	96.41	0.77	0.13	1.00	0.05	99.27	0.54	0.11	4.92	0.65	5.77	0.90
A11-2272	23	5	95.05	0.79	0.26	2.05	0.04	99.28	0.55	0.21	2.62	0.76	3.07	1.05
A11-2272	23	5	96.53	0.49	0.41	1.22	0.01	99.70	0.34	0.34	1.01	0.67	1.18	0.90

A11-2272	23	5	96.87	1.26	0.40	1.02	0.03	100.55	0.88	0.33	2.68	1.21	3.15	1.66
A11-2272	23	5	96.04	0.75	0.03	1.72	0.02	99.48	0.53	0.02	23.77	0.55	27.85	0.78
A11-2272	23	5	97.82	1.01	0.06	0.77	0.02	100.55	0.70	0.05	15.61	0.75	18.29	1.06
A11-2272	23	5	98.04	0.73	0.15	0.60	0.00	100.39	0.51	0.12	4.18	0.63	4.90	0.88
A11-2272	23	5	96.26	1.16	0.58	1.66	0.02	100.52	0.81	0.48	1.70	1.29	1.99	1.74
A11-2272	23	5	96.00	0.92	0.59	1.62	0.01	100.12	0.64	0.48	1.33	1.12	1.56	1.50
A11-2272	23	5	98.36	0.73	0.00	0.29	0.01	100.44	0.51	0.00	0.00	0.51	0.00	0.73
Average			96.23	0.90	0.35	1.31	0.03	99.59	0.63	0.28	4.07	0.91	4.77	1.24